องค์ประกอบทางเคมีและฤทธิ์ทางชีวภาพของผักเชียงดา *Gymnema inodorum* Decne. และมะรุม *Moringa oleifera* Lam.

นางสาวดารารัตน์ แย้มหมื่นอาจ

วิทยานิพนธ์นี้เป็นส่วนหนึ่งของการศึกษาตามหลักสูตรปริญญาวิทยาศาสตรมหาบัณฑิต
สาขาวิชาเคมี ภาควิชาเคมี
คณะวิทยาศาสตร์ จุฬาลงกรณ์มหาวิทยาลัย
ปีการศึกษา 2550

CHEMICAL CONSTITUENTS AND THEIR BIOLOGICAL ACTIVITIES OF *Gymnema inodorum* Decne. AND *Moringa oleifera* Lam.

Miss Dararat Yammuenart

A Thesis Submitted in Partial Fulfillment of the Requirements

for the Degree of Master of Science Program in Chemistry

Department of Chemistry

Faculty of Science

Chulalongkorn University

Academic Year 2007

Thesis Title	CHEMICAL CONSTITUENTS AND THEIR BIOLOGICAL ACTIVITIES OF *Gymnema inodorum* Decne. AND *Moringa oleifera* Lam.
By	Miss Dararat Yammuenart
Field of Study	Chemistry
Thesis Advisor	Assistant Professor Warinthorn Chavasiri, Ph.D.
Thesis Co-advisor	Associate Professor Klai-upsorn Pongrapeeporn, Ph.D.

Accepted by the Faculty of Science, Chulalongkorn University in Partial Fulfillment of the Requirements for the Master's Degree

S. Hannongbua .....Dean of the Faculty of Science

(Professor Supot Hannongbua, Ph.D.)

THESIS COMMITTEE

Udom Kokpol ..... Chairman

(Professor Udom Kokpol, Ph.D.)

Warinthorn Chavasiri ..... Thesis Advisor

(Assistant Professor Warinthorn Chavasiri, Ph.D.)

Klaiupsorn S. Pongrapeeporn ..... Thesis Co-Advisor

(Associate Professor Klai-upsorn Pongrapeeporn, Ph.D.)

Padet Sidisun ..... Member

(Professor Padet Sidisunthorn, Ph.D.)

Khanitha Pudhom ..... Member

(Assistant Professor Khanitha Pudhom, Ph.D.)

ดารารัตน์ แย้มหมื่นอาจ : องค์ประกอบทางเคมี และฤทธิ์ทางชีวภาพของผักเชียงดา *Gymnema indorum* Decnc. และมะรุม *Moringa oleifera* Lam. (CHEMICAL CONSTITUENTS AND THEIR BIOLOGICAL ACTIVITIES OF *Gymnema indorum Decnc.* AND *Moringa oleifera* Lam.) อาจารย์ที่ปรึกษา: ผศ.ดร.วรินทร ชวศิริ, อาจารย์ที่ปรึกษาร่วม: รศ.ดร.คล้ายอัปสร พงศ์รพีพร, 124 หน้า.

สิ่งสกัดไดคลอโรมีเทนและบิวทานอลของผักเชียงดาและรากมะรุมแสดงฤทธิ์ยับยั้งอนุมูลอิสระและแอลฟาเอไมเลสที่น่าสนใจ การแยกด้วยเทคนิคโครมาโทกราฟีของสิ่งสกัดไดคลอโรมีเทนของผักเชียงดาได้สาร 3 ชนิดได้แก่ แอลกอฮอล์โซ่ตรง, คีโทนโซ่ตรง และของผสมสเตอรอยด์ที่มี stigmasterol เป็นองค์ประกอบหลัก ขณะที่ซาโปนิน 2 ชนิด คือ (3β,4α,6β)-16,23,28-trihydroxyolean-12-en-3-yl-β-D-glucopyran osiduroic acid และ (3β,16β,22α)-16,28-dihydroxyolean-12-en-3-yl-O-β-D-glucopyranosyl-β-D-glucopyranosiduroic acid แยกได้จากสิ่งสกัดบิวทานอล สาร 4 ชนิด คือ แอลกอฮอล์โซ่ตรง, คีโทนโซ่ตรง, ของผสม β-sitosterol, campesterol และ stigmasterol และของผสม 1,3-dilinoleoyl-2-olein, 1,3-dioleoyl-2-linolein และ 1,2,3-trilinolein แยกได้จากสิ่งสกัดไดคลอโรมีเทนของรากมะรุม นอกจากนั้นแยกสารบริสุทธิ์ได้อีก 5 ชนิดคือ linoleic acid, isothiocyanatomethylbenzene, 1,2,3-triolein, benzamide, β-sitosteryl linoleate และ β-sitosterol-3-O-β-D-glucopyranoside เมื่อทดสอบฤทธิ์ต้านอนุมูลอิสระ DPPH ฤทธิ์ยับยั้งโคลีนเอสเทอเรสและฤทธิ์ยับยั้งแอลฟาเอไมเลสของสารที่แยกได้ทั้งหมดมีเพียง (3β,16β,22α)-16,28-dihydroxyolean-12-en-3-yl-O-β-D-glucopyranosyl-β-D-glucopyranosiduroic acid แสดงฤทธิ์ต้านอนุมูลอิสระ DPPH ส่วนฤทธิ์ยับยั้งแอลฟาเอไมเลสของ (3β,16β,22α)-16,28-dihydroxyolean-12-en-3-yl-O-β-D-glucopyranosyl-β-D-glucopyranosiduroic acid (38.59%) ดีกว่า (3β,4α,16β)-16,23,28-trihydroxyolean-12-en-3-yl-β-D-glucopyranosiduroic acid (9.80%) นอกจากนี้ benzamide ที่แยกได้จากสิ่งสกัดไดคลอโรมีเทนของรากมะรุมแสดงฤทธิ์ต้านอนุมูลอิสระ DPPH ดีที่สุด ขณะที่ β-sitosterol-3-O-β-D-glucopyranoside แสดงฤทธิ์ยับยั้งแอลฟาเอไมเลสที่ดีด้วยค่า IC_{50} 0.326 mM

ได้สังเคราะห์อนุพันธ์คาร์บอกซาไมด์และเอสเทอร์เพื่อทดสอบฤทธิ์ต้านอนุมูลอิสระ DPPH พบว่า *N*-(2-hydroxylphenyl)-5-(3,4-methylenedioxyphenyl)-*2E,4E*-pentadieneyl amide แสดงฤทธิ์ต้านอนุมูลอิสระสูงด้วยค่า IC_{50} 0.470 mM เมื่อทดสอบฤทธิ์ต้านอนุมูลอิสระ ABTS ได้ค่าใกล้เคียงกับ trolox ซึ่งแสดงให้เห็นว่าสารดังกล่าวมีประสิทธิภาพในการต้านอนุมูลอิสระ

ภาควิชา.....เคมี.....ลายมือชื่อ.....

สาขาวิชา.....เคมี.....ลายมือชื่ออาจารย์ที่ปรึกษา.....

ปีการศึกษา.....2550..... ลายมือชื่ออาจารย์ที่ปรึกษาร่วม.....

4872290323: MAJOR CHEMISTRY
KEY WORD: ANTIOXIDANT/ MORINGA OLEIFERA/ GYMMENA INODORUM
DARARAT YAMMUENART: CHEMICAL CONSTITUENTS AND THEIR BIOLOGICAL ACTIVITIES OF *Gymnema inodorum* Decne. AND *Moringa oleifera* Lam. THESIS ADVISOR: ASST. PROF. WARINTHORN CHAVASIRI, PH.D. THESIS CO-ADVISOR: ASSOC. PROF. KLAI-UPSORN PONGRAPEEPORN, PH.D. 124 pp.

The CH_2Cl_2 and *n*-BuOH crude extracts of *G. inodorum* and those of the roots of *M. oleifera* revealed a promising antioxidant and α-amylase inhibitor activities. Chromatographic separation of the CH_2Cl_2 extract of *G. inodorum* led to the isolation of three known substances: a long chain alcohol, a long chain ketone and a mixture of steroids containing stigmasterol as a major component. While two known saponins, (3*β*,4α,16*β*)-16,23,28-trihydroxyolean-12-en-3-yl-*β*-D-glucopyranosiduroic acid and (3*β*,16*β*,22α)-16,28-dihydroxyolean-12-en-3-yl-O-*β*-D-glucopyranosyl-*β*-D-glucopyranosiduroic acid were isolated from the *n*-BuOH crude extract. Four known substances: a long chain alcohol, a long chain ketone, a mixture of *β*-sitosterol, campesterol and stigmasterol along with a mixture of triglycerides as 1,3-dilinoleoyl-2-olein, 1,3-dioleoyl-2-linolein and 1,2,3-trilinolein were isolated from the CH_2Cl_2 crude extract of the roots of *M. oleifera*. In addition, five known compounds were isolated and identified as linoleic acid, isothiocyanatomethylbenzene, 1,2,3-triolein, benzamide, *β*-sitosteryl linoleate and *β*-sitosterol-3-O-*β*-D-glucopyranoside. All isolated substances were assayed for antioxidant, the inhibition of cholinesterase activity and α-amylase inhibitor. Only (3*β*,16*β*,22α)-16,28-dihydroxyolean-12-en-3-yl-O-*β*-D-glucopyranosyl-*β*-D-glucopyranosiduroic acid was active for radical scavenging effect on DPPH radical. The α-amylase inhibition of (3*β*,16*β*,22α)-16,28-dihydroxyolean-12-en-3-yl-O-*β*-D-glucopyranosyl-*β*-D-glucopyranosiduroic acid (38.59%) was better than that of (3*β*,4α,16*β*)-16,23,28-trihydroxyolean-12-en-3-yl-*β*-D-glucopyranosiduroic acid (9.80%). Moreover, benzamide isolated from the CH_2Cl_2 crude extract of *M. oleifera* roots showed the highest scavenging activity on DPPH, while *β*-sitosterol-3-O-*β*-D-glucopyranoside was found as a good inhibitor for α-amylase inhibition with IC_{50} of 0.326 mM.

The synthetic derivatives of certain carboxamides and esters were also prepared to test for scavenging effects on DPPH radical. *N*-(2-hydroxylphenyl)-5-(3,4-methylenedioxyphenyl)-*2E,4E*-pentadieneyl amide showed highly active toward radical scavenging effect on DPPH radical with IC_{50} of 0.470 mM and ABTS value being similar to that of trolox revealing good potent for antioxidant activity.

Department.....Chemistry.....Student's signature...Dararat Yammuenart...
Field of study.....Chemistry.....Advisor's signature....Warinthorn Chavasiri
Academic year.....2007..... Co-advisor's signature..Klaiupsorn S. Pongrapeeporn

ACKNOWLEDGEMENTS

The author would like to express her appreciation to her advisor and co-advisor, Assistant Professor Dr. Warinthorn Chavasiri and Associate Professor Dr. Klai-upsorn Pongrapeeporn for their very kind assistance and opinions during this course of research. Thanks are also extended to Natural Products Research Unit, Department of Chemistry, Faculty of Science, Chulalongkorn University for the support of chemicals.

The author also acknowledged Professor Dr. Udom Kokpol, Professor Dr. Padet Sidisunthorn and Assistant Professor Dr. Khanitha Pudhom serving as the chairman and members of this thesis committee, respectively, for their valuable discussion and suggestion.

Finally, the author would like to express her gratitude to her parents and family members for their inspiration, understanding, great support and encouragement throughout the entire study.

CONTENTS

CHAPTER **Page**

CHAPTER **Page**

CHAPTER **Page**

List of Tables

List of Figures

Figures **Page**

APPENDIX

Figures **Page**

List of Schemes

List of abbreviations

ABTS	=	2,2′-azinodi-3-ethylbenzthiazoline sulphonate
br	=	broad
ºC	=	degree Celsius
$CDCl_3$	=	deuterated chloroform
CH_2Cl_2	=	dichloromethane
$CHCl_3$	=	chlorofrom
^{13}C NMR	=	Carbon-13 Nuclear Magnetic Resonance
d	=	doublet (NMR)
dd	=	doublet of doublet (NMR)
ddd	=	doublet of doublet of doublet (NMR)
EtOAc	=	Ethyl acetate
g	=	Gram (s)
h	=	hour
^{1}H NMR	=	Proton-1 Nuclear Magnetic Resonance
HMBC	=	heteronuclear multiple bond correlation experiment
HMQC	=	heteronuclear multiple quantum coherence experiment
H_2O	=	Water
Hz	=	Hertz (NMR)
J	=	Coupling constant
m	=	multiplet (NMR)
MeOH	=	Methanol
mg	=	Milligram (s)
min	=	Minute
mL	=	Milliliter (s)
mm	=	Millimeter (s)
m.p.	=	Melting point
MS	=	Mass Spectrometry
MW	=	Molecular weight

List of abbreviations (continued)

No.	=	Number
ppm	=	Part per million
R_f	=	Retarding facter in chromatography
s	=	Singlet (NMR)
t	=	Triplet (NMR)
TLC	=	Thin Layer Chromatography
δ	=	Unit of chemical shif

CHAPTER I

INTRODUCTION

Many plants in Thailand are medicinal potent. It has been estimated that plants are the most important source of medicine for more than 80% of the world's population. Medicinal plants are a vital source of medication in developing countries. Nowadays, certain diseases have no drug for treatment while new diseases have still discovered. Therefore, searching for new drugs is necessary. Secondary metabolites in plant have involved in nature as biologically active compounds with particular effects on other organisms. Thus, the study on chemical constituents from medicinal plants together with their pharmacological activities is important to disclose and develop for new medicinal drugs [1].

Under normal condition balance exists between the generation and detoxification of reactive oxygen species in cells. However, diseases, aging, sunlight and chemical environments such as drugs, pesticides, herbicides and various pollutants can disrupt this balance by inhibition of the cellular antioxidant defense or by stimulation of the formation of reactive oxygen species. These reactive oxygen species can damage macromolecules in cell such as proteins, lipids, amino acids and DNA to cause serious diseases. As a result, it is interesting to search for new antioxidant agents that may lead to new medicinal drugs for treatment or prevention of these diseases. Other physiological activities of natural antioxidants have been described, such as antibacterial, antiviral, antimutagenic, antiallergic, anticarcinogenic effects, antimetastasis activity, platelet aggregation inhibition, blood-pressure increase inhibition, antiulcer activity and anticariogenicity. Their uses as chemopreventive agents by inhibiting radical generation have been suggested since free radicals are responsible for DNA damage and radical scavengers are probably important in cancer prevention. Other studies have reported antimicrobial and antifungal properties of the polyphenolic extracts from *Sempervivum tectorum*, potato peel, vanillin and liquid smoke. During *in vivo* antioxidant assays of red wine polyphenols, these compound

exhibited a co-antioxidant role, similar to that of vitamin C and a sparing role toward vitamin E, which increases due to supplementation with phenols. However, a pro-oxidant effect of phenolics has also been reported. More research is needed in order to establish the activity, bioavailability and others *in vivo* effects of natural antioxidants. Many of the antioxidants other than vitamin C, vitamin E and carotenoids, occur as dietary constituents [2-3]. Table 1.1 shows a list of antioxidants and the structures of these compounds are shown in Fig 1.1.

Table 1.1 A list of antioxidant compounds

Antioxidant	Sources	Antioxidant activity (mM)
Vitamin C	fruit and vegetables	1.0 ± 0.02
Vitamin E	grains, nuts and oils	1.0 ± 0.03
Narirutin	citrus fruit	0.8 ± 0.5
Caffeic acid	white grapes, olive, cabbage and asparagus	1.3 ± 0.01
Chlorogenic acid	apple, pear, cherry, tomato and peach	1.3 ± 0.02
Ferulic acid	apple, pear, cherry, tomato and peach	1.9 ± 0.02
p-Cumaric acid	white grapes, tomato, cabbage and asparagus	2.2 ± 0.06
Theaflavin	black tea	2.9 ± 0.08
Theaflavin-3-gallate	black tea	4.7 ± 0.16
Theaflavin-3′-gallate	black tea	4.8 ± 0.19
Theaflavin digallate	black tea	6.2 ± 0.43

The history of drug discovery showed that plants are highly rich sources in the search for new active compounds and become a challenge to modern pharmaceutical industry.

In this research, a primary screening test of selected medicinal plants was based on radical scavenging activity. 2,2-Diphenyl-1-(2,4,6-trinitrophenyl)hydrazyl (DPPH) radical was used as a radical source in this test model. DPPH is a kind of nitrogen-centered radical and stable with their resonance system so it long-lived enough to detect any change that occurred when reacted with test compounds. The

detection of the color change was employed since the property of DPPH having different color between radical form (DPPH, purple color) and non radical form (DPPHn, colorless). The structures of DPPH and DPPHn are shown in Fig 1.2.

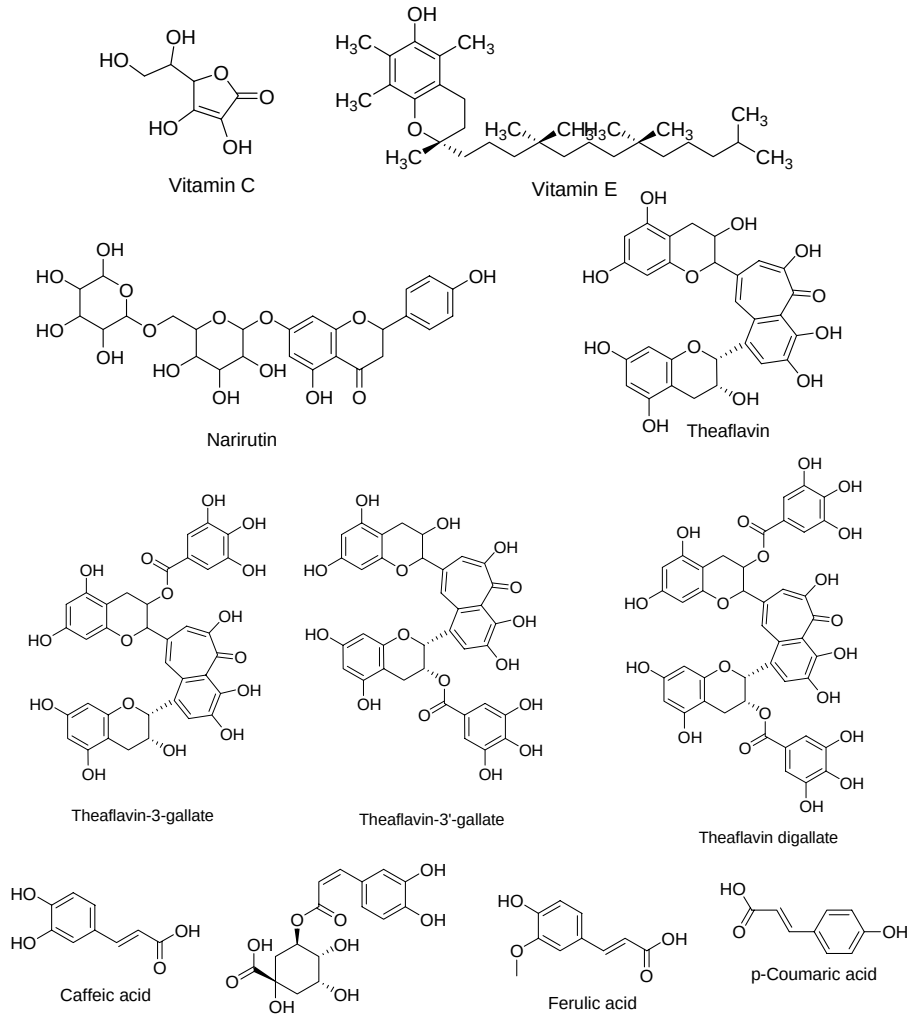

Figure 1.1 Structures of selected antioxidant compounds

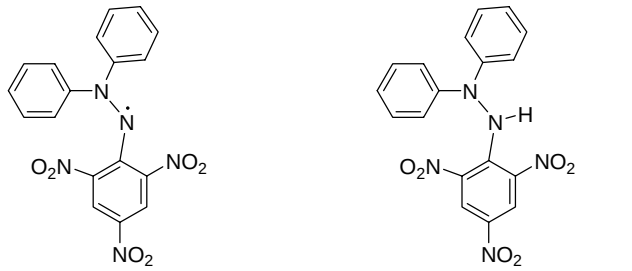

DPPH (purple color, λ_{max} 517 nm) DPPHn (colorless)

Figure 1.2 The structures of DPPH and DPPHn

1.1 Botanical characteristics of *M. oleifera*

Moringa oleifera Lam. (Synonym *Moringa perygosperma Gaern*.) is found in the East or Southeast Asia, Polynesia and West Indies [4]. *M. oleifera* is a tree with 3-10 m high. Leaves: tripinnate, atternate; leaflets elliptic, ovate, oblong or obovate, 0.7-2 cm wide, 1-3 cm long, inflorescence in auxillary panicle; flowers white or yellowish white, fruit capsule: linear, stem bark: carminative (Fig 1.3) [4].

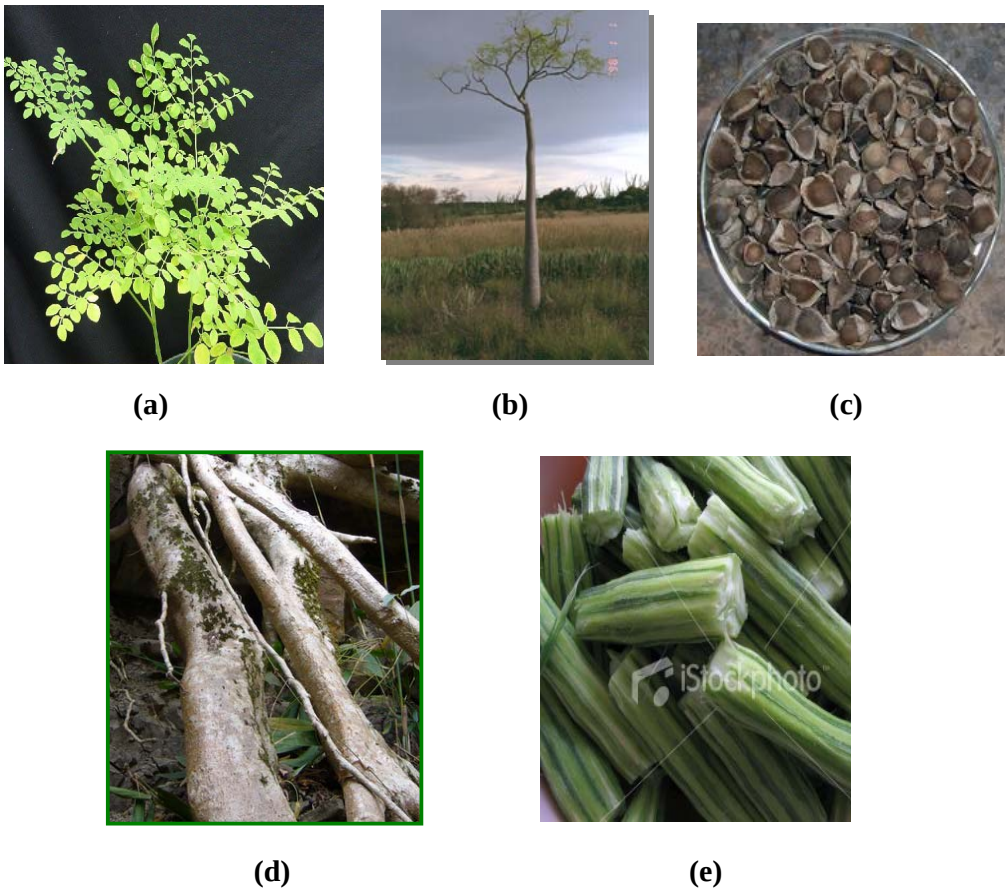

Figure 1.3 (a) leaves, (b) stem, (c) seed old, (d) root and (e) fruits and seeds young

1.2 Biological activity screening test of *M. oleifera*

In USA, fresh leaves are taken as a diuretic [5]. Hot water extract of the dried roots is taken orally as a cardiotonic, a stimulant for fainting [6], an antihistamine and papaverine-like action [7]. Pharmacological studies showed that juices from the leaves and barks could inhibit *Staphylococcus aureus*, but inactive against *Escherichia Coli* [8]. 50% Ethanolic extract of the whole plant (excluding roots) showed anticancer activity in mice [9]. The leaves of this plant are traditionally

known to have various biological activities, including hypocholes-terolemic effect [10], thyroid hormone regulation [11], antidiabetic action [12] and antigastric ulcer activity [13]. The fresh beans after roasting made a palatable dish. Seeds were also consumed after frying and reported to taste like peanuts. A number of medicinal and therapeutic properties have been ascribed to various parts of this multipurpose tree.

M. oleifera can be found in various parts of the world. Geographical origins determine the differences in bioactivity and the amount of active ingredients. In Thailand the tender pods and leaves have been eaten as vegetable for more than 100 years and other parts are used as traditional medicine. However, these uses are not well established. To take more advantage of the root, more scientific research is required.

1.3 Literature survey on chemical constituents of *M. oleifera*

1.3.1 Chemical constituents of the seeds in *M. oleifera*

The literature on the chemical constituents of the EtOH extracts of the seeds of *M. oleifera* revealed the presence of *O*-ethyl-4-(α-L-rhamnosyloxyl)benzyl carbamate **(1)**, 4(α-L-rhamnosyloxy)–benzyl isothiocyante **(2)**, niazimicin **(3)**, niazirin **(4)**, β-sitosterol **(5)**, glycerol-1-(9-octadecanoate) **(6)**, 3-*0*-(6′-*0*-oleoyl-β-D-glucopyrano-syl)-β-sitosterol **(7)** and β-sitosterol-3-*0*-β-D-glucopyranoside **(8)**. These compounds were tested for their potential antitumor promoting activity using an *in vitro* assay on Epstein-Barr virus-early antigen (EBV-EA) activation in Raji cells induced by the tumor promoter, 12-0-tetradecanoyl-phorbol-15-acetate (TPA). All tested compounds displayed the inhibitory activity against EBV-EA activation, while compound **2**, **3** and **8** exhibited very significant activities. 4-(α-L-rhamnosyloxy)–benzylisothiocyante **(2)**, niazimicin **(3)** and β-sitosterol-3-*0*-β-D-glucopyranoside **(8)** [14].

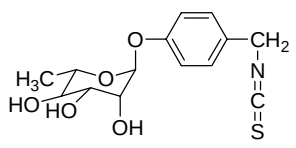

(**2**)

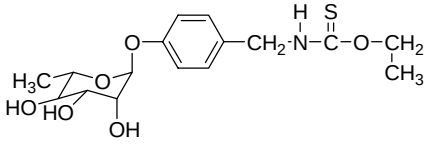

(**3**)

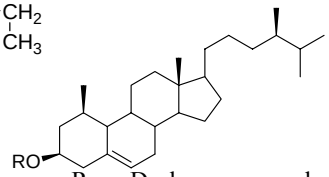

(**8**) R= α-D-glucopyranosyl

1.3.2 Chemical constituents of leaves in *M. oleifera*

The EtOH extract of the leaves of *M. oleifera* was reported to express hypotensive activity. This preliminary results led to the isolation of two nitrile glycoside: niazirin (**4**) and niazirinin (**9**), three mustard oil glycosides and 4-[(4′-*O*-acetyl-α-L-rhamnosyloxylbenzyl)isothiocyate (**10**). Niaziminin A and niziminin B. showed hypotensive activity while nitrile glycosides (**4**) and (**9**) were inactive [15].

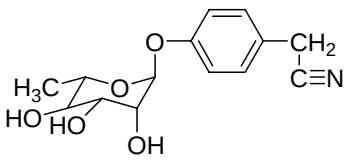

(**4**)

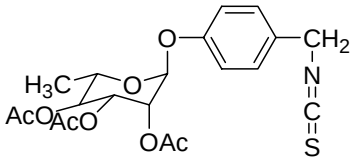

(**10**)

1.4 Botanical characteristics of *G. inodorum.*

G. inodorum lianas to 10 m stem glabrous; young branchlets pale gray, lenticellate, puberulent. Petiole 2-6 cm; leaf blade membranous, ovate-oblong to ovate or broadly ovate, 4-13×2-9 cm, glabrous or thin puberulent along veins, base rounded to shallowly cordate, apex acuminate to caudate; lateral veins 4-6 pairs (Fig 1.3) [4].

Figure 1.4 *G. inodorum*

1.5 Literature survey on chemical constituents of genus *Gymnema*

Ye and his co-workers separated the active principles from the EtOH extract of *G. sylvestre* as characterized as 21*β*-*O*-benzoylsitakisogenin-3-*O*-*β*-D-glucopyranosyl(1⟶3)-*β*-D-glucuronopyranoside (**11**), potassium salt of longispinogenin 3-*O*-*β*-D-glucopyranosyl (1⟶3)-*β*-D-glucuronopyranoside (**12**), potassium salt of 29-hydroxylongispinogenin-3-*O*-*β*-D-glucopyranosyl(1⟶3)-*β*-D-glucuronopyrano

side (**13**) and alternoside II (**14**). Compounds **11** and **14** exhibited antisweet activity [16].

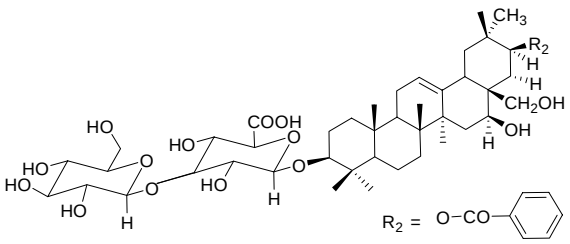

(11)

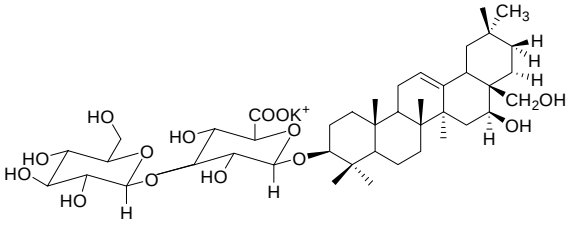

(12)

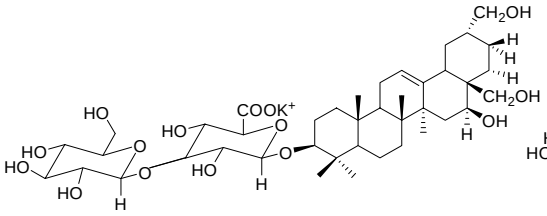

(13)

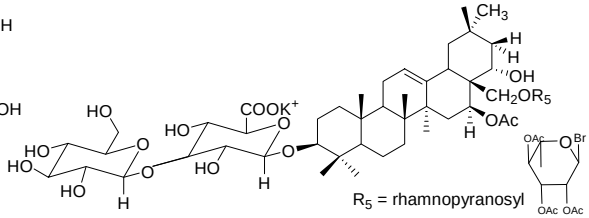

(14)

1.5.1 Chemical constituents and biological activity of *Gymnema inodorum*

From the literature survey, there was only one report in 2001 by Shimizu *et al*. on the chemical constituents of *G. Inodorum*. The active principles from the MeOH extract of *G. Inodorum* were identified as (3β,16β,22α)-16,28-dihydroxyolean-12-en-3-yl-*O*-β-D-glucopyranosyl-β-D-glucopyranosiduroic acid (**15**), (3β,4α,16β)16,23, 28-trihydroxyolean-12-en-3-yl-β-glucopyranosiduroic acid) (**16**), (3β,4α,16β, 22α)–22-(*N*-methylanthraniloxy)-16-23-28-trihydroxyolean-12-en-3-yl-*O*-β-D-glucopyrano -syl-β-D-glucopyranosiduroic acid) (**17**) and (3β,4α,16β,22α)-22-(*N*-methylanthraniloxy)-16,23,28-trihydroxyolean-12-en-3-yl-3-*O*-β-glucopyranosiduroic acid (**18**). Compounds **16**, **17** and **18** displayed good acitivity of glucose absorption [17].

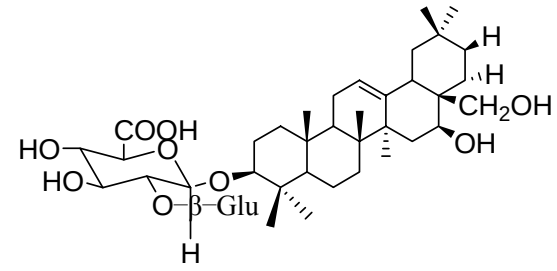

(15)

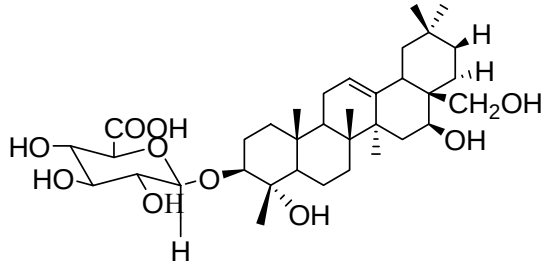

(16)

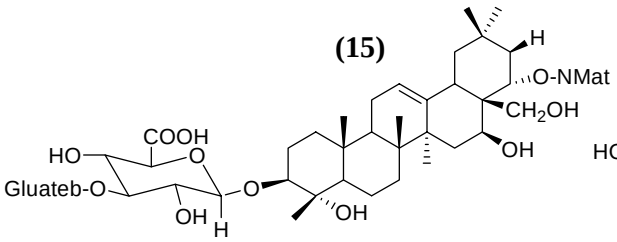

(17)

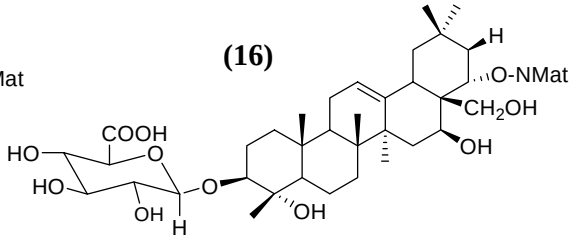

(18)

1.6 The goal of this research

From the primarily biological screening result, the extracts of *G. Inodorum* and *M. oleifera* showed excellent antioxidant activity. Therefore, the goal of this research could be summarized as follows:

1. To extract and isolate the chemical constituents of root of *M. oleifera*
2. To extract and isolate the chemical constituents of *G. inodorum*
3. To elucidate the structures of isolated substances.
4. To explore the biological activities of isolated substances.
5. To synthesize related compounds for studying structure-biological activity of isolated substances

CHAPTER II

EXPERIMENTAL

2.1 Plant materials

The stem, root, seed and leave of *Moringa oleifera* were collected from Tak Province in December 2006, whereas the whole plant of *Gymnema inodorum* was obtained from Changmai Province in June 2006.

2.2 Instruments and equipment

Thin layer chromatography (TLC) was preformed on an aluminium sheet precoated with silica gel (Merck's Kieselgel 60 PF_{254}). Column chromatography was performed on silica gel (Merck's Kieselgel 60G) 7734 and quick column chromatography was conducted on silica gel (Merck's Kieselgel 60 G) 7729.

The ^{1}H and ^{13}C-NMR spectra were preformed in $CDCl_3$ or otherwises stated with tetramethylsilane (TMS) as an internal reference on Fourier transform nuclear magnetic resonance spectrometer of Varian model Mercury+400. The Fourier Transform-infrared spectra (FT-IR) were recorded on Nicolet Impact 410 FT-IR spectrometer. Melting points were determined with a Fisher-Johns melting point apparatus and are uncorrected. GC analysis was carried out on a Shimadzu GC-9A instrument equipped with flame ionization detector with N_2 as a carrier gas. HPLC was performed on Water® 600 controllers equipped with a Water® 2996 dual UV wavelength detector (USA) using Econosphere 5 Cl8-ARII (25×250 mm) reversed phase column (Alltech Associates, IL, USA).

2.3 Color Test

Liebermann-Burchard's Test

The sample was dissolved in dry $CHCl_3$ 0.5 mL, then slowly added a few drops of acetic anhydride followed by a drop of concentrated H_2SO_4. Development of

the color suggests the presence of steroids or triterpenoids. If the solution was dark blue or greenish blue, the sample may contain steroidal nucleus, whereas if the solution turned reddish or purple, the sample should be a triterpenoidal compound.

2.4 Bioassay

2.4.1 Scavenging effects on DPPH radicals [18]

2,2-Diphenyl-1-picryhydrazyl (DPPH) radical is a stable radical with a purple color (λ_{max} 517nm). Upon reduction by a scavenger, the extensive conjugation is disrupted and the compound turns yellow.

TLC autographic assay

After developing and drying, TLC plates were sprayed with a 0.2% DPPH in MeOH solution. The plates were examined for 5 min after spraying. Active compounds appeared as yellow spots against purple background.

Spectrophotometric assay

Samples of various concentrations (0.5 mL) were added to 1 mL of MeOH solution of DPPH radical (final concentration of DPPH was 0.2 mM). The mixture was shaken vigorously and then left for 30 min. The absorbance of the resulting solution was measured at 517 nm with a spectrophotometer. All tests and analyses were run in three replicates and averaged. Calculate the percentage of radical scavenging by the following equation.

The percentage of radical scavenging = $(1-A_{sample}/A_{control}) \times 100$

A_{sample} = Absorbance of sample solution with DPPH

$A_{control}$ = Absorbance of only DPPH and used solvent

2.4.2 Trolox equivalent antioxidant capacity (TEAC) assay [19]

The action of *N*-(2-hydroxylphenyl)-5-(3,4-methylenedioxyphenyl)-*2E*,*4E*-pentadieneyl amide to inhibit 2,2′-azinodi-3-ethylbenzthiazoline sulphonate (ABTS) was kindly tested by Ms. Janpen Tangjitjaroenkun.

2.4.3 Cholinesterase activity assay [20-21]

The inhibition of cholinesterase activity of the isolated compounds from *M. oleifera* and seven synthesized benzamides was investigated using TLC. This assay was based on Ellman's method. The enzyme activity is measured by observing the increase of a yellow color produced from thiocholine. The principle of the reaction is shown in Scheme 2.1. Enzyme activity can be affected by other molecules. Inhibitiors

are naturally occurring or synthetic molecules that decrease enzyme activity. The inhibitor may interact with the enzyme and prevents any substrate molecules from reacting with the enzyme. The changes in color can be observed from light yellow to colorless.

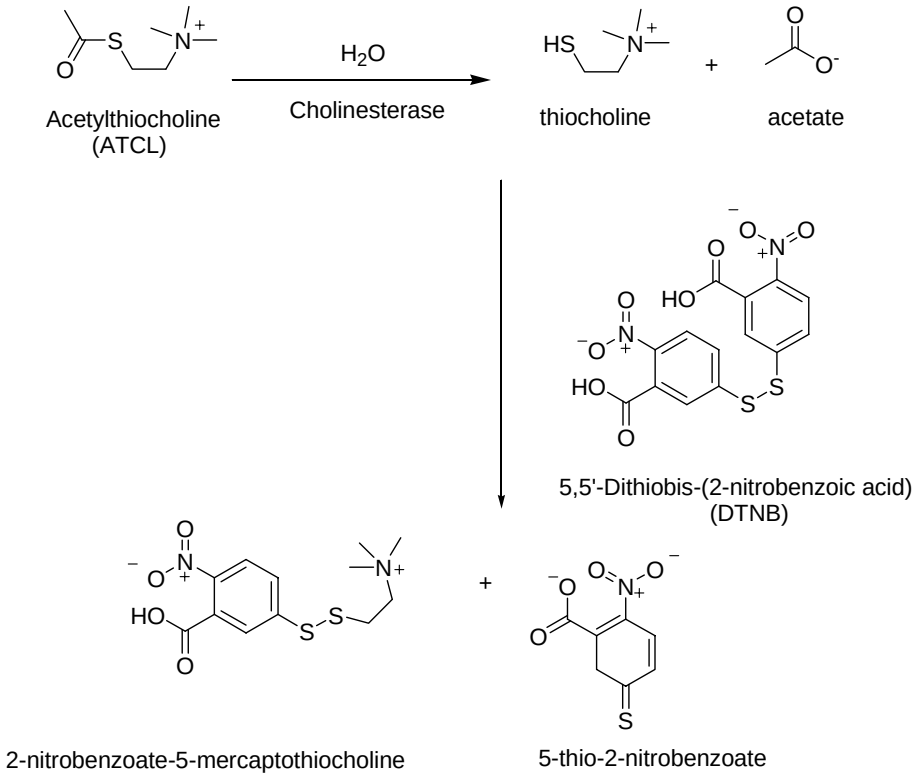

Scheme 2.1 Cholinesterase catalysed hydrolysis of acetylthiocholine and thiocholine reaction

TLC autographic assay

The samples were dissolved in an appropriate solvent to a concentration of 10 mg/mL for extract, 1 mg/mL for isolated compound (various concentrations: 1, 0.5, 0.25, 0.125, 0.0625 mg/mL) and standard compounds: galanthamine and eserine were obtained from Sigma (St.Louis, MO, USA). 10 µL of each sample was spotted on silica gel TLC plates and developed in a suitable solvent, dried for 1-2 h. After developing TLC plate, enzyme inhibitory activities of the developed spots were detected by spraying the substrate with DTNB/ATCL reagent until the silica was saturated with solvent. TLC was allowed to dry for 3-5 min and then 3 U/mL of enzyme solution was sprayed. A yellow background appeared with white spots for

inhibiting compounds becoming visible after 5 min. These were observed and recorded within 15 min because they would disappear after 20-30 min.

2.4.4 α-amylase inhibition

α-Amylase inhibition was assayed according to the method of Kanda [22]. The action of compounds and crude extracts of *M. oleifera* and *G. inodorum* to inhibit α-amylase was kindly tested by Dr. Sirichai adisakwattana.

2.5 Extraction procedure

2.5.1 Extraction of the roots of *M. oleifera*

The dried and minced roots of *M. oleifera* (4.5 kg) were extracted with CH_2Cl_2 using soxhlet. The extraction procedure was summarized as shown in Scheme 2.2.

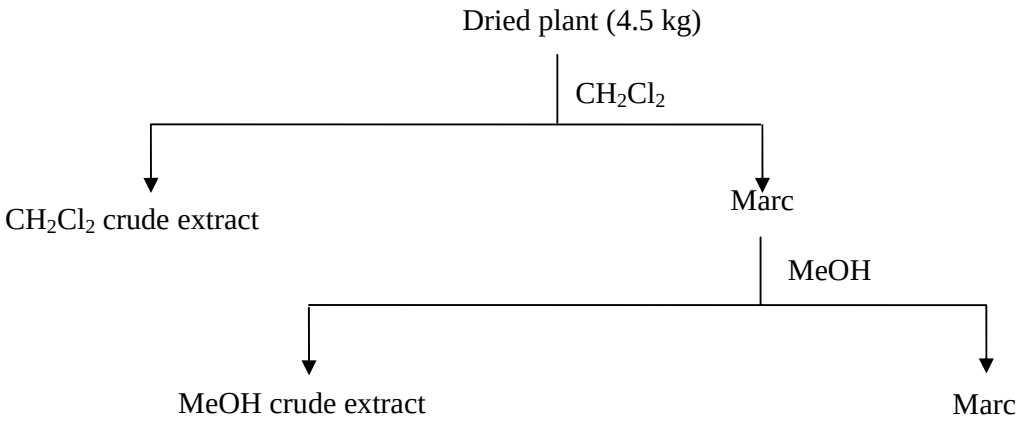

Scheme 2.2 The extraction procedure for the roots of *M. oleifera*

2.5.2 Extraction procedure of *G. inodorum*

The dried and minced whole plants of *G. inodorum* (4.5 kg) were extracted with CH_2Cl_2 by soxhlet. The marc was then similarly extracted with MeOH. The MeOH crude was further extracted by EtOAc for three times. The evaporation of solvent afforded the EtOAc extract. The marc was then partitioned with *n*-BuOH:H_2O, 1:1 (V/V) in a separatory funnel to gain *n*-BuOH soluble and water soluble parts. After separation of both *n*-BuOH soluble and water soluble parts, *n*-BuOH was removed to provide a dark greenish crude. Another part as H_2O layer, after the solvent was removed, a greenish crude was attained. The overview of general procedure for extraction is presented in Scheme 2.3.

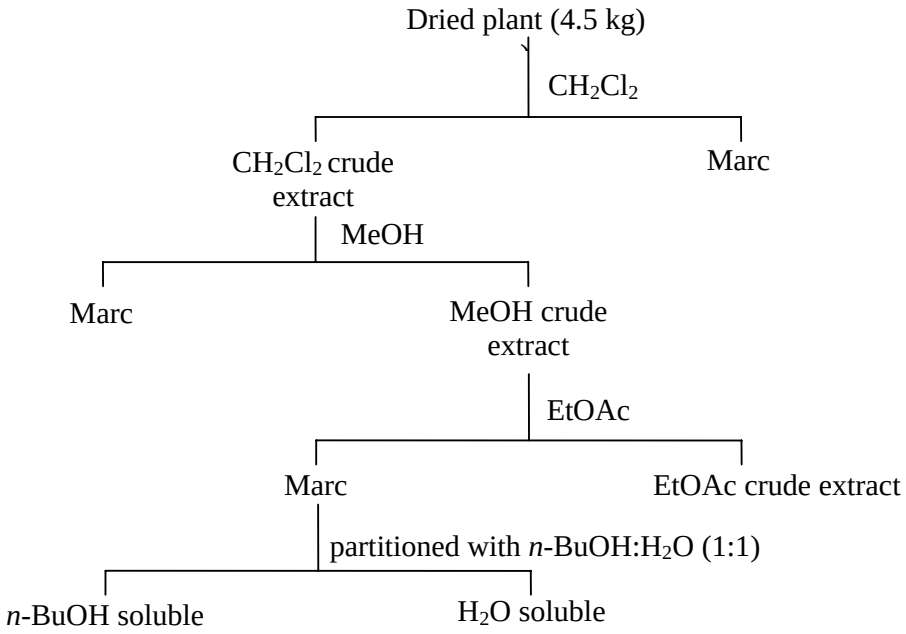

Scheme 2.3 The extraction procedure for the whole plant of *G. inodorum*

2.6 The synthesis of bezamides and esters

The synthesis of benzamides and esters was carried out using the reaction conditions described by Chaysripongkul [23].

2.6.1 General procedure

1 Equiv of carboxylic acid, 2 equiv of CCl_3CONH_2 and 2 equiv of PPh_3 were well mixed and refluxed in CH_2Cl_2 for 1 h. 1 Equiv of alcohol and 3 equiv of *4*-picoline were subsequently added under refluxing CH_2Cl_2 for 1 h for the preparation of ester. In case of the preparation of amide the second step was done at RT in CH_2Cl_2 for 30 min.

2.6.1.1 Synthesis of amides

***N*-(2-hydroxylphenyl)-5-methyl-*2E,4E*-pentadienoyl amide (**compound **A):** yellow soild (84% yield), R_f 0.50 (50% EtOAc/hexane). ^{1}H-NMR ($CDCl_3$) δ_H: 1.80 (3H, s, C*H*$_3$), 5.99-7.31 (4H, m, *H*C=C), 5.41, 6.80-7.10 (4H, Ar*H*). ^{13}C-NMR ($CDCl_3$) δ_C: 19.9, 119.0, 120.0, 122.0, 125.8, 126.0, 129.0, 145.0, 149.0 and 166.0.

***N*-(2-hydroxylphenyl)-5-(3,4-methylenedioxyphenyl)-*2E,4E*-pentadieneyl amide** (compound **B):** yellow soild (52% yield) R_f 0.48 (50% EtOAc/hexane). ^{1}H-NMR ($CDCl_3$) δ_H: 6.71-7.47 (4H, m, H-2, 4, 5 and 6, Ar*H*), 6.85-7.06 (4H, m,

*H*C=C), 6.94-7.41 (3H, m, H-2′′, 3′′ and 5′′, Ar*H*) and 6.06 (2H, s, C*H*$_2$). ^{13}C-NMR ($CDCl_3$) δ_C: 101.2, 111.5, 115.2, 116.1, 119.7, 121.7, 123, 123.4, 125.2, 127.4, 128.5, 131.2, 148, 148.7, 149.0 and 166.0.

***N*-(2-hydroxylphenyl)-3,4-methylenedioxycinnamoyl amide** (Compound **C**): yellow soild (95% yield), R_f 0.50 (50% EtOAc/hexane.) ^{1}H-NMR ($CDCl_3$) δ_H: 6.06 (2H, s, C*H*$_2$), 6.80-7.46 (2H, m, *H*C=C), 6.88-7.72 (4H, m, H-2,4, 5 and 6, Ar*H*), 6.88-7.20 (3H, m, H-2′′, 3′′ and 5′′, Ar*H*) a ^{13}C-NMR ($CDCl_3$) δ_C: 101.0, 106.0, 109.0, 116.0, 116.1, 119.0, 121.0, 122.0, 125.0, 128.0, 141.0, 148.0, 148.7 and 165.0.

***N*-(2-hydroxylphenyl)-piperonyl amide** (Compound **D)**: [24] yellow soil (84% yield), R_f 0.52 (50% EtOAc/hexane.) ^{1}H-NMR ($CDCl_3$) δ_H: 7.61 (1H, s, H-2′′, Ar*H*), 7.49 (1H, d, *J*=7.12 Hz, H-3′′, Ar*H*), 7.17 (1H, d, *J*=7.19 Hz, H-5′′, Ar*H*), 7.47 (1H, d, *J*=7.05 Hz, H-2, Ar*H*), 6.98 (1H, d, *J*=7.19 Hz, H-4, Ar*H*), 7.30 (1H, d, *J*=7.19 Hz, H-6, Ar*H*), 6.71 (1H, d, *J*=7.91 Hz, H-5, Ar*H*) and 6.06 (2H, s, C*H*$_2$.) ^{13}C-NMR ($CDCl_3$) δ_C: 101.0, 116.0, 119.0, 121.0, 123.0, 125.0, 127.0, 148.9, 149.0 and 164.7.

***N,N*-Diethylbenzamide** (Compound **E):** [25-26], yellow liquid (95% yield), R_f 0.58 (50% EtOAc/hexane). ^{1}H-NMR ($CDCl_3$) δ_H: 1.10 (3H, br s, CH_2CH_3), 1.25 (3H, br s, CH_2CH_3), 3.26 (2H, br s, CH_2CH_3), 3.55 (2H, br s, CH_2CH_3) and 7.38 (5H, br s, Ar*H*). ^{13}C-NMR ($CDCl_3$) δ_C: 12.8, 41.5, 127.2, 128.6, 129.6, 135.2 and 168.6.

***N*-(*sec*-butyl)-5-(3,4-methylenedioxyphenyl)-*2E,4E*-pentadieneylamide** (Compound **F):** white solid (77% yield), R_f 0.64 (77% EtOAc/hexane). ^{1}H-NMR ($CDCl_3$) δ_H: 7.38 (1H, t, *J*=14.8 Hz, =C*H*-), 7.02 (1H, s, Ar*H*), 6.92 (1H, d, *J*= 8.0 Hz, Ar*H*), 6.82-6.70 (3H, m, =C*H*-), 6.00 (2H, s, -C*H*$_2$-), 5.85 (1H, d, *J*= 14.9 Hz, =C*H*-), 5.28 (1H, d, *J*= 8.2 Hz, -N*H*-), 4.02 (1H, m, -CH-), 1.54 (m, 2H, -CH_2-), 1.20 (3H, d, *J*= 6.53 Hz, -C*H*$_3$) and 0.92 (3H, t, *J*= 7.37 Hz, C*H*$_3$) (^{13}C-NMR ($CDCl_3$) δ_C: 10.3, 20.5, 29.8, 46.7, 101.0, 105.0, 108.0, 123.0, 123.8, 128.2, 130.8, 140.8, 148.0 and 165.0.

***N*-(cyclohexyl)-5-(3,4-methylenedioxyphenyl)-*2E,4E*-pentadieneylamide** (Compound **G):** yellow solid (61% yield), R_f 0.54 (50% EtOAc/hexane). ^{1}H-NMR ($CDCl_3$) δ_H: 7.38 (m, 1H, =CH-), 7.00 (s, 1H, Ar*H*), 6.92 (d, *J*=8.1 Hz, 1H, Ar*H*), 6.80-6.60 (m,3H, Ar*H* and =C*H*-), 6.01(s, 2H, -C*H*$_2$-), 5.90 (d, *J*=14.8 Hz, 1H, =C*H*-), 5.40 (d, *J*=6.9 Hz, 1H, N*H*), 1.95 (m, 2H, -C*H*$_2$-), 1.63 (m, 2H, -C*H*$_2$-), 1.40 (m, 4H, C*H*$_2$-) and 1.16 (m, 2H, -C*H*$_2$-). ^{13}C-NMR ($CDCl_3$) δ_C: 24.9, 25.6, 33.3, 48.2, 101.3, 105.7, 108.5, 122.5, 123.5, 124.7, 130.7, 140.8, 148.2 and 165.1.

***N*-(*tert*-butyl)-5-(3,4-methylenedioxyphenyl)-*2E,4E*-pentadieneylamide** (Compound **H**)**:** greenless solid (96% yield), R_f 0.53 (50% EtOAc/hexane). ^{1}H-NMR ($CDCl_3$) δ_C: 7.34 (m, =C*H*-), 7.01 (s, 1H, Ar*H*), 6.90 (d, *J*=7.9Hz, 1H, Ar*H*), 6.81 (d, *J*=7.9 Hz, 1H, Ar*H*), 6.70 (m, 2H, =C*H*-), 6.01 (s, 2H, -CH_2-), 5.89 (d, *J*=14.51 Hz, 1H, =C*H*-), 5.40 (s, 1H, N*H*) and 1.44 (s, 9H, -CH_3) ^{13}C-NMR ($CDCl_3$) δ_C: 28.9, 51.4, 101.3, 105.7, 108.4, 122.5, 124.4, 124.6, 130.5, 140.3, 148.1, 148.2 and 165.4.

2.6.1.2 Synthesis of ester compounds

Piperic acid 2-acetoxy-phenyl-ester (Compound **I)**: yellowless soild (60% yield), R_f 0.65 (50% EtOAc/hexane**).** ^{1}H-NMR ($CDCl_3$) δ_H: : 6.71-7.47 (4H, m, H-2, 4, 5 and 6, Ar*H*), 6.83-7.76 (8H, m, *H*C=C), 6.65-7.06 (6H, m, H-2′′, 3′′ and 5′′, Ar*H*) and 6.06 (4H, s, CH_2). ^{13}C-NMR ($CDCl_3$) δ_C: 101.2, 108.0, 114.8, 115.2, 119.4, 126.0x4, 128, 128.8x2, 132.7, 146.1x2, 148.0x4, 148.7x2 and 166.0.

Cinnamic acid 2-acetoxy-phenyl-ester (Compound **J)**: yellow soild (75% yield), R_f 0.61 (50% EtOAc/hexane) ^{1}H-NMR ($CDCl_3$) δ_H: 7.29-7.30 (4H, m, H-2,4, 5 and 6, Ar*H*), 6.40-7.70 (4H, m, *H*C=C), 6.41-7.00 (6H, m, H-2′′, 3′′ and 5′′, Ar*H*) and 6.06 (4H, s, CH_2). ^{13}C-NMR ($CDCl_3$) δ_C: 101.0, 106.0x2, 109.0x2, 114.0, 115.0x2, 122.0, 126.0, 128.0x2, 146.1, 148x4, 150x2, and 164.0.

Cholesteryl benzoate (Compound **K**) **:** white solid (81%), R_f 0.81 (50% EtOAc/hexane). ^{1}H-NMR ($CDCl_3$) δ_H: 0.69 (3H, s, CH_3), 0.87 (6H ,d, *J*= 6.80 Hz, (CH_3)$_2$CH), 0.92-2.04 (30H, m, alkyl group), 2.46 (2H, d, *J*= 7.60 Hz, CCH_2), 4.86 (1H, m, C*H*O), 5.41 (1H, d, *J*= 4.40 Hz, *H*C=C), 7.43 (2H, t, *J*= 7.20 Hz, *m*-Ar*H*), 7.54 (1H, t, *J*= 7.20 Hz, *p*-Ar*H*) and 8.03 (2H, d, *J*= 7.20 Hz, *o*-Ar*H*). ^{13}C-NMR ($CDCl_3$) δ_C: 11.9, 18.7, 19.4, 21.0, 22.6, 22.8, 23.8, 24.3, 27.9, 28.0, 28.2, 31.8, 31.9, 35.8, 36.2, 36.6, 37.0, 38.2, 39.5, 39.7, 42.3, 50.0, 56.1, 56.7, 74.6, 122.8, 128.2, 129.5, 130.8, 132.7, 139.6 and 165.9.

***β*-sitosteryl benzoate (**Compound **L**)**:** white solid (85%), R_f 0.81 (50% EtOAc/hexane). ^{1}H-NMR ($CDCl_3$) δ_H: 0.69 (3H, s, CH_3), 0.87 (6H, d, *J*= 6.80 Hz, (CH_3)$_2$CH), 0.92-2.04 (30H, m, alkyl group), 2.46 (2H, d, *J*= 7.60 Hz, CCH_2), 4.86 (1H, m, C*H*O), 5.41 (1H, d, *J*= 4.40 Hz, *H*C=C), 7.43 (2H, t, *J*= 7.20 Hz, *m*-Ar*H*), 7.54 (1H, t, *J*= 7.20 Hz, *p*-Ar*H*) and 8.03 (2H, d, *J*= 7.20 Hz, *o*-Ar*H*). ^{13}C-NMR ($CDCl_3$) δ_C: 11.9, 12.1, 18.7, 19.4, 21.0, 22.6, 22.8, 23.8, 24.3, 25.0, 27.9, 28.0, 28.2,

31.8, 31.9, 35.8, 36.2, 36.6, 37.0, 38.2, 39.5, 42.3, 45.8, 50.0, 56.1, 56.7, 74.6, 122.8, 128.2, 129.5, 130.8, 132.7, 139.6 and 165.9.

CHAPTER III

RESULTS AND DISCUSSION

3.1 Extraction of selected plants

The whole plants of *G. inodorum* accumulated for preliminarily biological screening testwere extracted with CH_2Cl_2 and MeOH by Soxhlet. The general extraction is shown in scheme 3.1.

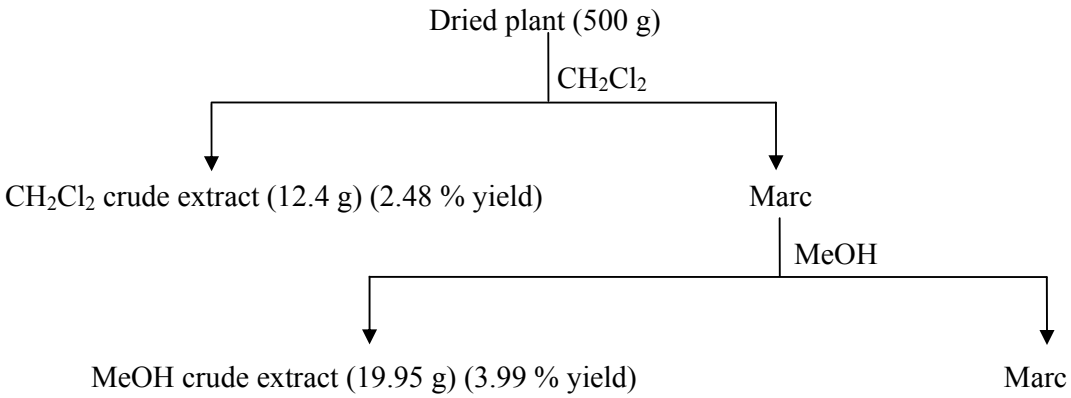

Scheme 3.1 Extraction procedure for preliminary screening test

3.2 Results of preliminary antioxidant activity of *G. inodorum*

3.2.1 Antioxidant activity

The CH_2Cl_2 and MeOH extracts of *G. inodorum* were preliminarily screened for radical scavenging effect on DPPH radical by TLC autographic assay. The results are demonstrated in Table 3.1

Table 3.1 The antioxidant activity of crude extracts of *G. inodorum*

Crude extract	Radical savenging effection DPPH
CH_2Cl_2	+
MeOH	+++

Note : + positive results observed within 10 min,
++ positive results observed within 5 min
+++ positive immediately

The MeOH extract of *G. inodorum* revealed a white spot on TLC plate immediately, whereas the observation of the white spot could be visualized within 10 min in the case of the CH_2Cl_2 extract. Therefore, both extracts were selected for further study.

3.3 Extraction of *M. oleifera*

The stems, old seeds, young seeds, leaves and roots of *M. oleifera* were separately collected and dried. The dried crushes of each part were extracted with CH_2Cl_2 and MeOH by Soxhlet. The results of extraction are tabulated in Table 3.2.

Table 3.2 The results of the extraction of various parts of *M oleifera*

Part	Weight of dried plant (g)	Percentage yield	
		CH_2Cl_2 extract	MeOH extract
Young seed	247	6.64	22.68
Old seed	198	5.75	8.45
Stem	86	1.12	7.90
Leaves	250	6.20	17.97
Root	250	2.20	16.60

3.4 Results of preliminary antioxidant activity of *M.oleifera*

3.4.1 Antioxidant activity

The CH_2Cl_2 and MeOH of various parts of *M. oleifera* were preliminarily screened for radical scavenging effect on DPPH radical by TLC autographic assay. The results are demonstrated in Table 3.3.

Table 3.3 The results of antioxidant activity screening test of *M. oleifera* extract

part	Radical savenging effect on DPPH	
	CH_2Cl_2 extract	**MeOH extract**
Young Seed	++	++
Old Seed	++	++
Leaves	+++	+++
Stem	++	+++
Root	++	+++

Note : + positive results observed within 10 min

++ positive results observed within 5 min

+++ positive immediately

From these preliminary antioxidant activity results, the MeOH extracts of the leaves, stem and root and the CH_2Cl_2 of the leaves exhibited the highest level of antioxidant activity while the ability of the scavenging of free radial of the CH_2Cl_2 and MeOH extracts of young and old seeds, stem and root also showed good activity.

Part I: Chemical constituents and biological activities of *G. inodorum*

3.5 α-Amylase inhibitors of *G. inodorum*

n-BuOH crude extract was tested for α-Amylase inhibition. The result of α-amylase inhibition was displayed in Table 3.4.

Table 3.4 Biological activity screening test result of *n*-BuOH crude extract

Plant	Crude extract	% inhibition α-Amylase
G. Inodorum	*n*-BuOH	43.34

The *n*-BuOH crude extract was preliminary tested the α-amylase inhibition. This extract showed moderate activity.

3.6 Results of extraction of *G. inodorum*

General procedure for extraction

The dried whole plants of *G. inodorum* (4.5 kg) were collected from Changmai province in June 2006, and extracted with CH_2Cl_2 and MeOH, respectively by soxhlet apparatus as outlined in Scheme 3.2.

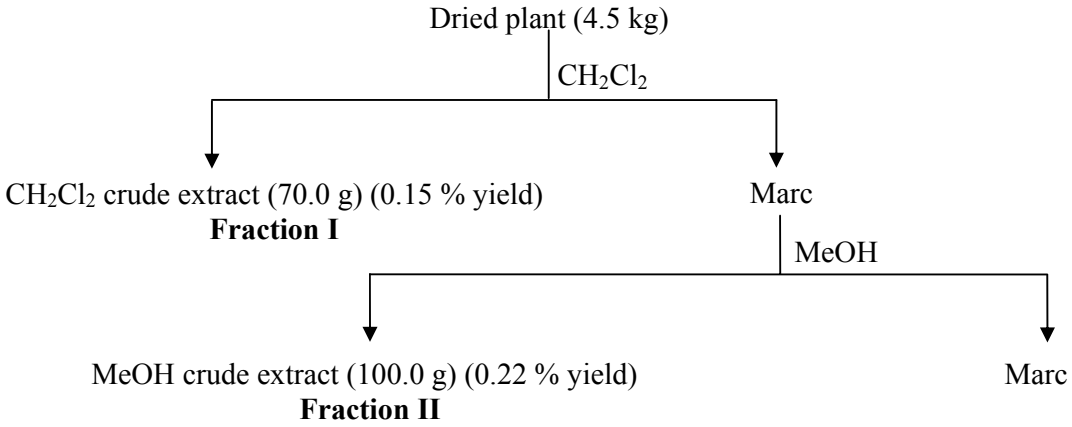

Scheme 3.2 The results of the extraction of *G. inodorum*

3.7 Separation of the CH_2Cl_2 extract (Fraction I)

The CH_2Cl_2 extract (Fraction I)**,** 70 g as dark brown material was subjected to silica gel quick column using gradient solvent starting from hexane and increased polarity by mixing with EtOAc and MeOH. The fractions were collected and combined according to the TLC results to obtain three sub-fractions, **GIC1-GIC3** (Scheme 3.3). The results are summarized as presented in Table 3.5.

Table 3.5 The results of the separation of Fraction I

Fraction	Solvent system	Remarks	Weight(g)
GIC1	100%hexane-10% EtOAc/hexane	Brownish solid	6.03
GIC2	10-15% EtOAc/hexane	Brownish solid	8.57
GIC3	20%EtOAc/hexane-50%EtOAc/MeOH	Brownish solid	42.54

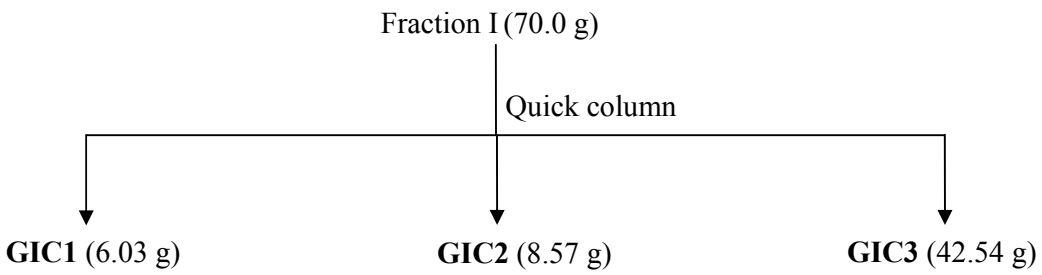

Scheme 3.3 The results of the separation of Fraction I

Sub-fractions **GIC1-GIC3** were re-separated on silica gel column using step gradients of hexane-EtOAc and EtOAc-MeOH.

3.8 Separation of sub-fraction GIC1

Sub-fraction **GIC1** 5.0 g was re-separated by silica gel column eluting with 100%hexane-20%MeOH/EtOAc. The results of the separation of sub-fraction **GIC1** are shown in Table 3.6.

Table 3.6 The results of the separation of sub-fraction **GIC1**

Fraction	Solvent system	Remarks	Weight(g)
GICC1	100%hexane-15%EtOAc/hexane	orange solid	1.79
GICC2	15-30%EtOAc/hexane	green brown solid	0.77
GICC3	30-50%EtOAc/hexane	dark brown syrup + substance **1**	0.72
GICC4	50-70%EtOAc/hexane	dark brown syrup	0.76
GICC5	70%EtOAc/hexane-20%MeOH/EtOAc	dark brown syrup	1.03

3.8.1 Structural elucidation of substance 1

Substance **1** was obtained as bright white plate (21.5 mg, 0.055% w/w of Fraction I) with R_f 0.80 (40% EtOAc/hexane), m.p. 51-53°C. This substance was soluble in $CHCl_3$, CH_2Cl_2 and EtOAc. According to the ^{1}H-NMR spectrum (Fig 3.1), a high intensity signal at δ_H 1.27 suggesting the presence of several interlinking of methylene groups in the molecule. The signal of the methylene group connecting to a hydroxyl group was detected at δ_H 3.50. The signal of a methyl group exhibited a high intensity signal at δ_H 0.89. It was thus considered that this substance contained a

hydroxyl group. This postulation was confirmed by the ^{13}C-NMR spectrum (Fig 3.2) which displayed a significant signal at δ_C 63.11 of –COH-. The structure of substance **1** was clarified as a long chain alcohol.

$$H_3C-(CH_2)_n-CH_2\cdot OH$$

Substance 1

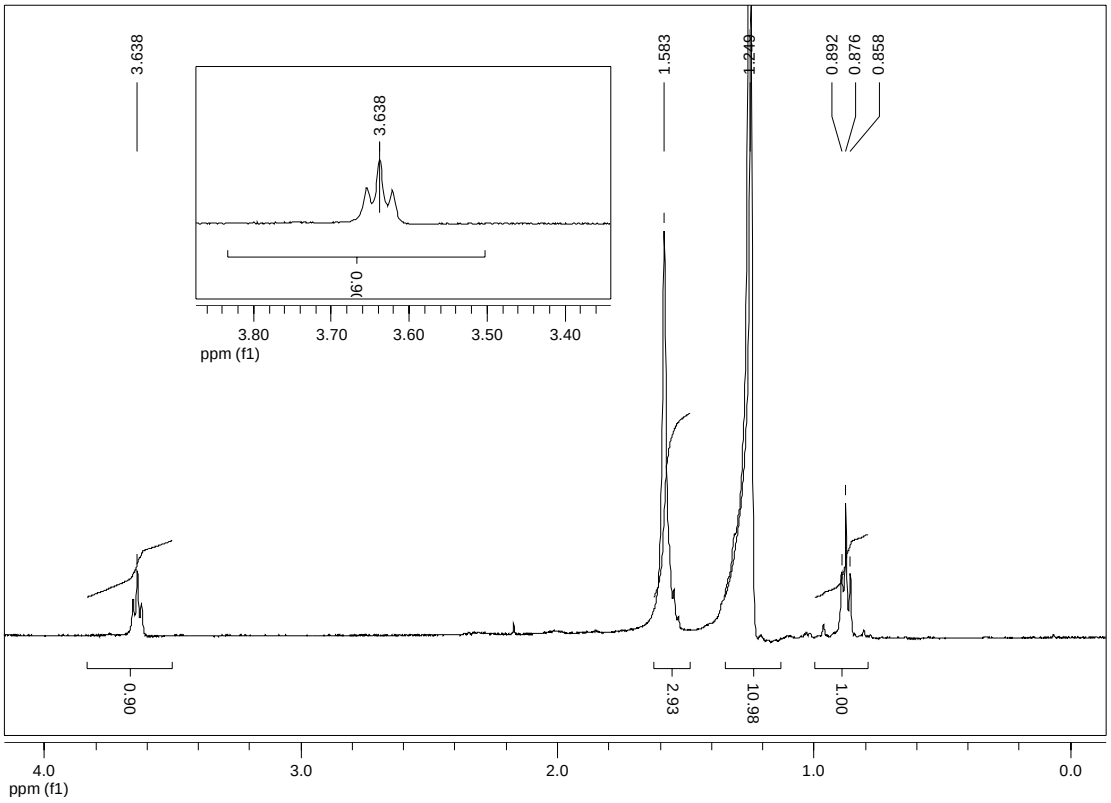

Figure 3.1 The ^{1}H-NMR spectrum of substance **1**

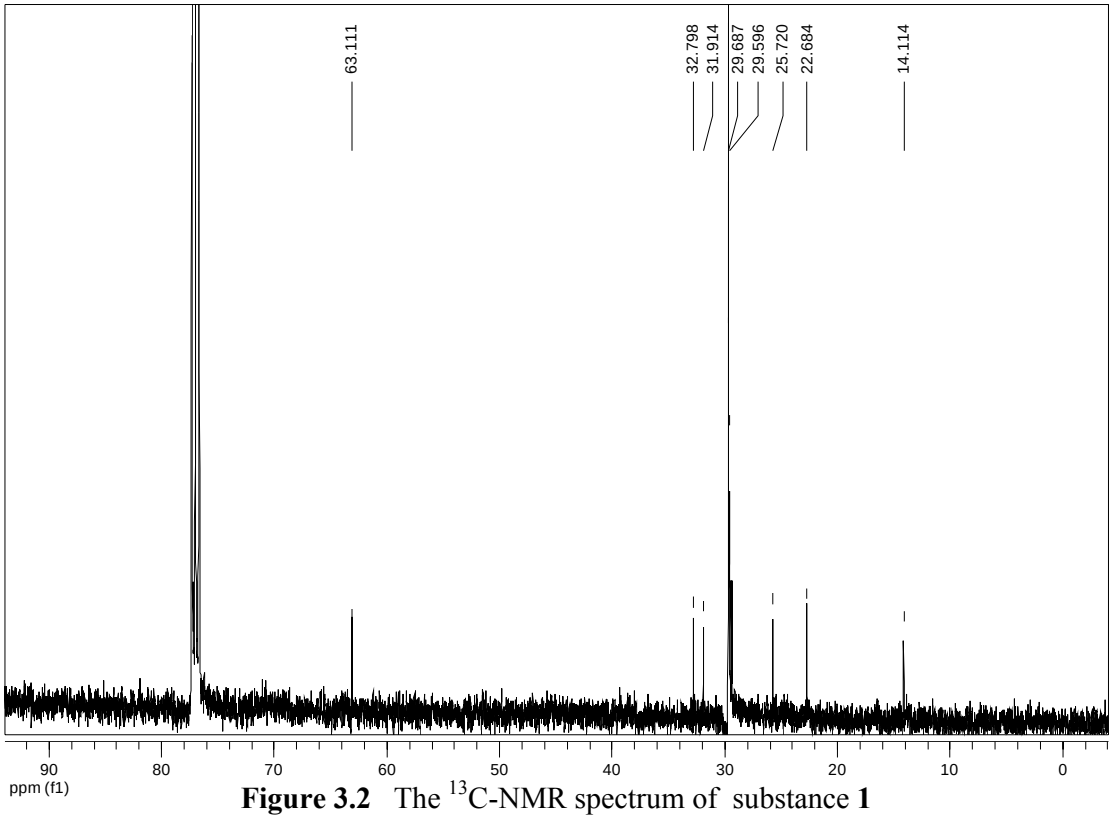

Figure 3.2 The ^{13}C-NMR spectrum of substance **1**

3.9 Separation of sub-fraction GICC4

Sub-fraction **GICC4** 0.76 g was re-separated by silica gel column eluting with 100% hexane-40%EtOAc-hexane. The results of the separation of sub-fraction **GICC 4** was shown in Table 3.7.

Table 3.7 The results of the separation of sub-fraction **GICC4**

Fraction	Solvent system	Remarks	Weight (g)
GICC41	100%hexane 15%EtOAc/hexane	Orange soild + substance **2**	0.41
GICC42	20-40%EtOAc/hexane	Green brown soild + mixture **3**	0.11

3.9.1 Structural elucidation of substance 2

Substance **2** was obtained as white powder solid (55.6 mg, 0.0794% w/w of Fraction I) with m.p. 79-80°C and R_f 0.74 (40% EtOAc/hexane). This substance was soluble in $CHCl_3$, CH_2Cl_2 and EtOAc. Concerning with the ^{1}H-NMR spectrum (Fig 3.3), it exhibited a high intensity signal at δ_H 1.25 suggesting several interlinking of

methylene groups in the molecule. The signal of the methylene groups connecting to a carbonyl group was detected at δ_H 2.34. The signal of a methyl group was detected at δ_H 0.87. This postulation was also confirmed by the ^{13}C-NMR spectrum (Fig 3.4) which displayed a significant signal at δ_C 179.6 of a carbonyl carbon of ketone group. These results comfirmed truly that substance **2** was a long chain ketone.

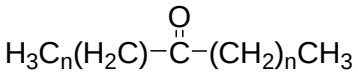

Substance 2

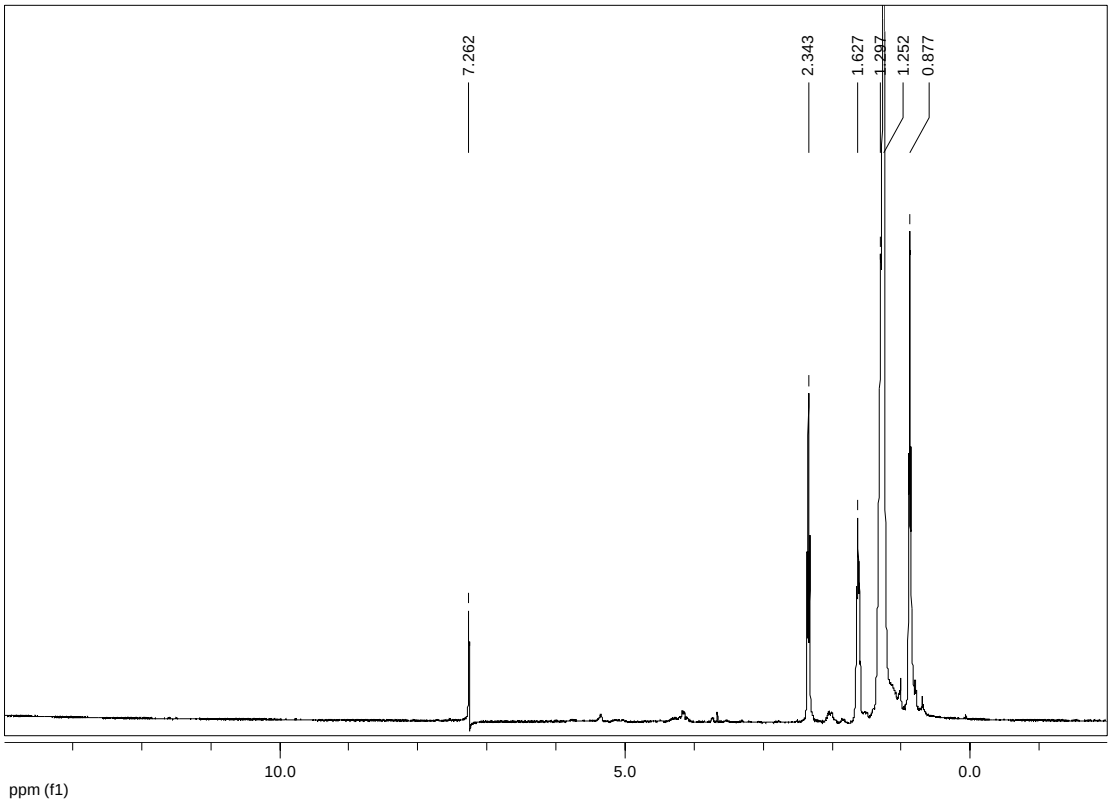

Figure 3.3 The ^{1}H-NMR spectrum of substance **2**

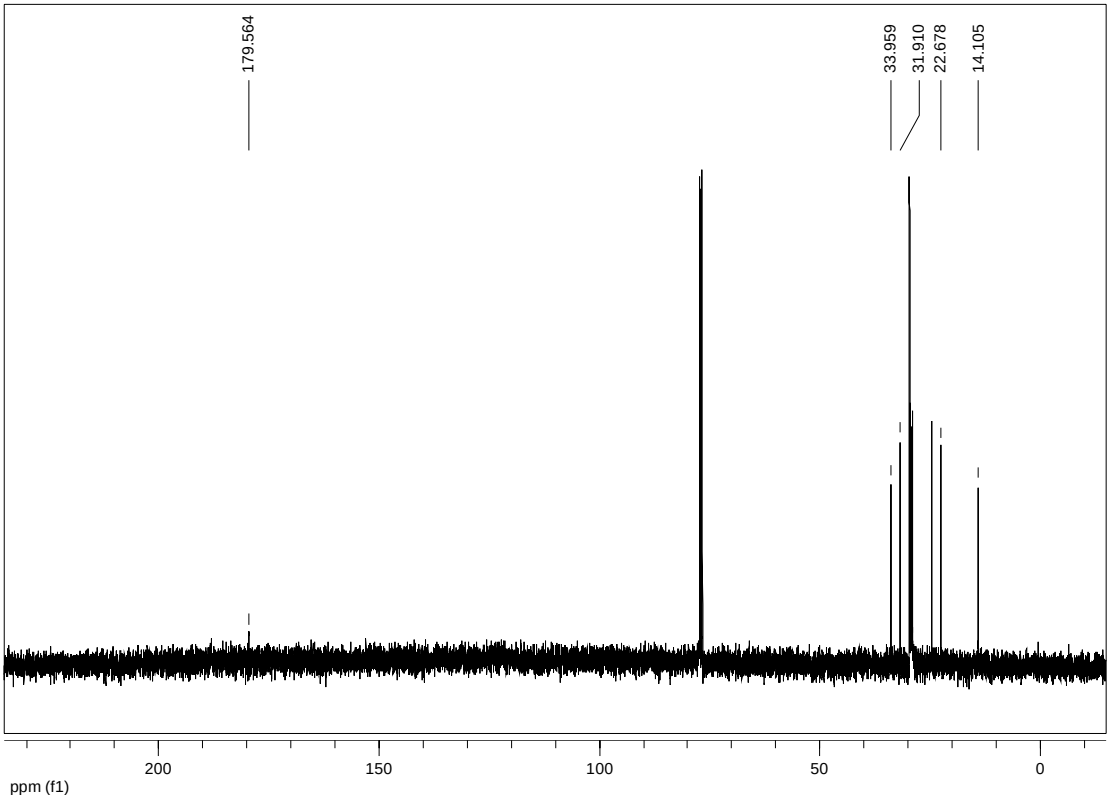

Figure 3.4 The ^{13}C-NMR spectrum of substance **2**

3.9.2 Strutural elucidation of mixture 3

Mixture **3** was obtained as white powder solid (1.70 mg, 0.00242% w/w of Fracton I) with m.p.131.1-143.4°C and R_f 0.47 (40% EtOAc/hexane). This soild was soluble in $CHCl_3$, CH_2Cl_2 and EtOAc. It could not be detected on TLC under UV, but could be detected with 10% H_2SO_4 in MeOH indicating that there was no conjugated double bond in this molecule.

According to the spectroscopic data, the ^{1}H-NMR spectrum of substance (Fig 3.5) exhibited a significant signal at δ_H 0.68-2.35(m) of methylene and methyl groups. The signals of three olefinic protons were detected at δ_H 5.04-5.02 (m), 5.12-5.18 (m) and 5.35 (m). The signal belonging to the proton connecting to a hydroxyl group was detected at δ_H 3.40. From this spectroscopic data, it could be assumed that this substance may be a steroid. However, the steroids in nature contained a mixture of steroids with similar polarity. For this reason provided the obtained mixture **3** inclined to be a steroid mixture of β-sitosterol or stigmasterol [27]. To investigate this remark, this substance was then analyzed its purity by GC. The GC chromatogram

(Fig 3.6) showed three peaks at R_t 16.34, 16.71 and 17.42 min. Compared with a standard mixture, the component could be analyzed as β-sitosterol (25%), campesterol (24%) and stigmasterol (51%), respectively. According to the obtained results, it could be noticably concluded that this mixture contained stigmasterol as a major component mixed with β-sitosterol and campesterol.

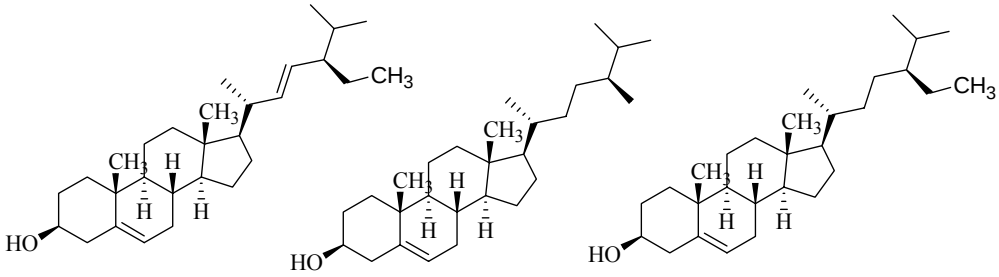

Stigmasterol Campesterol β-sitosterol

Mixture 3

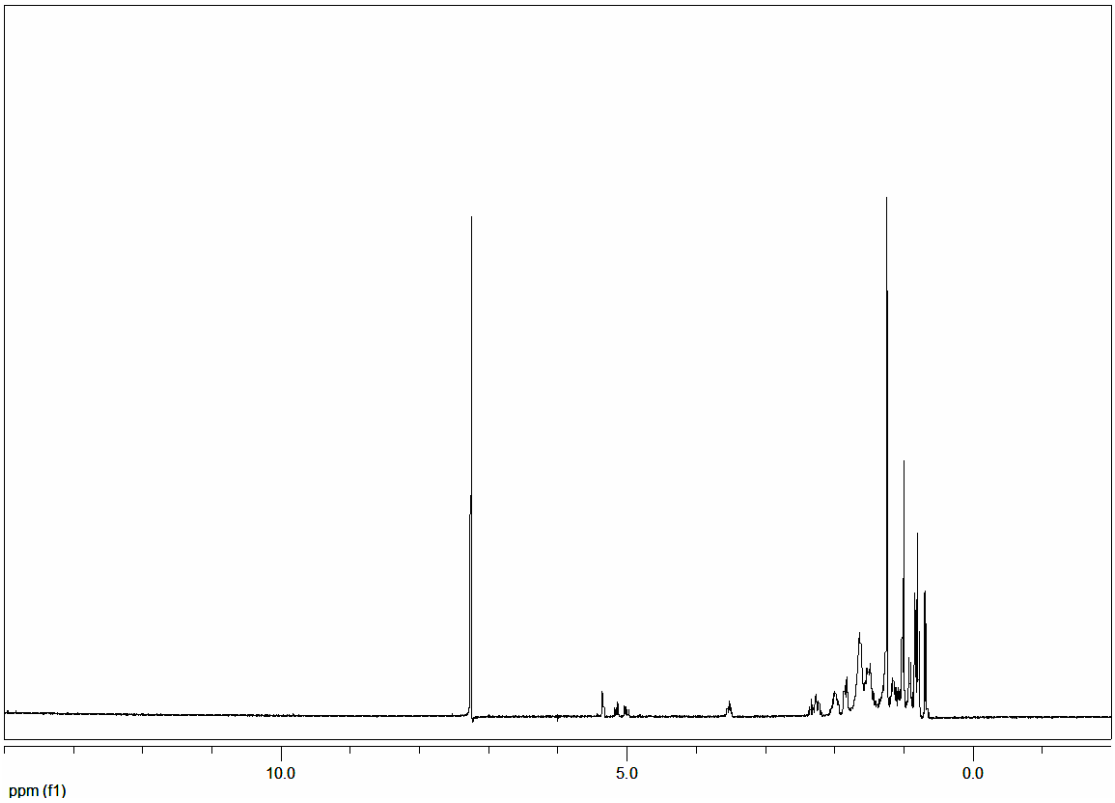

Figure 3.5 The ^{1}H-NMR spectrum of mixture **3**

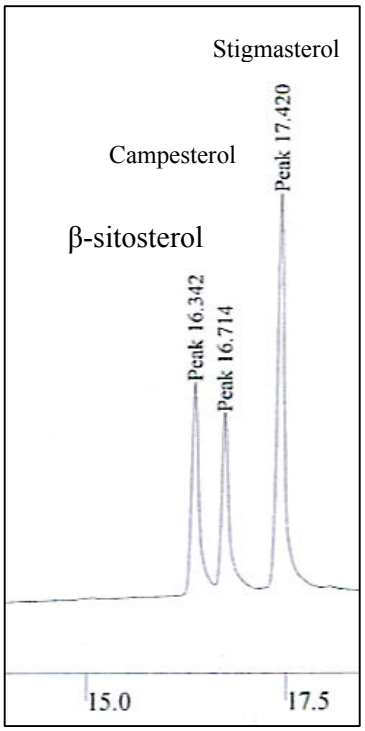

Figure 3.6 The GC chomatogram of mixture **3**

3.10 Separation of the MeOH extract (Fraction II)

From the general extraction scheme (Scheme 3.2), the marc was further extracted with MeOH by soxhlet apparatus. The MeOH extract (Fraction II) was evaporated yielding 100 g of crude extract. The concentrated 100 g of Fraction II was then extracted by EtOAc for three times. The evaporation of the solvent afforded the EtOAc extract (Fraction III). The EtOAc extract was then partitioned with *n*-BuOH:H_2O 1:1(V/V) in a separatory funnel to gain *n*-BuOH soluble and water soluble parts. After evaporating *n*-BuOH, a dark greenish crude designated as Fraction IV 50 g was obtained. Another part, the aqueous layer was achieved as a greenish crude (Fraction V) 10 g after removal of water. The overview of the general procedure for the extraction of Fraction II is presented in Scheme 3.4.

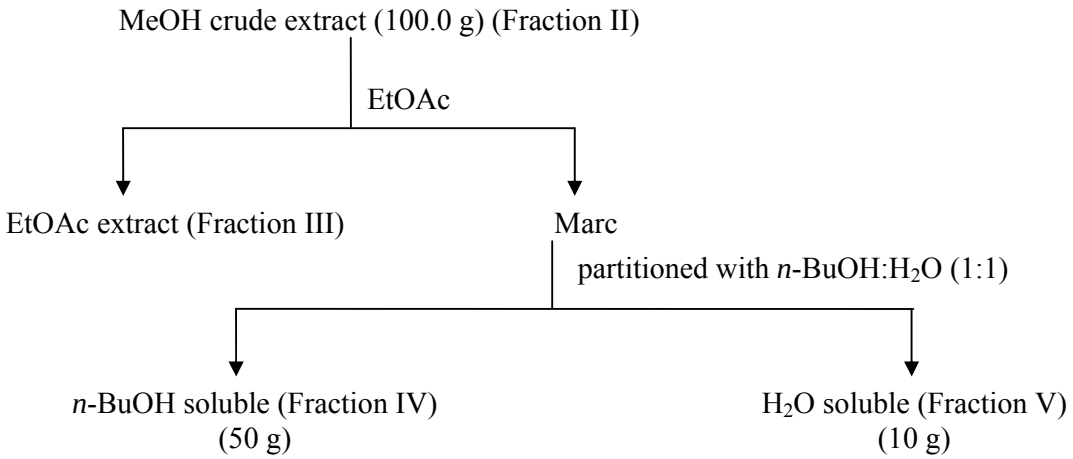

Scheme 3.4 The results of the further extraction of Fraction II

3.11 Separation of the *n*-BuOH extract (Fraction IV)

The *n*-butanol extract (70.0 g) (Fraction IV) was chromatographed on dianion column to separate into small fractions according to their polarity, using gradient eluent started from 100%H_2O followed by a mixture of H_2O/MeOH, MeOH/acetone and 100%acetone, respectively. The eluted solution was collected approximately 2L each. Monitoring each fraction by TLC, the fractions that demonstrated similar features were combined. The results of the separation of Fraction IV and the scavenging effects on DPPH radicals of separated fractions are shown in Table 3.8.

Table 3.8 The separation of Fraction IV and the scavenging effects on DPPH radicals of separated fractions.

Fraction	Solvent system	Remarks	Weight (g)	Scavenging effects on DPPH radicals
GGM1	25%MeOH/DI	Brown syrup	4.66	++
GGM2	50%MeOH/DI	Brown syrup	8.05	++
GGM3	75%MeOH/DI	Brown syrup	6.36	+
GGM4	100%MeOH	Brown syrup	10.03	++
GGM5	100%MeOH	Brown syrup	15.23	+++
GGM6	100%MeOH	Brown syrup	6.03	+++
GGM7	25%Acetone/MeOH	Brown syrup	11.02	++
GGM8	50%Acetone/MeOH	Brown syrup	6.06	++

Note : + positive results within 10 min
++ positive results within 5 min
+++ positive immediately

Sub-fractions **GGM5** and **GGM6** showded good activity on the scavenging effects on DPPH radicals. These inhibitory effect results are used as a guide to select the active fractions for further fractionation.

3.12 Separation of sub-fraction GGM5

Sub-fraction **GGM5** as brown syrup, 15.23 g was obtained from the separation of Fraction IV by dianion column. This fraction was re-chromatographed on Sephedex LH-20 system: 100%MeOH. The eluted solution was collected approximately 8 mL for each fraction. Each eluted portion was monitored by TLC and the equivalent ones were combined. The results of the separation of sub-fraction **GGM5** and the scavenging effects on DPPH radicals of the separated fractions are presented in Table 3.9.

Table 3.9 The separation of sub-fraction **GGM5**

Fraction	Remarks	Weight (g)	Scavenging Effects on DPPH radicals
GGM51	Yellow semi solid	2.58	+
GGM52	Yellow solid	2.36	_
GGM53	Yellow semi solid	1.25	++
GGM54	Yellow semi solid	1.25	+
GGM55	Yellow solid	2.56	+
GGM56	Yellow solid	0.84	+
GGM57	White solid + compound **4**	2.85	+++

Sub-fraction **GGM57** revealed good activity on the scavenging effects on DPPH radicals. This sub-fraction was thus purified by crystallizion using MeOH to obtain compound **4**.

3.12.1 Strutural elucidation of compound 4

Compound **4** (3.5 mg, 0.005%w/w of Fraction I) was obtained from the separation of sub-fraction **GGM5** by eluting with 100%MeOH using Sephedex L-20 column, m.p. 203-206 °C, R_f 0.75 ($MeOH/H_2O$ 4:1). Compound **4** gave a violet color to Liebermann-Burchard′ reagent indicating the presence of triterpenoidal skeleton.

The IR spectrum of compound **4** (Fig 3.7) revealed a very broad absorption band at 3400 cm^{-1} due to the –OH stretching vibration of alcohol. Other characteristic absorption peaks were observed at 1608 cm^{-1} for C=C stretching vibration and two sharp peaks at 1183 and 1111 for C-O stretching vibration, 2939-2858 cm^{-1} (C-H stretching of CH_2,CH_3) and 620 cm^{-1} (C-H stretching of β-sugar).

The ^{1}H-NMR spectrum (DMSO-d_6) (Fig 3.8) showed the signals in the range of δ_H 0.53-2.39 which were the signals of CH_3, CH_2 and CH groups. The multiplet signals at δ_H 2.85-3.15 could be assigned to the protons of a sugar moiety. The proton on the carbon attached to a hydroxyl group appeared as the multiplet signal at δ_H 3.53 and the signal at δ_H 4.20 belonged to the anomeric proton. The multiplet signal at δ_H 5.30 was the proton of trisubstituted vinyl group (-CH=C-).

The ^{13}C-NMR spectrum (DMSO-d_6) (Fig 3.9) revealed a group of five carbon signals resonated at δ_C 72.0, 75.8, 76.6, 77.4 and 106.0 [17] as presented in Table

3.10. The signal of trisubstituted vinyl carbon was observed at δ_C 122.0 and 143.0. The presence of the carbon signal at δ_C 171.0 was belonged to a carbonyl carbon of carboxylic acid of glucose part. From the aforementioned data, it could conclude that this substance contained an aglycone connecting with a sugar and was additionally compared its identity with that of a known compound [17]. The structure of compound **4** was proved to be (3*β*,4*α*,16*β*)-16,23,28-trihydroxyolean-12-en-3-yl-*β*-D-glucopyranosiduroic acid.

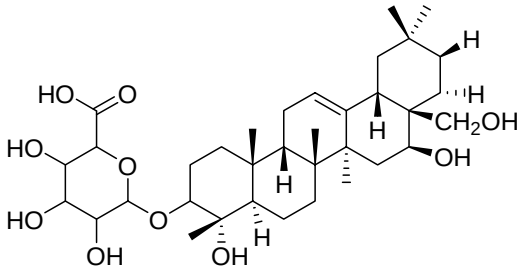

Compound 4

Table 3.10 The ^{13}C-NMR chemical shift assignment of compound **4** and (3β,4α,16β)-16,23,28 trihydro-xyolean-12-en-3-yl-β-D-glucopyranosiduroicacid)

Carbon	Chemical Shift (ppm)		Carbon	Chemical Shift (ppm)	
	Compound **4**	**Ref [17]**		Compound **4**	**Ref [17]**
C1	38.5	39.6	C29	33.5	33.7
C2	26.1	26.3	C30	24.1	24.3
C3	88.4	83.3	β-Glu		
C4	43.1	43.9	C1′	105.9	105.9
C5	46.7	48.1	C2′	75.7	75.2
C6	18.2	18.8	C3′	77.4	77.8
C7	33.6	33.3	C4′	72.0	73.2
C8	40.5	41.1	C5′	76.6	76.5
C9	46.7	48.2	C6	171.1	172.5
C10	36.5	37.5			
C11	24.1	24.7			
C12	122.1	123.9			
C13	143.7	144.3			
C14	43.3	44.7			
C15	36.5	36.7			
C16	65.4	67.9			
C17	40.5	41.6			
C18	46.6	45.1			
C19	46.7	47.9			
C20	30.9	31.7			
C21	33.5	34.8			
C22	27.9	26.1			
C23	64.9	64.8			
C24	15.7	13.4			
C25	16.8	16.6			
C26	18.1	17.4			
C27	27.9	27.5			
C28	64.9	69.1			

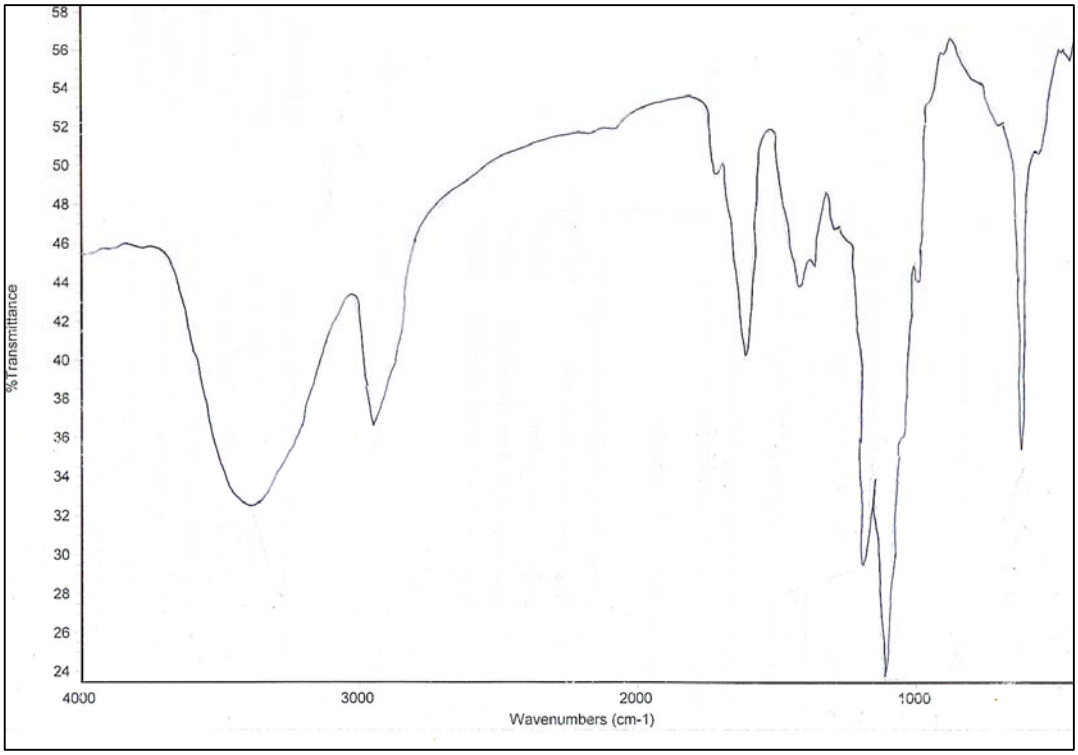

Figure 3.7 The IR spectrum of compound **4**

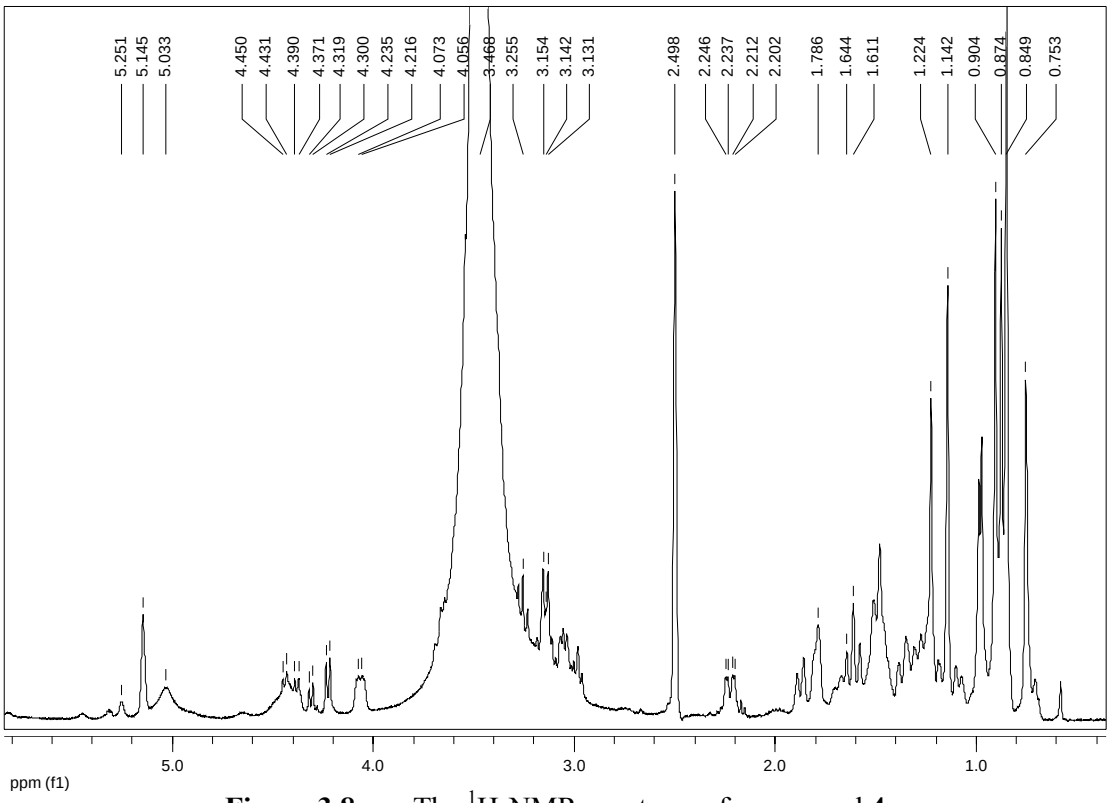

Figure 3.8 The ^{1}H-NMR spectrum of compound **4**

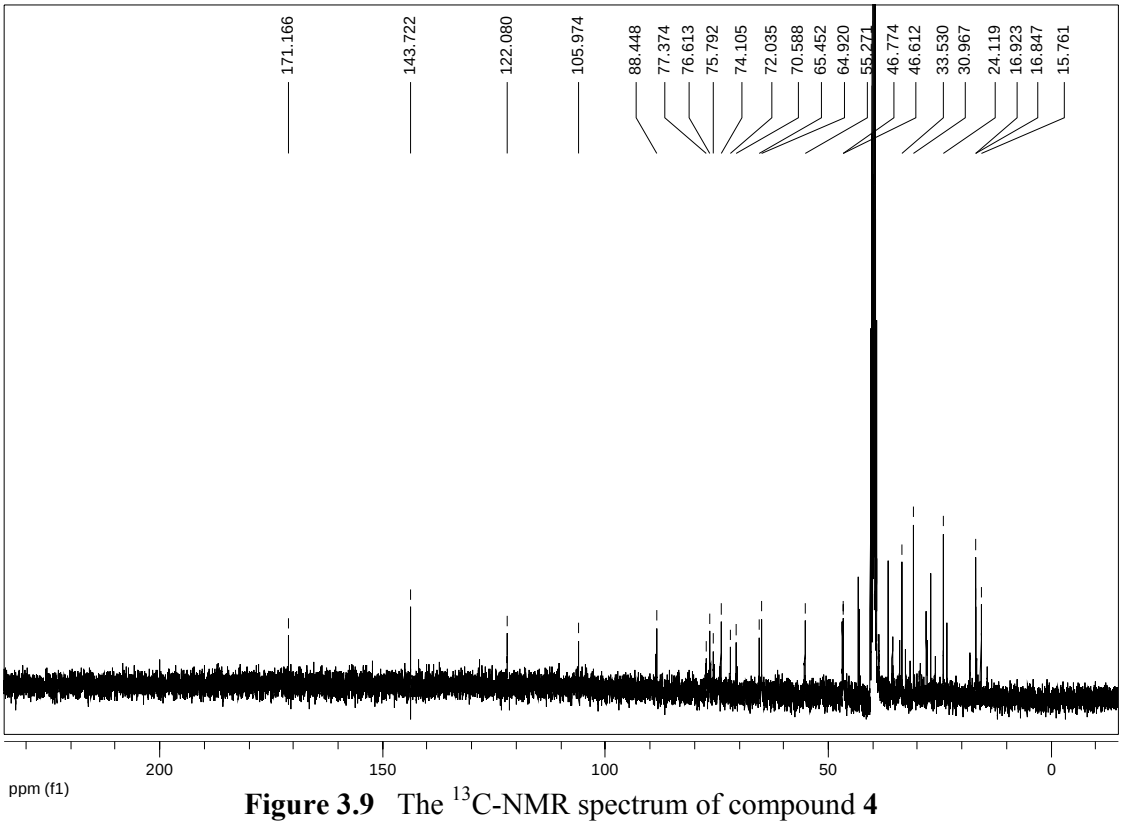

Figure 3.9 The ^{13}C-NMR spectrum of compound **4**

3.13 Separation of sub-fraction GGM6

Sub-fraction **GGM6** was obtained as brown syrup, 6.03 g from dianion column of Fraction IV. This fraction was re-chromatographed on Sephedex L-20, system: 100%MeOH. The eluted solution was collected approximately 8 mL for each fraction. Each eluted portion was monitored by TLC and the equivalent ones were combined. The results of the separation of sub-fraction **GGM6** are presented in Table 3.11.

Table 3.11 The separation of sub-fraction **GGM6** and the scavenging effects on DPPH radicals of separated fractions.

Fraction	Remarks	Weight (g)	Scavenging effects on DPPH radicals
GGM61	Yellow solid	trace	+
GGM62	Yellow solid	0.89	++
GGM63	Yellow solid	1.10	+
GGM64	Yellow semisolid	2.56	++
GGM65	Yellow semisolid	1.59	++
GGM66	Yellow solid	trace	++

According to the results presented in Table 3.8, sub-fractions **GGM62, GGM64**, **GGM65** and **GGM66** showed good scavenging effects on DPPH radicals. Since the amount of sub-fractions **GGM62** and **GGM66** was limited for further separation, these two fractions were thus not further explored.

3.14 Separation of sub-fraction GGM64

Sub-fraction **GGM64** as yellow semisolid, 2.56 g was re-chromatographed on Sephedex LH-20 system: 100%MeOH. The procedure of separation was the same as that described for sub-fraction **GGM6.** The results of the separation of sub-fraction **GGM64** are presented in Table 3.12.

Table 3.12 The separation of sub-fraction **GGM64**

Fraction	Remarks	Weight (g)
GGM64A	Yellow wax	trace
GGM64B	White solid + compound **5**	0.87
GGM64C	Yellow wax	1.56
GGM64D	Yellow wax	0.36

3.15 Separation of sub-fraction GGM65

Sub-fraction **GGM65** as yellow semisolid, 1.59 g was re-chromatographed on Sephedex LH-20 system: 100%MeOH. The procedure of the separation was the same as that described for sub-fraction **GGM65**. The results of the separation of sub-fraction **GGM65** are presented in Table 3.13.

Table 3.13 The separation of sub-fraction **GGM65**

Fraction	Remarks	Weight (g)
GGM65A	Yellow wax	trace
GGM65B	White solid + compound **5**	0.77
GGM65C	Yellow wax	0.36
GGM65D	Yellow wax	0.16
GGM65E	Yellow wax	trace

3.15.1 Strutural elucidation of compound 5

Compound **5** (650 mg, 0.93 % w/w of Fracton I) was obtained from sub-fraction **GGM65** using Sephedex LH-20 system: 100%MeOH, m.p. 212-215 °C, R_f 0.83 (solvent system MeOH/H_2O 4:1). Compound **5** gave a violet color to Liebermann-Burchard′s reagent indicating the presence of triterpenoidal skeleton.

The ^{1}H-NMR spectrum (DMSO-d_6) (Fig 3.10) showed the signals in the range of δ_H 0.72-2.97 which were the signals of CH_3, CH_2 and CH groups. The multiplet signals at δ_H 2.98-3.12 were assigned to the protons of a sugar moiety. The proton on the carbon attached to a hydroxyl group appeared as the multiplet signal at δ_H 3.53 and the signal at δ_H 4.21 belonged to the anomeric proton. The multiplet signal at δ_H 5.45 was the signal of trisubstituted vinyl proton (-CH=C-).

The ^{13}C-NMR spectrum (DMSO-d_6) (Fig 3.11) revealed twenty-six signals of twenty-six sp^3 carbons of aglycone. Two carbons of aglycone connecting to hydroxyl groups were observed at δ_C 65.4 and 70.2. The presence of an olefinic carbon was assigned from the apperance of two carbon signals at δ_C 123.0 and 144.6 as presented in Table 3.14. The obtained spectroscopic data of this compound was similar to that of compound **4**. Certain additional signals indicated more glucose being linked to C2′ of compound **4**, characterized by the shift of carbon signal from δ_C 75.7 to 88.6. These results suggested that compound **5** contain an aglycone and two glucoses as (3*β*,16*β*,22*α*)-16,28-dihydroxyolean-12-en-3-yl-*O*-*β*-D-glucopyranosyl-*β*-D-gluco-pyranosiduroic acid [17].

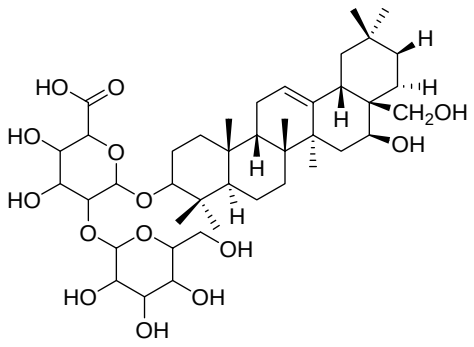

Compound 5

Table 3.14 The ^{13}C-NMR assignment of compound **5** and (3*β*,16*β*,22*α*)-16,28-dihydroxyolean-12-en-3-yl-*O*-*β*-D-glucopyranosyl-*β*-D-glucopyranosiduroicacid

Carbon	Chemical Shift (ppm)		Carbon	Chemical Shift (ppm)	
	Compound **4**	**Ref [17]**		Compound **4**	**Ref [17]**
C1	40.9	40.0	C29	33.5	33.7
C2	27.0	27.1	C30	24.1	24.3
C3	88.5	91.6	*β*-Glu		
C4	40.5	40.4	C1′	104.7	105.6
C5	57.5	57.0	C2′	88.6	80.9
C6	18.2	19.4	C3′	77.2	77.9
C7	33.5	33.9	C4′	73.4	73.0
C8	42.9	41.2	C5′	76.3	76.4
C9	48.1	48.2	C6	172.3	172.4
C10	36.4	37.8	Glu		
C11	25.4	24.7	C1″	104.2	104.7
C12	123.0	123.9	C2″	76.3	76.4
C13	144.6	144.3	C3″	77.2	77.9
C14	43.3	44.7	C4″	72.5	72.0
C15	36.4	36.7	C5″	81.6	78.3
C16	65.4	67.9	C6″	64.9	63.2
C17	40.9	41.6			
C18	46.6	45.2			
C19	48.2	48.0			
C20	30.9	31.7			
C21	33.5	34.8			
C22	25.8	26.2			
C23	27.9	28.6			
C24	16.9	17.0			
C25	16.5	16.2			
C26	18.2	17.5			
C27	27.9	27.5			
C28	70.2	69.2			

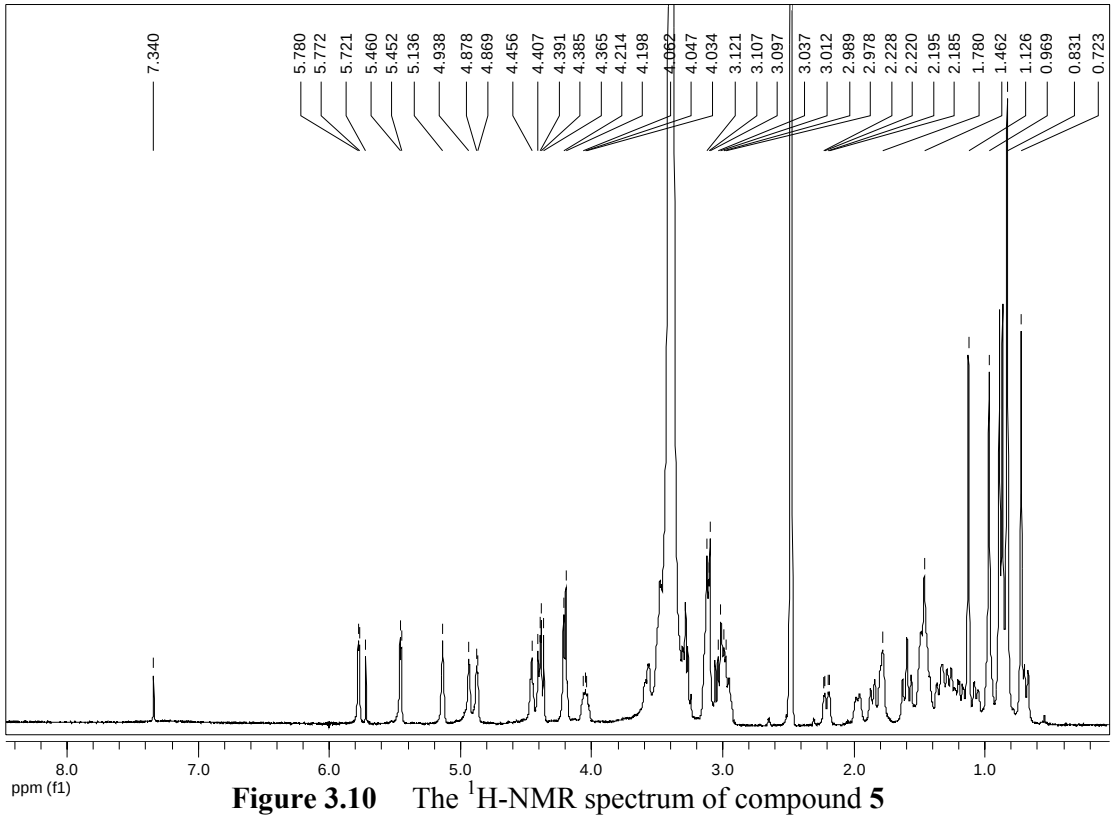

Figure 3.10 The ^{1}H-NMR spectrum of compound **5**

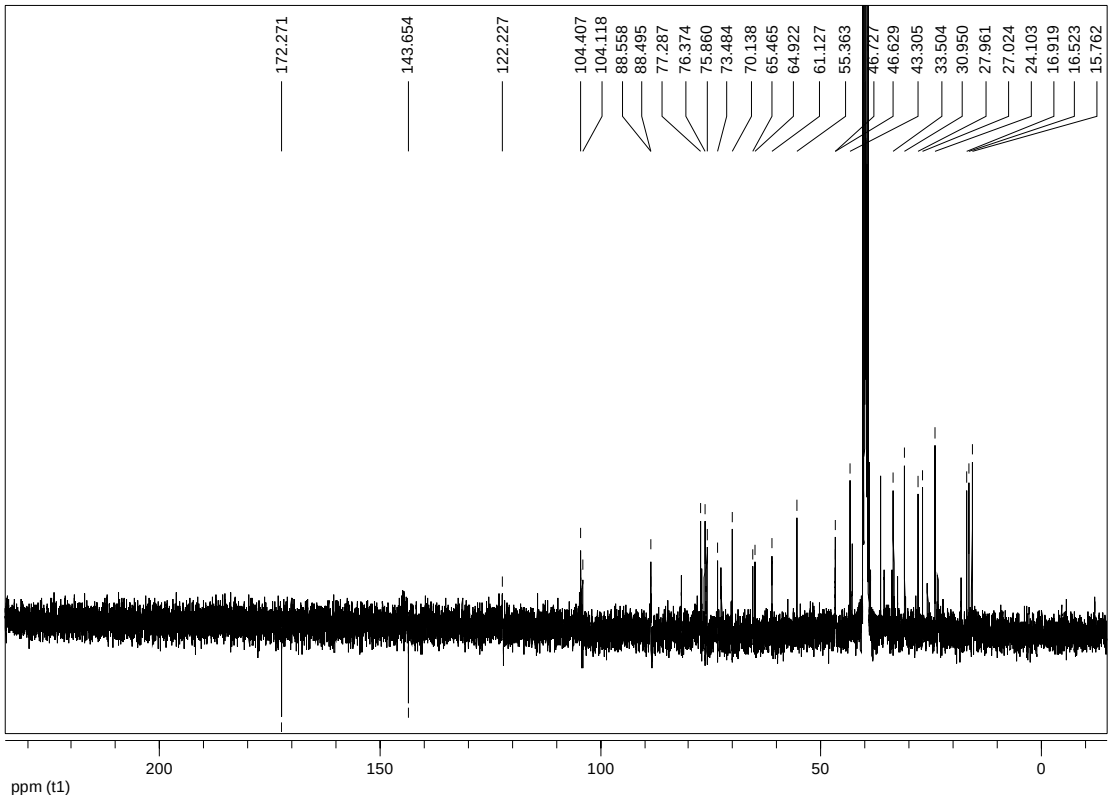

Figure 3.11 The ^{13}C-NMR spectrum of compound **5**

3.16 Biological activities of isolated substances from Fractions I and IV

All isolated substances from those mentioned extracts were assayed for antioxidant, the inhibition of cholinesterase activity and α-amylase inhibitor.

3.16.1 Antioxidant

The radical scavenger effect on DPPH radical of substances **1**, **2**, mixture **3** and compound **5** was tested by TLC autographic assay. The results are demonstrated in Table 3.15.

Table 3.15 The radical scavenging effect on DPPH radical of isolated substances from Fraction I and IV

Substance	**DPPH radical scavenging activity by TLC autographic method**
Substance **1**	-
Substance **2**	-
Mixture **3**	-
Compound **5**	++
Ascorbic acid	+++

Note : + positive results observed within 10 min
++ positive results observed within 5 min
+++ positive immediately

From the antioxidant test of substances **1**, **2**, mixture **3** and compound **5**, only compound **5** was active for radical scavenging effect on DPPH radical. According to the only report in literature, the biological activities addressed of extract *G. inodorum* was the inhibition of glucose absorption **[17]**. There was however no report on the evaluation of antioxidant activity of this compound. Therefore, natural compound **5** was first addressed as a new antioxidant agent.

3.16.2 Inhibition of cholinesterase activity

The inhibition of cholinesterase activity of substances **1**, **2**, mixture **3**, compounds **4** and **5** was assayed. All did not show any activity against acetylchlolinesterase or butyrylcholinesterase.

3.16.3 α-Amylase inhibitor.

Compounds **4** and **5** were tested for α-amylase inhibition. The results of α-amylase inhibition of these compounds at concentration of 2 mg/mL are presented in Table 3.16.

Table 3.16 The α-amylase inhibition result of compounds **4** and **5**

Compound	% α-Amylase inhibition
Compound **4**	9.80
Compound **5**	38.59

Based on the results obtained, the α-amylase inhibition of compound **5** (38.59 %) was better than that of compound **4** (9.80 %). Nevertheless, both of their activities were still in low activities.

It was found that Butanol crude extract showed moderate activity in the inhibition of α-amylase with 43.34 %. α-amylase inhibition of compound **5** (38.59 %) was better than that of compound **4** (9.80 %) four times at 1 mM. This result indicated that the activity of α-amylase inhibition of the *n*-BuOH extract arised from the active compound **5.**

The relative inefficacy of α-amylase inhibitors in affecting human digestion of starch has been highlighted by recent scientific and public controversy over the commercial sales of so-called starch-blockersor slimming pills. α-amylase and its inhibitors is drug-design targets for the development of compounds for treatment of diabetes obesity and hyperlipaemia. Studies on the structures of the numerous enzyme inhibitors found in cereal grains have led to the recognition of a super family of homologous proteins which includes inhibitors of α-amylase, proteinase and bifunctional inhibitors active against two or more classes of enzymes.

The reaction mechanisms involved in the inhibition of alpha-amylase by plant protein inhibitors are not clearly understood. But there are suggestion that reducing sugars which are covalently bound to the inhibitor polypeptide chain may play a major role in the mechanism or that the inhibitor may induce conformational changes in the enzyme molecule [28].

Part II: Chemical constituents and biological activities of the roots of *M.oleifera*

2.17 Results of biological activity α-amylase inhibitors of *M.oleifera*

The CH_2Cl_2 extracts of various parts of *M. oleifera* were further examined for α-amylase inhibitors. The results are demonstrated in Table 3.17.

Table 3.17 The results of α-amylase inhibitors of various crude extracts from *M. oleifera*

Part	% Inhibition α-amylase
Young seed	93.43
Leaf	72.40
Stem	58.25
Root	98.64

The results showed that the CH_2Cl_2 extract from the roots and the seeds of *M. oleifera* exhibited high activity for inhibiting α-amylase. There was no report on the investigation the chemical constituents of the CH_2Cl_2 extract of the roots of *M. oleifera* and their biological activities. Thus, the roots of *M. oleifera* were chosen for further investigation of their chemical constituents and bioactivities.

3.18 Results of extraction

General procedure for extraction

The dried roots of *M. oleifera* (4.5 kg) were collected from Tak province in December 2006, and extracted with CH_2Cl_2 and MeOH, respectively by soxhlet as outlined in Scheme 3.5.

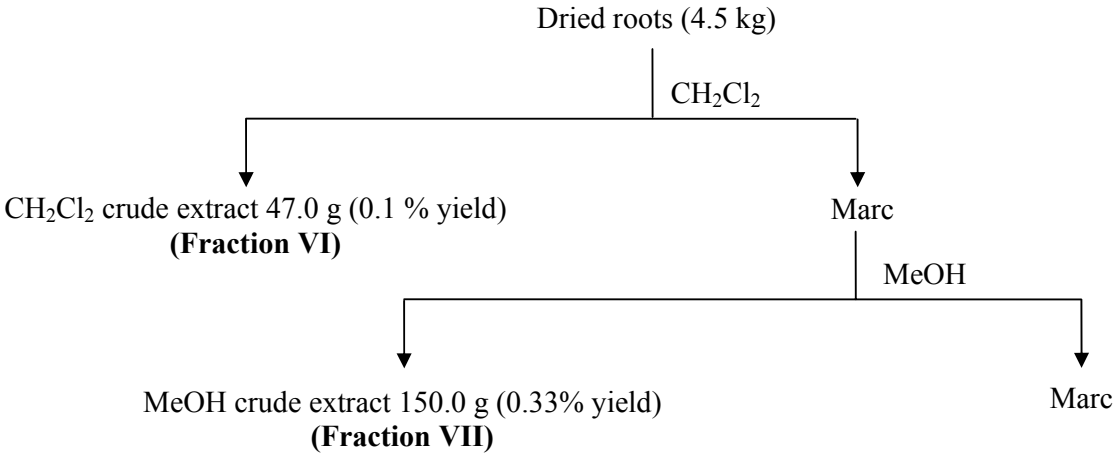

Scheme 3.5 The extraction of the roots of *M. oleifera*

3.19 Separation of the CH_2Cl_2 extract (Fraction VI) and its preliminary antioxidant activities

47 g of Fraction VI was subjected to silica gel column using step gradient of hexane/EtOAc and EtOAc/MeOH. The eluted fractions were collected and combined according to TLC results to obtain eight fractions, **Mor1-Mor8**. Each fraction was preliminarily tested for radical scavenging properties in the DPPH assay. The results of each fraction and its activities are shown in Table 3.18.

Table 3.18 The separation of Fraction VI and its radical scavenging properties

Sub-fraction	Solvent system	Remarks	Weight (g)	Activities
Mor1	100% hexane	Brown yellow soild + compound **6**	2.78	++
Mor2	10%EtOAc/hexane	Brown yellow soild	1.57	++
Mor3	20%EtOAc/hexane	Yellow oil	17.73	++
Mor4	20%EtOAc/hexane	Brown yellow semi soild	3.45	++
Mor5	30% EtOAc /hexane	White soild	3.46	++
Mor6	40-60% EtOAc/hexane	Yellow soild	2.56	+++
Mor7	60-70% EtOAc/hexane	White soild	4.23	++
Mor8	80% EtOAc/hexane - 5%EtOAc/MeOH	Dark brown syrup	1.28	++

Note: + positive results observed within 10 min
++ positive results observed within 5 min
+++ positive immediately

From the preliminary results of DPPH assay, only sub-fraction **Mor6** displayed the best activity for radical scavenging property while other fractions showed moderate antioxidant activity.

3.19.1 Structural elucidation of compound 6

The brown oil (2.78 g, 0.031% w/w of dried plant material) with R_f 0.64 in 10%MeOH/$CHCl_3$ was obtained from sub-fraction **Mor1**. This compound was soluble in hexane, $CHCl_3$ and MeOH.

The IR spectrum of this compound (Fig 3.12) exhibited the absorption peaks of hydroxyl group of carboxylic acid in the region of 3100-3400 cm^{-1}, and a carbonyl group at 1715 cm^{-1}. Other signals were tentatively assigned in Table 3.19.

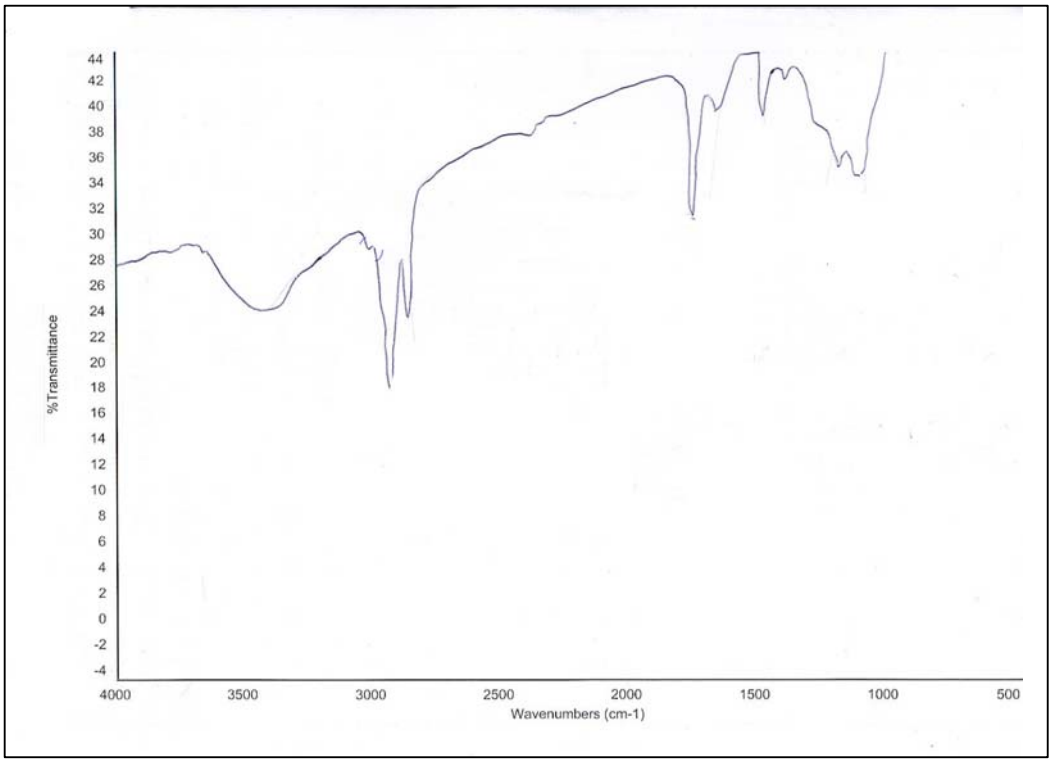

Figure 3.12 The IR spectrum of compound **6**

Table 3.19 The IR absorption band assignments of compound **6**

Wavenumber (cm^{-1})	Intensity	Tentative assignments
3100-3400	broad	O-H stretching vibration of carboxylic acid.
2921, 2856	strong	C-H stretching vibration of CH_2 and CH_3
1715	strong	C=O stretching vibration of carboxylic acid
1446	medium	C-H bending vibration of CH_2 and CH_3

The ^{1}H-NMR spectrum (Fig 3.13) exhibited the chemical shift of an olefinic proton at δ_H 5.22. The presence of the signal at δ_H 2.60 was assigned to a bisallylic proton. The protons at α-position of a carbonyl group and at allylic position could be detected δ_H 2.20 and 1.90 respectively. The triplet signal with three protons integration at δ_H 0.87 was belonged to terminal methyl group.

The ^{13}C-NMR spectrum (Fig 3.14) displayed 18 carbon signals. The important signals are as follows: at δ_C 175.4 for a carbonyl carbon of carboxylic acid and four olefinic carbons at δ_C 127.9, 128, 130.0 and 130.2.

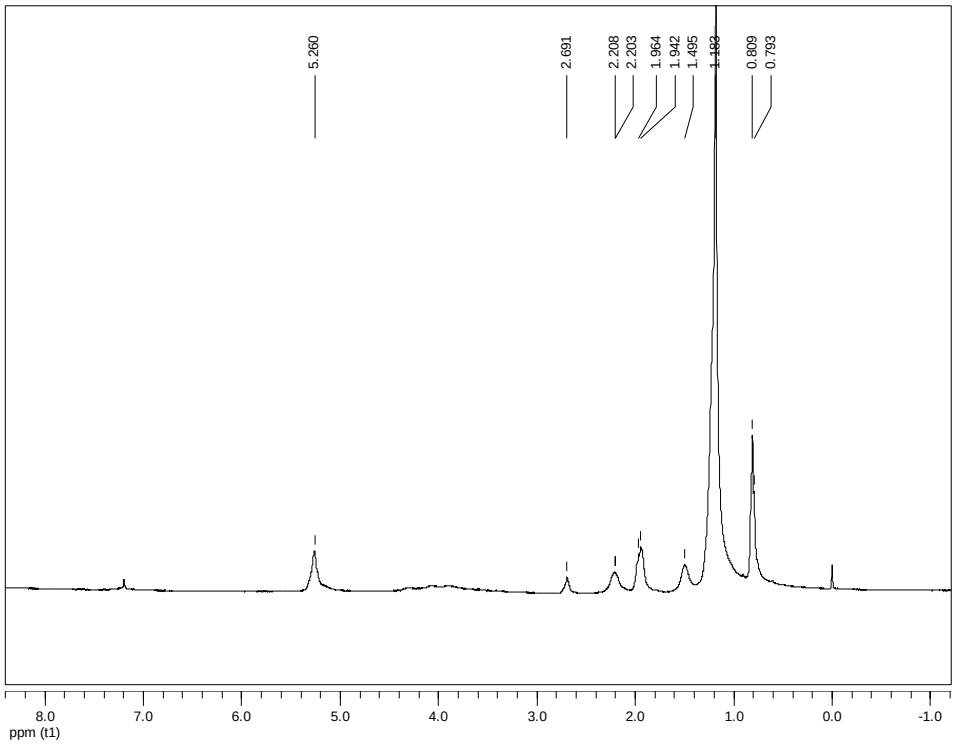

Figure 3.13 The ^{1}H-NMR spectrum of compound **6**

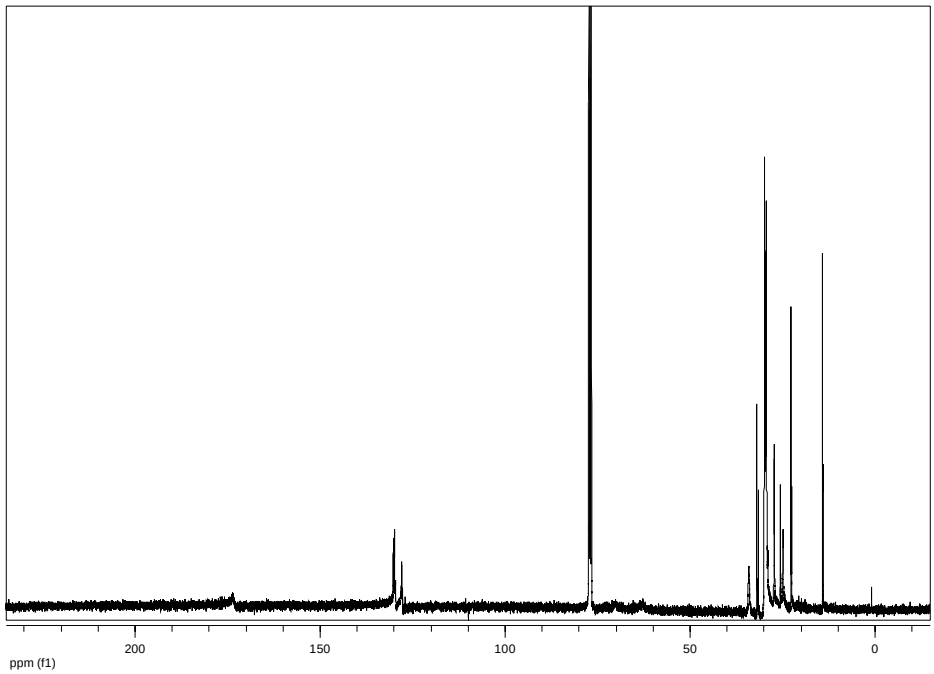

Figure 3.14 The ^{13}C-NMR spectrum of compound **6**

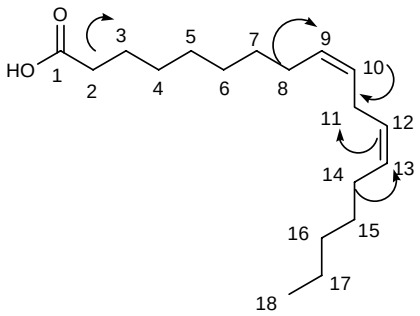

The COSY spectrum of compound **6** (Fig 3.15) reasonably exposed the correlations between H-2 (δ_H 2.20) and H-3 (δ_H 1.49), between allylic protons H-8, H-14 (δ_H 1.96) and olefinic protons H-9, H-13 (δ_H 5.26), and between bisallylic proton H-11 (δ_H 2.69) and olefinic protons H-10 (δ_H 5.26) and H-12 (δ_H 5.26), respectively.

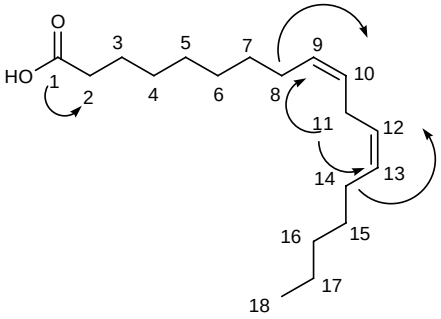

The HMBC spectrum (Fig 3.16) clearly manifested the correlations between C-1 (δ_C 175.4), and H-2 between C-8 (δ_C 27.1) and H-10 (δ_H 5.26) between C-14 (δ_C 27.2) and H-12 (δ_H 5.26) and C-11 (δ_C 25.6) and H-9, H-13 (δ_H 2.26), respectively.

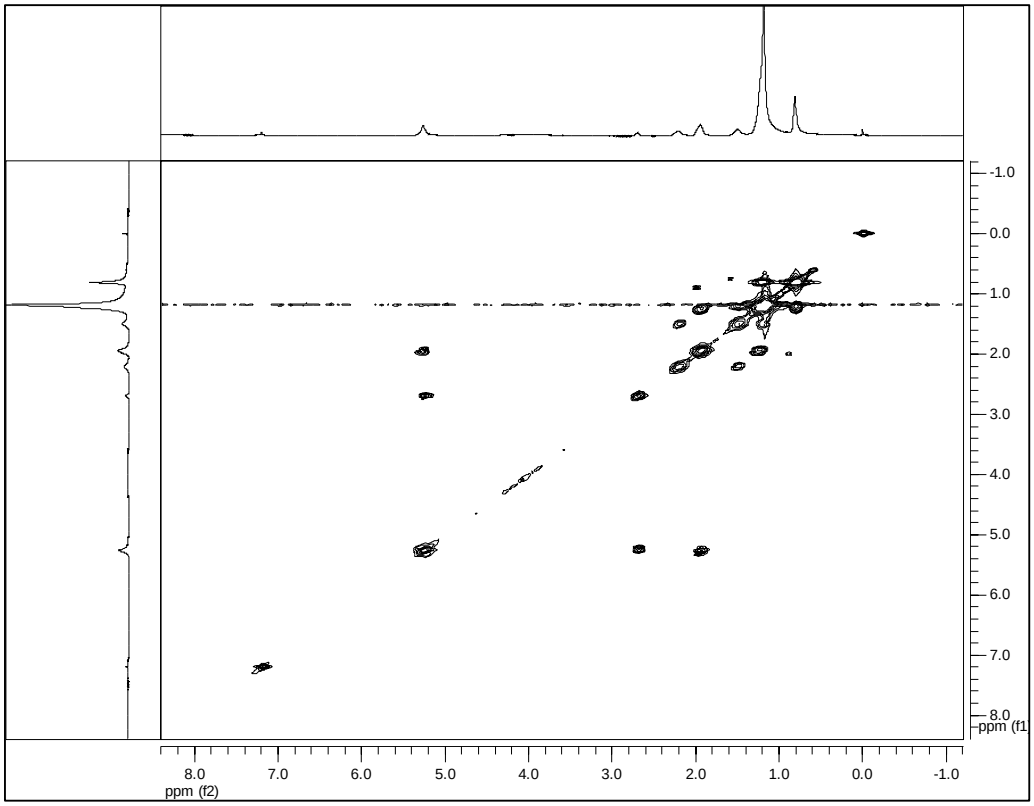

Figure 3.15 The COSY spectrum of compound **6**

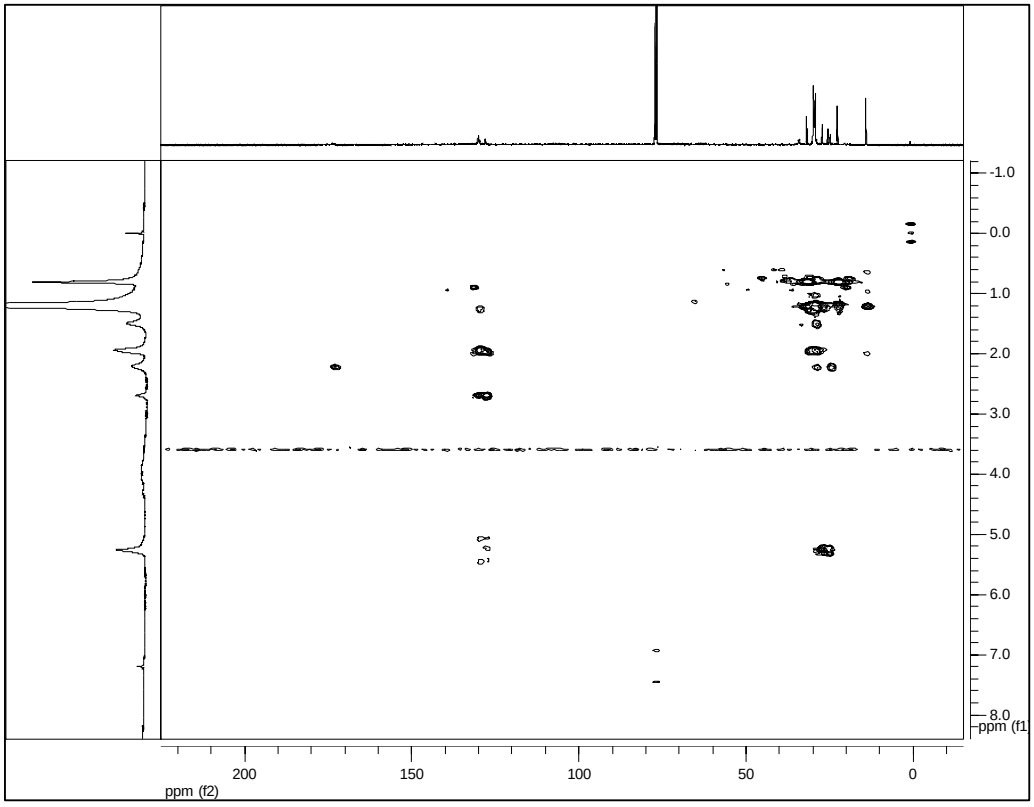

Figure 3.16 The HMBC spectrum of compound **6**

The spectroscopic data of this compound was compared with that of known linoleic acid to confirm the expected structure. The results are displayed in Table 3.20.

Table 3.20 The ^{1}H and ^{13}C chemical shift assignments of compound **6** compared with linoleic acid [29]

Position	Chemical shift (ppm)			
	Compound 6		linoleic acid [29]	
	^{1}H	^{13}C	^{1}H	^{13}C
1	-	175.4	-	177.0
2	2.20 (br, 2H)	34.0	2.37 (t, 2H, *J*= 7.1 Hz)	35.8
3	1.49 (m, 2H)	24.8	1.67 (m, 2H)	25.1
4	*	29.7	**	29.7
5	*	29.5	**	30.1
6	*	29.3	**	30.4
7	*	29.1	**	30.3
8	1.96 (m, 2H)	27.1	2.10 (m, 2H)	27.4
9	5.26 (m, 2H)	130.1	5.32 (m, 2H)	131.0
10		129.7		128.4
11	2.70 (t, 2H, *J*= 5.5 Hz)	25.6	2.80 (m, 2H)	25.2
12	5.26 (m, 2H)	127.8	5.32 (m, 2H)	128.0
13		129.9		130.6
14	1.96 (m,2H)	27.2	2.10 (m, 2H)	27.4
15	*	29.1	**	30.0
16	*	31.9	**	32.6
17	*	22.6	**	23.2
18	0.89 (t, 3H, *J*= 6.87)	14.1	0.91 (t, 3H, *J*= 7.4 Hz)	14.0

Note : The methylene signals of linoleic acid * were resonated at 1.29 ppm

According to the obtained spectroscopic data, it could be thoroughly concluded that the isolated compound from sub-fraction **Mor1** was octadeca-9,12-dienoic acid or linoleic acid and its structure is shown below.

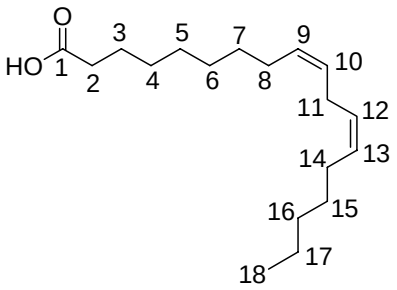

Linoleic acid

Since the amount of sub-fractions **Mor2** and **Mor8** were limited for further separation, these two fractions were not explored. Sub-fractions **Mor3, Mor4,** and **Mor6** were then separated by silica gel column using step gradients of hexane-EtOAc and EtOAc-MeOH.

3.20 Separation of sub-fraction Mor3

17.73 g of sub-fraction **Mor3** was re-separated by silica gel column eluting with 100%hexane-50%EtOAc/hexane. The results of the separation are shown in Table 3.21.

Table 3.21 The results of the separation of sub-fraction **Mor3**

Fraction	Solvent system	Remarks	Weight(g)
Mor3A	100% hexane	yellow oil	1.25
Mor3B	2%EtOAc/hexane	yellow oil	8.26
Mor3C	4%EtOAc/hexane	yellow oil	0.26
Mor3D	10%EtOAc/hexane	yellow oil	1.25
Mor3E	20%EtOAc/hexane	yellow oil	2.84
Mor3F	30-50% EtOAc/hexane	yellow oil	0.78

3.21 Separation of sub-fraction Mor3B

8.26 g of sub-fraction **Mor3B** was re-separated by silica gel column eluting with 100%hexane-60%EtOAc/hexane. The results of the separation are presented in Table 3.22.

Table 3.22 The separation of sub-fraction **Mor3B**

Fraction	Solvent system	Remarks	Weight(g)
Mor3B1	100%hexane	yellow oil +compound **7**	15 mg
Mor3B2	2%EtOAc/hexane	white soild	0.01
Mor3B3	4%EtOAc/hexane	yellow liquid	0.48
Mor3B4	10%EtOAc/hexane	dark brown semisoild	0.36
Mor3B5	20%EtOAc/hexane	dark brown semisoild	0.02
Mor3B6	40%EtOAc/hexane	yellow liquid	1.12
Mor3B7	40-50%EtOAc/hexane	yellow oil	4.31
Mor3B8	60%EtOAc/hexane	dark brown semisoild	0.51

3.21.1 Structural elucidation of compound 7

The yellow oil (15 mg, 0.03% w/w of Fraction VI) revealed the spot at R_f 0.69 (2%EtOAc/hexane). This compound was soluble in $CHCl_3$, CH_2Cl_2 and EtOAc.

The IR spectrum of this compound (Fig 3.17), exhibited the absorption peaks of isothiocyanate group in region of 2162 cm^{-1} and aromatic group at 1479 cm^{-1}. Other signals were tentatively assigned in Table 3.23.

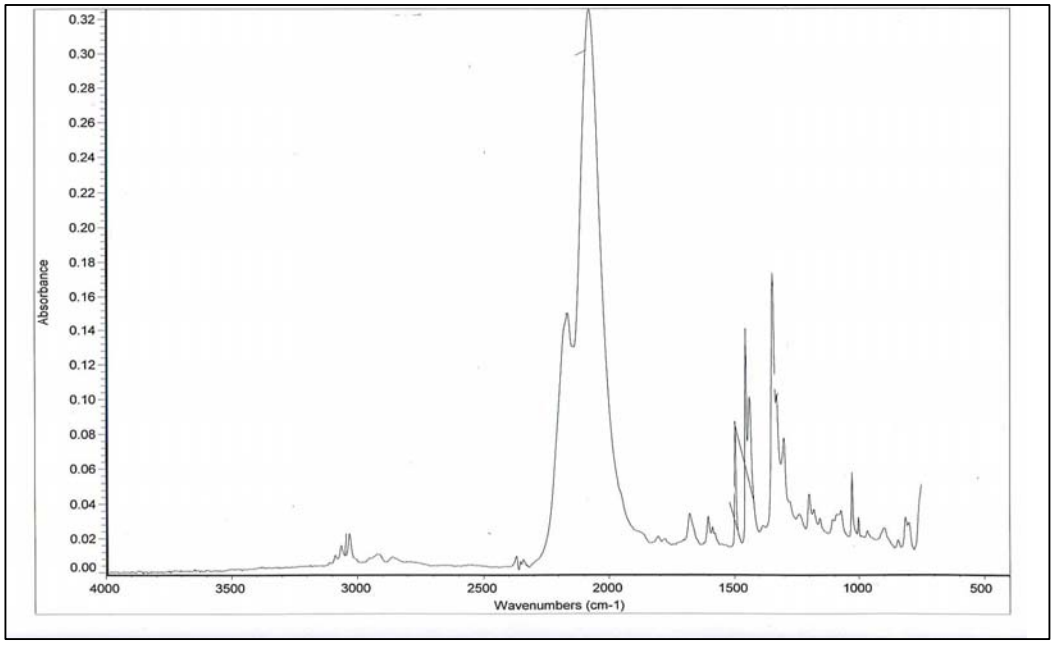

Figure 3.17 The IR spectrum of compound **7**

Table 3.23 The IR absorption band assignment of compound **7**

Wavenumber (cm^{-1})	Intensity	Tentative assignments
2162	Strong	-N=C=S stretching vibration of isothiocyanate
1479	strong	C-C stretching vibration of aromatic
1333	strong	=CH bending vibration in plane

The ^{1}H-NMR spectrum ($CDCl_3$) (Fig 3.18) exhibited the chemical shift of aromatic protons at H-1 (δ_H 7.44), H-2,6 (δ_H 7.38) and H-3,5 (δ_H 7.32). The chemical shift of methylene protons of H-7 was observed at δ_H 4.80.

The ^{13}C-NMR spectrum ($CDCl_3$) (Fig 3.19) displayed eight carbon signals. The aromatic carbon signals of C-1, C-2,6, C-3,5 and C-4 were resonated at δ_C 128.4 128.9, 126.8 and 134.0, respectively. The chemical shift of methylene carbon of C-7 was observed at δ_C 48.0, whereas the isothiocyanate carbon of C-8 was detected at δ_C 132.0.

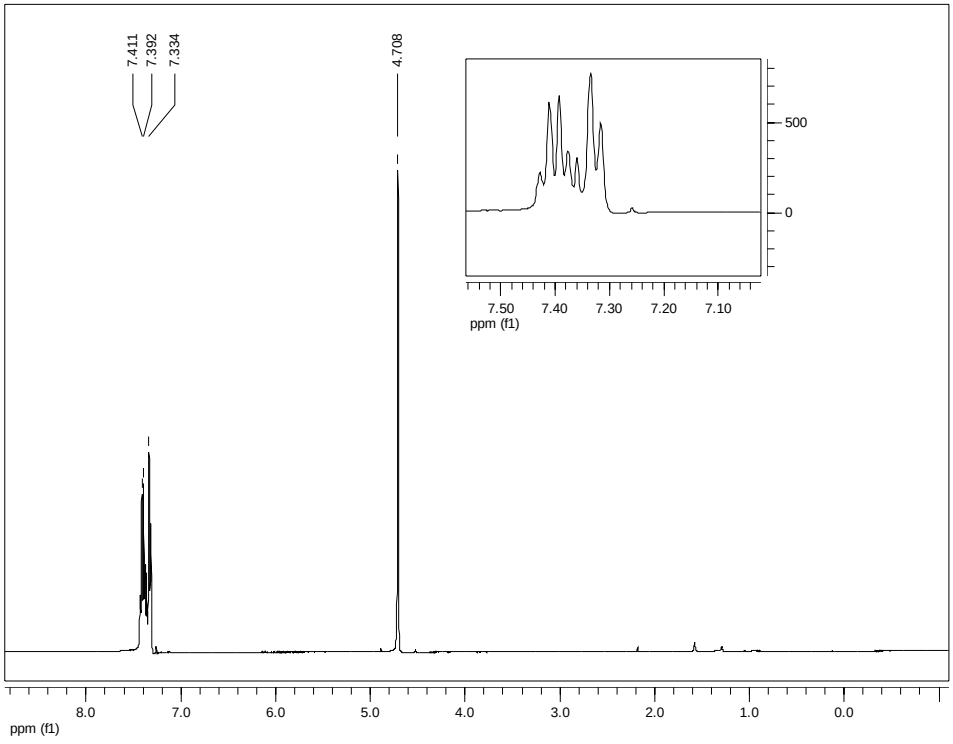

Figure 3.18 The ^{1}H-NMR spectrum of compound **7**

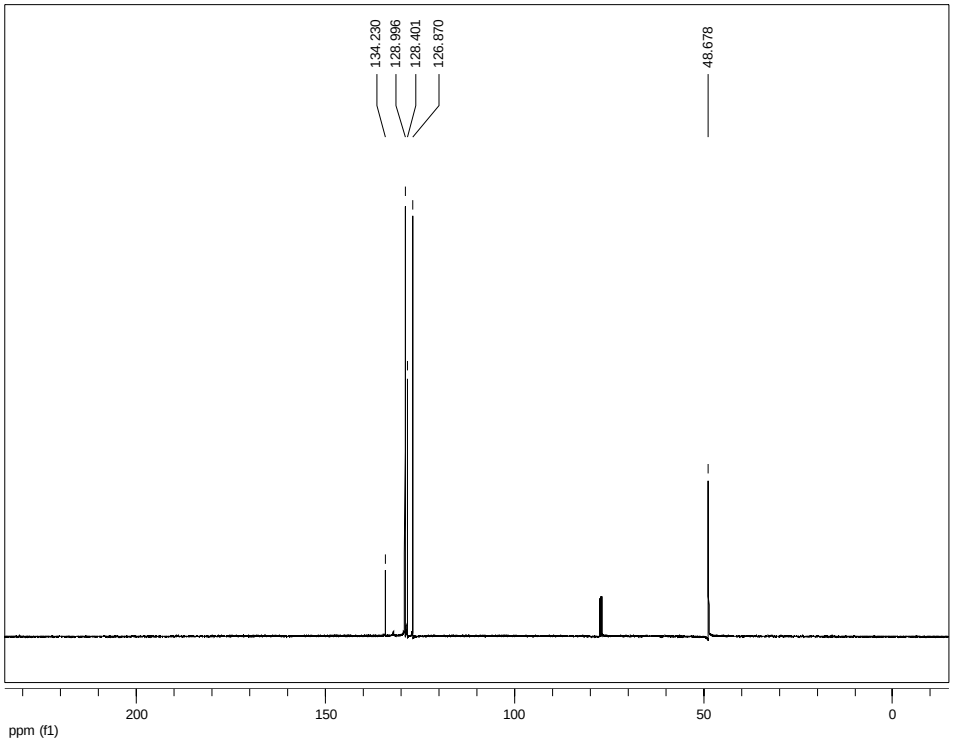

Figure 3.19 The ^{13}C-NMR spectrum of compound **7**

Table 3.24 The ^{1}H and ^{13}C chemical shift assignments of compound **7** [30]

Position	Chemical shift (ppm) compound 8		Position	Chemical shift (ppm) Benzylisothiocyanate [30]	
	^{1}H	^{13}C		^{1}H	^{13}C
1	7.48 (t, 1H, *J*= 7.48 Hz)	128.4	1	7.41 (t, 1H, *J*= 7.80 Hz)	128.3
2	7.38 (t, 2H, *J*= 6.87 Hz)	128.9	2	7.36 (t, 2H, *J*= 7.80 Hz)	129.2
3	7.32 (d, 2H, *J*= 7.36 Hz)	126.8	3	7.33 (d, 2H, *J*= 7.80 Hz)	126.3
4	-	134.0	4	-	131.7
5	7.32 (d, 2H, *J*= 7.36 Hz)	126.8	5	7.33 (d, 2H, *J*=7.80 Hz)	126.7
6	7.38 (t, 2H, *J*= 6.87 Hz)	128.9	6	7.36 (t, 2H, *J*=7.80 Hz)	129.2
7	4.8 (s, 2H)	48.0	7	4.75 (s, 2H)	48.25
8	-	132.0	8	-	132.6

The structure of compound **7** was additionally elucidated based on the results from COSY and HMBC spectra.

The COSY spectrum of compound **7** (Fig 3.20) reasonably exposed the correlations between H-1a (δ_H 7.44) and H-6,-2b (δ_H 7.38), between H-6,2b (δ_H 7.38) and H-3,5c (δ_H 7.32).

COSY

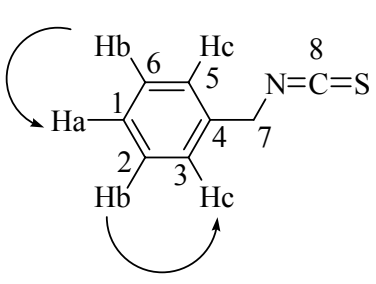

HMBC

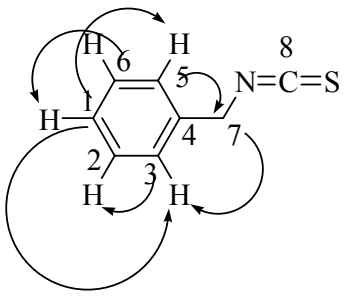

The HMBC spectrum (Fig 3.21), revealed the correlations between C-3,5 (δ_C 127.0) and H-7 (δ_H 4.70) and between C-1 (δ_C 128.4) with H-3,5 (δ_H 7.32) between C-3,5 (δ_C 127.0) with H-2,6 (δ_H 7.38) between C-2,6 (δ_C 128.9) with H-1 (δ_H 7.48) and between C-7 (δ_C 48.0) and H-3,5 (δ_H 7.32), respectively.

Compound **7** was further confirmed its structure by MS (Fig 3.22). The MS showed the mass per charge (m/z) at 149, corresponding to the molecular weight of (isothiocyanatomethyl)benzene. The presence of m/z at 91 was assigned to the base peak of benzyl ion.

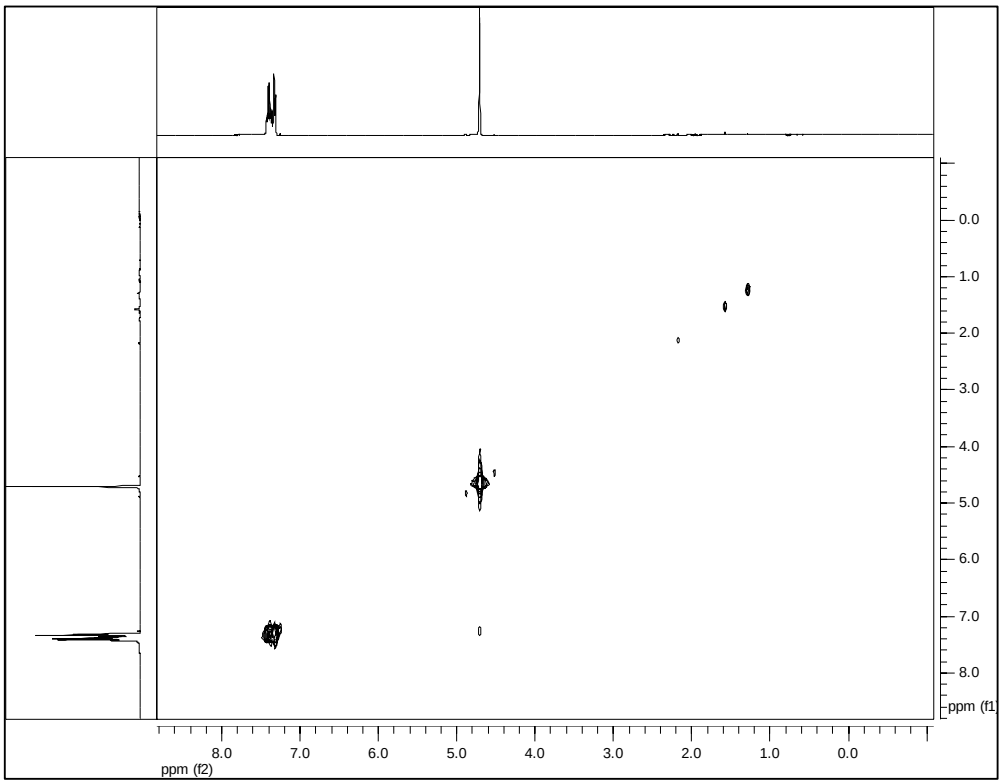

Figure 3.20 The COSY spectrum of compound **7**

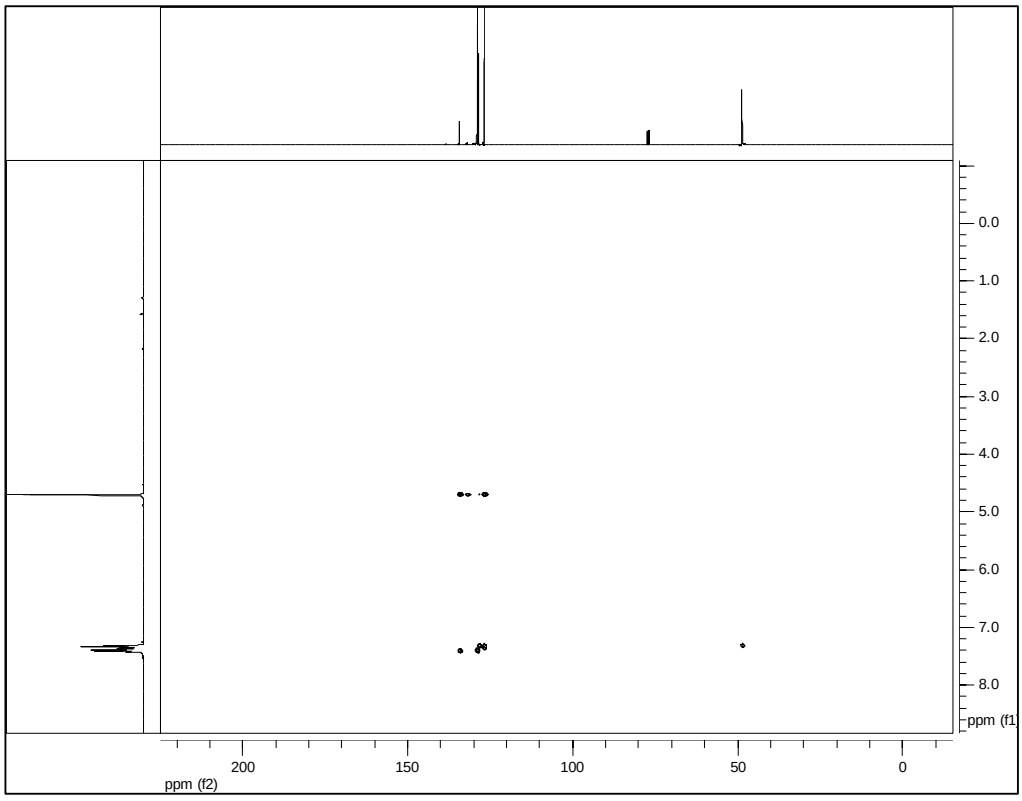

Figure 3.21 The HMBC spectrum of compound **7**

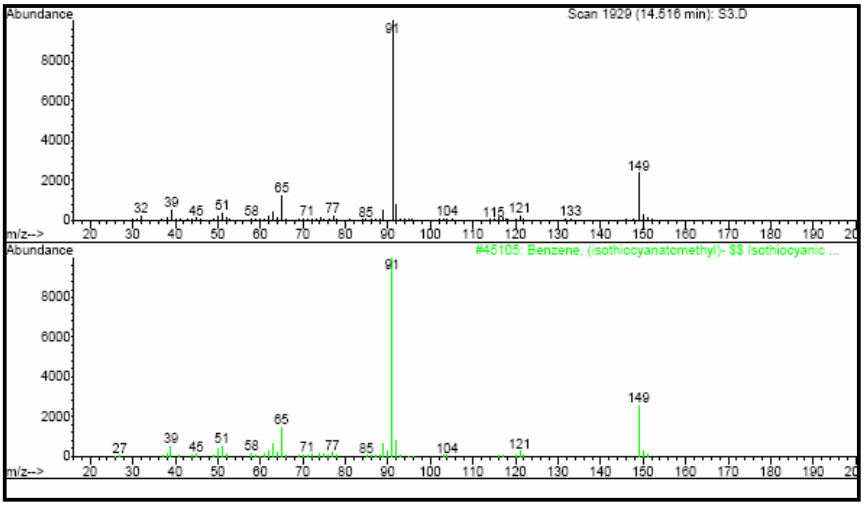

Figure 3.22 The mass spectrum of compound **7**

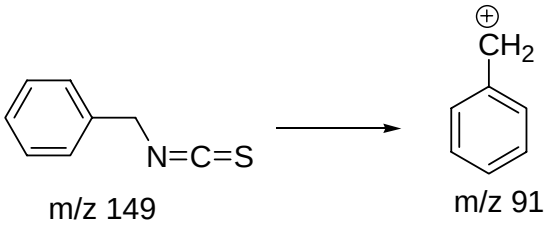

According to all spectroscopic data, it could be summarized that the separated compound from sub-fraction **Mor3B1** was (isothiocyanatomethyl)benzene.

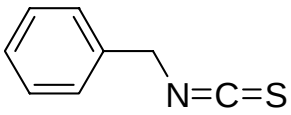

(isothiocyanatomethyl)benzene

3.22 Separation of sub-fraction of Mor3B7

4.31 g of sub-fraction **Mor3B7** was re-separated by silica gel column eluting with 100%hexane-50%EtOAc/hexane. The results of the separation are shown in Table 3.25.

Table 3.25 The separation of sub-fraction **MorB37**

Fraction	Solvent system	Remarks	Weight(g)
Mor3B71	100% hexnae	Yellow oil	0.23
Mor3B72	2% EtOAc/hexane	Yellow oil + mixture **8**	2.45 g
Mor3B73	4% EtOAc/hexane	Yellow liquid +compound **9**	45 mg
Mor3B74	10% EtOAc/hexane	Yellow liquid	0.36
Mor3B75	20% EtOAc/hexane	Dark brown semisoil	0.02

3.22.1 Structural elucidation of mixture 8

Mixture **8** as a pale yellow oil 2.45 g (5.21% w/w of Fraction VI) revealed R_f 0.65 (15%hexane/ether). This mixture was subjected to HPLC analysis to explore the components using Nova–Pak normal phase column and isocratic system of 99% hexane/isopropanol. The chromatogram of mixture **8** displayed three peaks as shown in Fig 3.23.

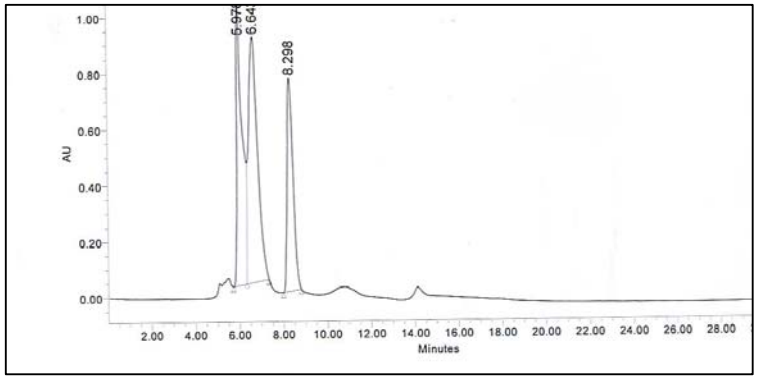

Figure 3.23 The HPLC chromatogram of mixture **8**

Table 3.26 The composition of mixture **8**

Component	Retention time (min)	% Composition
1	5.98	31
2	6.64	44
3	8.30	25

The HPLC analysis of this mixture revealed the retention time at R_t 5.98, 6.64 and 8.30 min with 31, 44 and 25%composition, respectively (Table 3.26). This clearly indicated that this mixture was the mixture of three substances.

To confirm the structure of the component, this mixture was in addition characterized by NMR technique. The ^{1}H-NMR spectrum (Fig 3.24) exhibited the multiplet signal of the olefinic proton at δ_H 5.33 (m, 10H, H-(9′, 10′, 12′, 13′)x2 and H-(9″,10″). The bisallylic proton was observed from the presence of the signal at δ_H 2.75 (m, 4H, H-11″x2). The signals at δ_H 4.12 (dd, 2H, H-1^{a}) and 4.28 (dd, 2H, H-1b, 3b) were assigned for two methylene protons connecting to an oxygen atom. The NMR data for all three compounds were identical since they were either linoleic or oleic acid esters.

The structure of this mixture was also confirmed by comparison its ^{1}H-NMR spectrum with that published in a previous report [29]. From the aforementioned results, it could be concluded that one of the components was a triglyceride, 1,3-dilinoleoyl-2-olein and others were two triglycerides: 1,3-dioleoyl-2-linolein and 1,2,3-trilinolein. The assignments of proton and carbon signals of mixtures **8** are summarized in Tables 3.27-3.28.

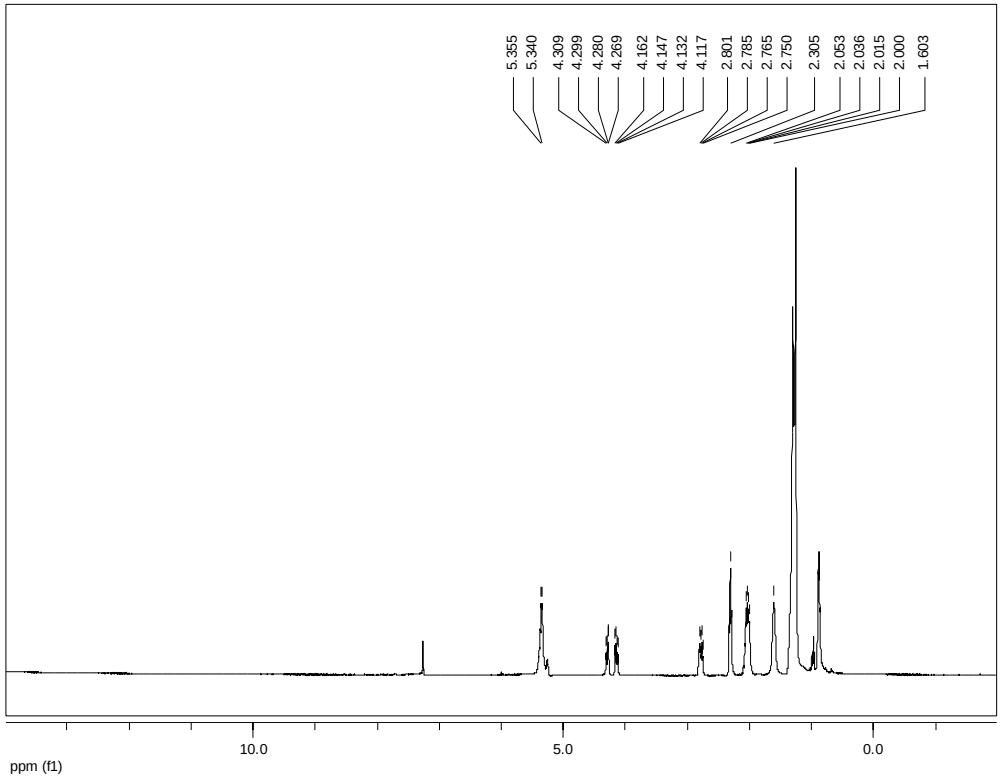

Figure 3.24 The ^{1}H-NMR spectrum of mixture **8**

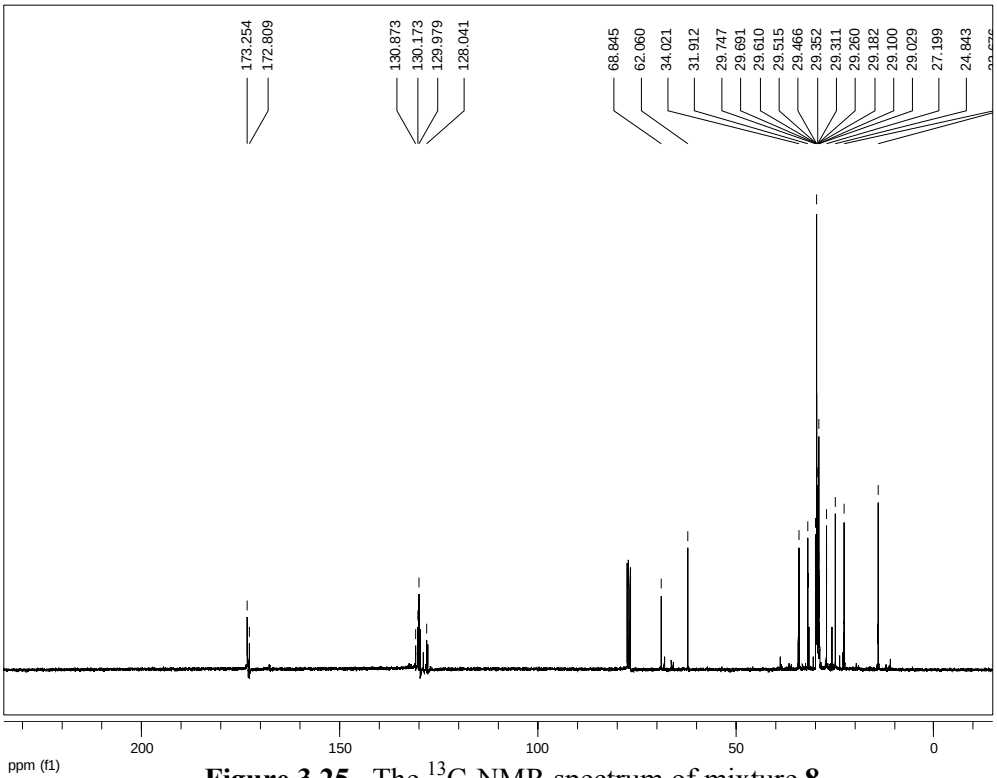

Figure 3.25 The ^{13}C-NMR spectrum of mixture **8**

Table 3.27 The ^{1}H and ^{13}C chemical shifts assignment of 1,3-dilinoleoyl-2-olein [29]

Position	Chemical shift (ppm)		Position	Chemical shift (ppm)	
	^{1}H	^{13}C		^{1}H	^{13}C
1′	-	174.3	1″	-	173.1
2′	2.28	34.2	2″	2.29	34.2
3′	1.59	24.8	3″	1.59	24.8
4′	*	29.7	4″	*	29.7
5′	*	29.6	5″	*	29.6
6′	*	29.2	6″	*	29.2
7′	*	29.1	7″	*	29.1
8′	2.02	27.2	8″	2.02	27.2
9′	} 5.33	129.9	9″	} 5.33	129.9
10′		129.6	10″		129.6
11′	2.75	25.6	11″	2.02	27.2
12′	} 5.33	129.9	12″	1.59	29.3
13′		129.6	13″	*	29.3
14′	2.02	27.2	14″	*	29.1
15′	1.59	29.2	15″	*	29.6
16′	*	29.5	16″	*	30.0
17′	*	24.7	17″	*	23.8
18′	0.86	14.2	18″	0.86	14.2
1	4.16	62.1			
2	5.20	68.9			
3	4.26	62.1			

Note : The methylene signals of 1,3-dilinoleoyl-2-olein * were resonated at 1.29 ppm

Table 3.28 The ^{1}H and ^{13}C chemical shift assignments of mixture **8**

Position	Chemical shift (ppm)		Position	Chemical shift (ppm)	
	^{1}H	^{13}C		^{1}H	^{13}C
1′	-	174.3	1″	-	173.1
2′	2.33	34.2	2″	2.32	34.2
3′	1.60	24.8	3″	1.61	24.8
4′	*	29.7	4″	*	29.7
5′	*	29.6	5″	*	29.6
6′	*	29.2	6″	*	29.2
7′	*	29.1	7″	*	29.1
8′	2.04	27.2	8″	2.05	27.2
9′	5.33	129.9	9″	5.33	129.9
10′		129.6	10″		129.6
11′	2.76	25.6	11″	2.05	27.2
12′	5.33	129.9	12″	1.61	29.3
13′		129.6	13″	*	29.2
14′	2.04	29.1	14″	*	29.1
15′	1.61	27.4	15″	*	14.2
16′	*	29.5	16″	*	30.0
17′	*	24.7	17″	*	23.8
18′	0.86	14.2	18″	0.86	14.2
1	4.08	62.1			
2	5.20	68.9			
3	4.12	62.1			

Note : The methylene signals of mixture **8*** were resonated at 1.29 ppm

Additionally, the structure of mixture **8** was deduced from COSY and HMBC. The COSY spectrum (Fig 3.26) revealed the correlations between H-1 (δ_H 4.16) and H-2 (δ_H 5.20), between H-3 (δ_H 4.28) and H-2 (δ_H 5.20), between H-2′ (δ_H 2.33) and H-3′ (δ_H 1.60) between allylic proton H-8, H-14′ (δ_H 2.04) and olefinic protons at H-

9′,H-13′ (δ_H 5.33) and between bissallylic proton H-11′ (δ_H 2.76) and olefinic protons at H-10′, H-12′ (δ_H 5.33), respectively.

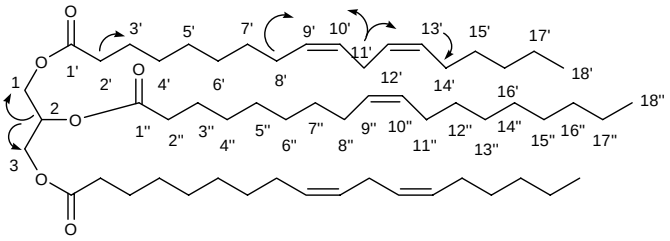

The HMBC spectrum (Fig 3.27) was clearly manifested the correlations between carbon and proton signals as follows: the correlations of C-1′ (δ_C 174.3) with H-1 (δ_H 4.08), H-2 (δ_H 5.20) and H-3′ (δ_H 1.59), that of C-4′ (δ_C 29.7) with H-3′ (δ_H 1.59), that of C-8′ (δ_C 27.2) with H-10′ (δ_H 5.33), that of C-14′ (δ_H 29.1) with H-12′ (δ_H 5.33) and that of C-11′ (δ_C 25.6) with H-9′,13′ (δ_H 5.33) and that of C-1″ (δ_C 173.1) with H-3 (δ_H 4.26).

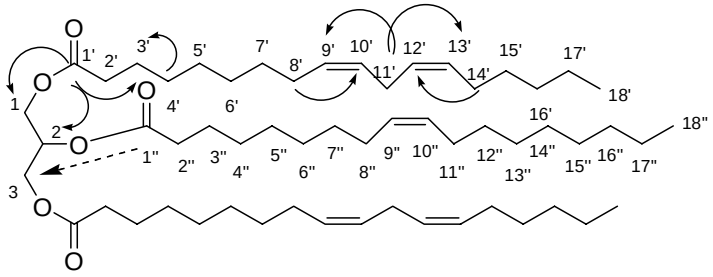

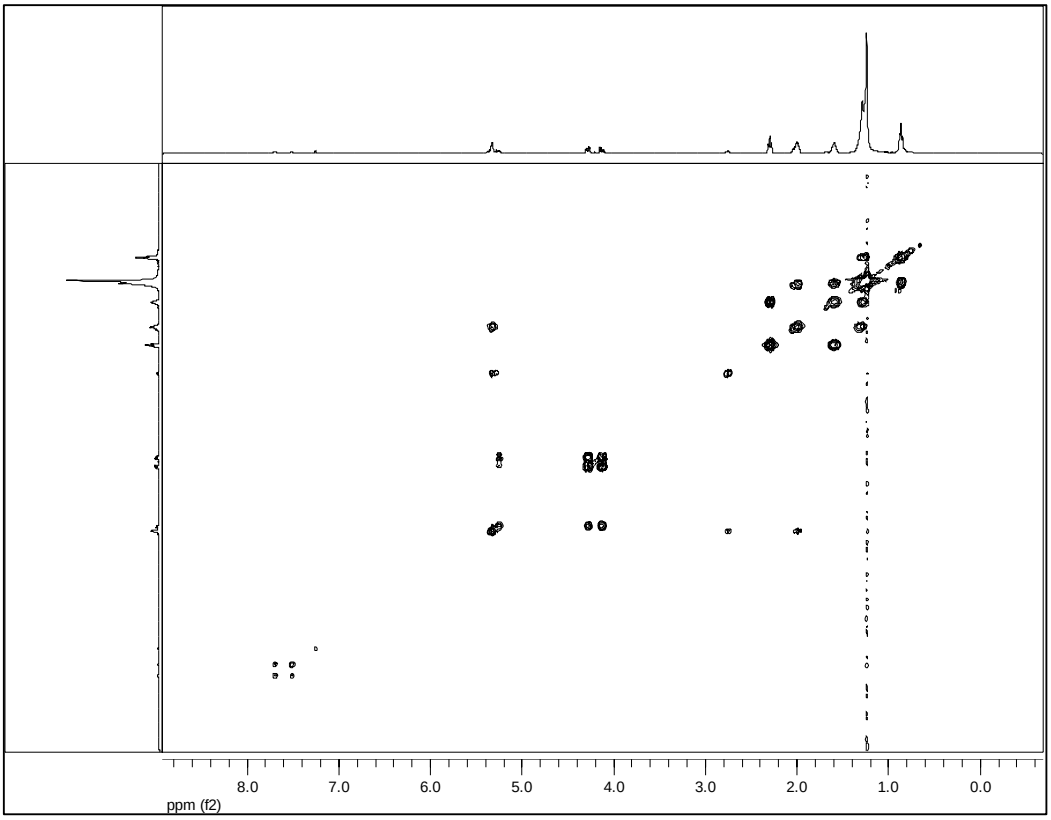

Figure 3.26 The COSY spectrum of mixture **8**

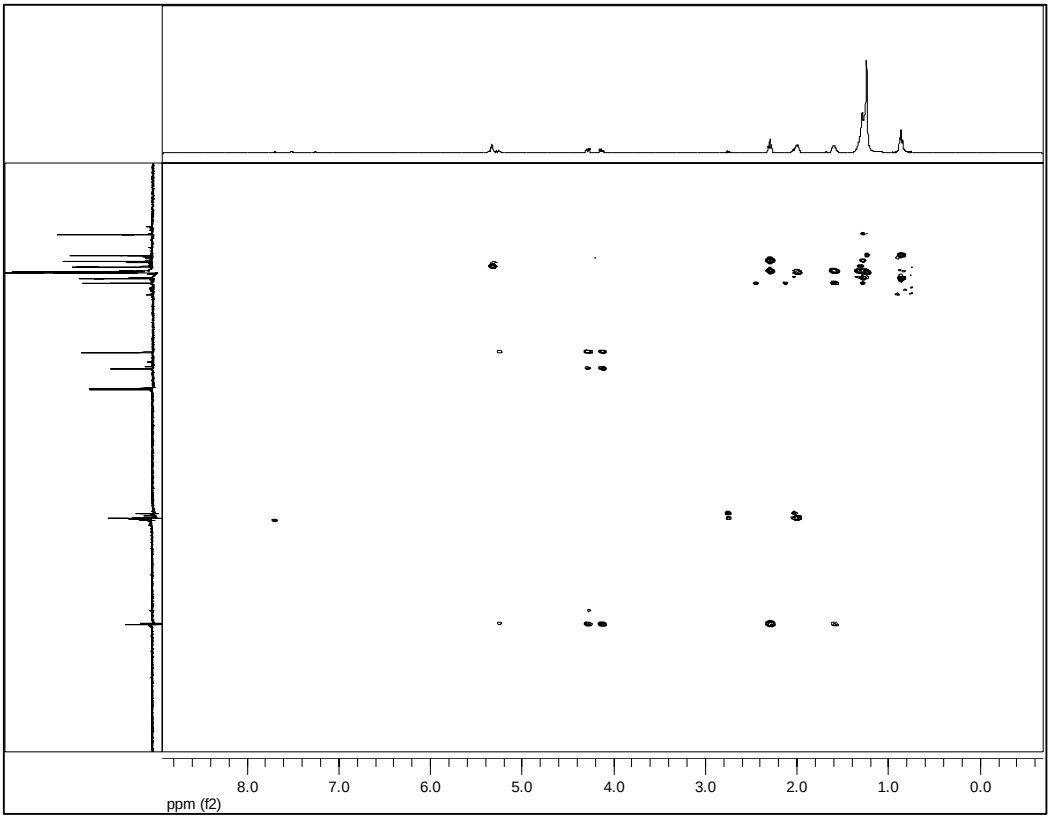

Figure 3.27 The HMBC spectrum of mixture **8**

According to all spectroscopic data, it could be summarized that the separated substance from sub-fraction **Mor3B72** composed of three kinds of triglycerides: 1,3-dilinoleoyl-2-olein, 1,3-dioleoyl-2-linolein and 1,2,3-trilinolein.

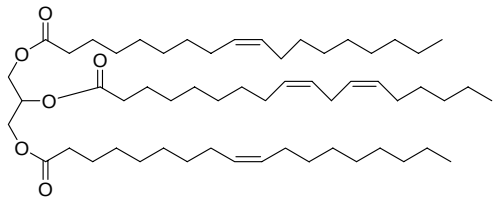

1,3-dilinoleoyl-2-olein

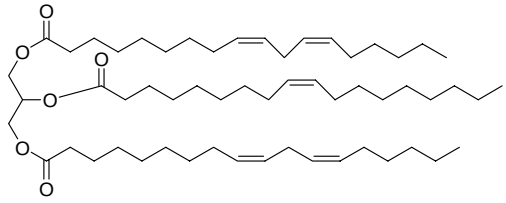

1,3-dioleoyl-2-linolein

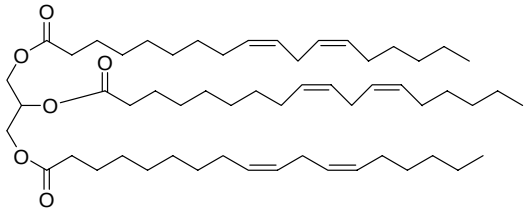

1,2,3-trilinolein

3.22.2 Structural elucidation of compound 9

Compound **9** was obtained as yellow wax (45 mg, 0.02%w/w of Fraction VI) with R_f 0.60 (20%EtOAc/hexane).

The ^{1}H-NMR spectrum ($CDCl_3$) (Fig 3.28) exhibited the chemical shift of the olefinic proton at δ_H 5.30, the bisallylic proton at δ_H 2.70, the α-proton of H-2 at δ_H 2.25 and β-proton of H-3 at δ_H 1.56. The methylene signal was detected as overlapped peaks around δ_H 1.23. The terminal methyl protons were observed at δ_H 0.82. The signal at δ_H 4.50 was assigned to a proton next to an oxygen atom.

The ^{13}C-NMR spectrum ($CDCl_3$) (Fig 3.29) displayed the carbonyl signal of ester group at δ_C 173.0, six olefinic carbons at δ_C 122.5, 128.3, 128.2, 129.7 129.9 and 139.6 and an oxygen-bearing carbon signal at δ_C 56.6. The presence of thirty-three aliphatic carbons of linoleic part could be assigned for the carbon signal at δ_C 14.1, 22.6, 24.7, 25.6, 27.2x2, 29.0x2, 29.1, 29.3, 29.8, 31.5 and 34.6. Two signals at δ_C 36.4 and 41.8 were observed as two quaternary carbons of *β*-sitosterol group. Twenty-seven sp^3 carbons of *β*-sitosterol part were observed in the range of δ_C 11.9-56.3. The assignments of proton and carbon signals of compound **9** are summarized in Table 3.29

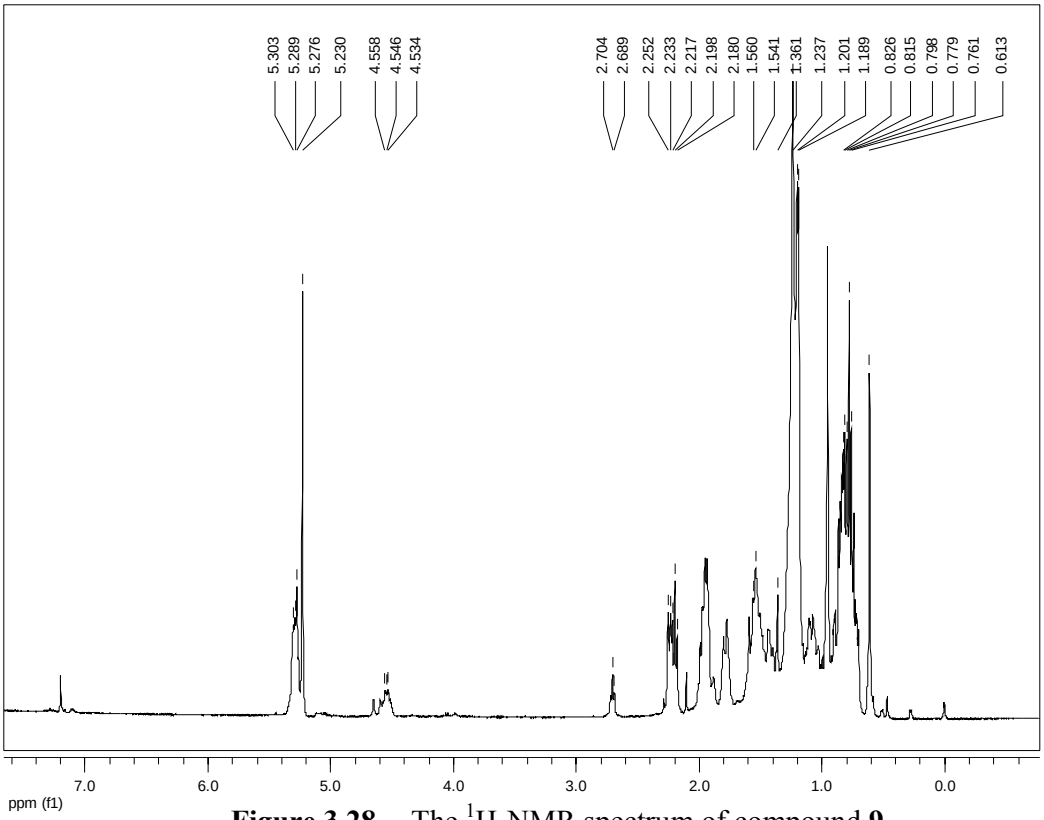

Figure 3.28 The ^{1}H-NMR spectrum of compound **9**

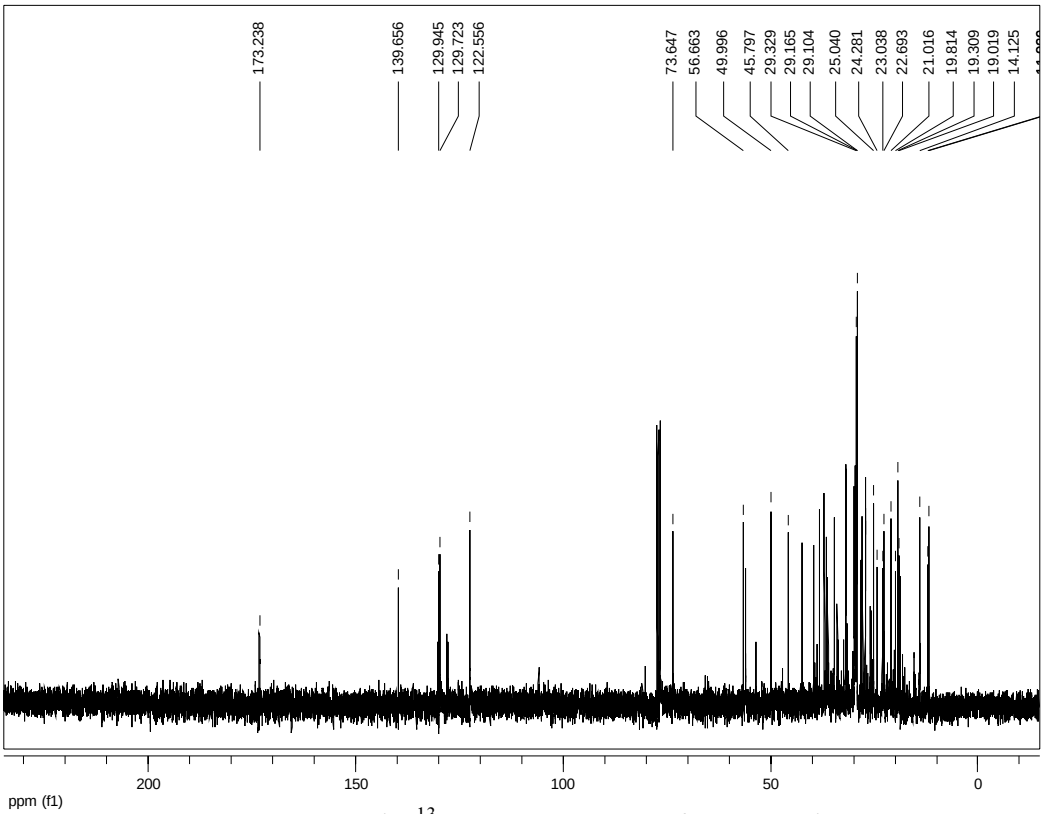

Figure 3.29 The ^{13}C-NMR spectrum of compound **9**

Table 3.29 The ^{1}H- and ^{13}C-NMR chemical shift assignment of compound **9**

Position	^{1}H	^{13}C	Position	^{1}H	^{13}C
C1	*	36.8	C28	*	25.0
C2	*	29.3	C29	0.82	11.9
C3	4.55 (m, 1H)	70.2	C1′	-	173.6
C4	2.20 (t, 2H, *J*= 7.60 Hz)	42.7	C2′	2.21 (br, 2H)	34.6
C5	-	140.0	C3′	1.54 (m, 2H)	24.7
C6	5.20 (m, 1H)	121.3	C4′	*	29.8
C7	2.18 (m, 2H)	31.4	C5′	*	29.3
C8	1.36	31.4	C6′	*	29.1
C9	1.36	49.7	C7′	*	29.0
C10	-	36.4	C8′	1.96 (m, 2H)	27.2
C11	*	21.3	C9′	5.32 (m, 2H)	129.9
C12	*	38.7	C10′	5.32 (m, 2H)	129.7
C13	-	41.8	C11′	2.70 (t, 2H, *J*= 5.5Hz)	25.6
C14	1.36	56.3	C12′	5.26 (m, 2H)	129.7
C15	*	23.9	C13′	5.26 (m, 2H)	129.9
C16	*	28.6	C14′	1.96 (m, 2H)	27.2
C17	1.36	55.6	C15′	*	29.0
C18	0.82	12.5	C16′	*	31.5
C19	0.82	19.6	C17′	*	22.6
C20	1.20	40.8	C18′	0.95 (t, 3H, *J*= 6.87)	14.1
C21	0.82	21.0			
C22	*	21.5			
C23	*	21.6			
C24	1.36	46.02			
C25	1.23	29.34			
C26	0.96 (t, 3H, *J*=6.88)	19.0			
C27	0.96 (t, 3H, *J*=6.88)	19.0			

Note : The methylene signals of compound **9*** were resonated at 1.29 ppm

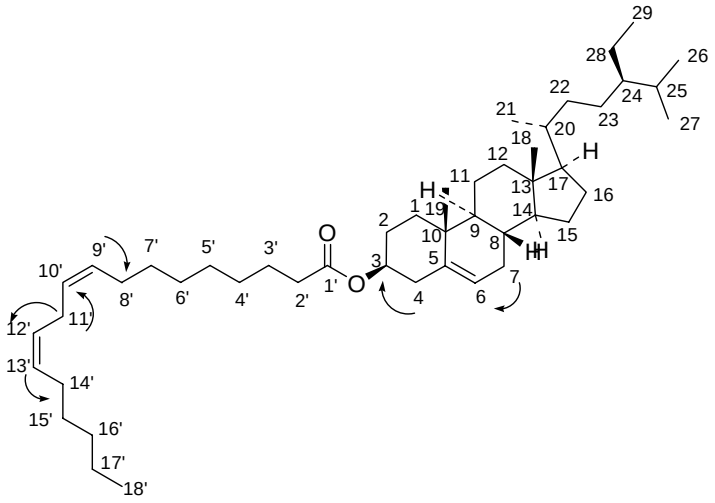

The COSY spectrum of compound **9** (Fig 3.30) reasonably exposed the correlations between H-8′ (δ_H 1.96) and H-9′ (δ_H 5.32), between allylic protons H-8′ (δ_H 1.96), H-14′ (δ_H 1.96) and olefinic protons H-9′, H-13′ (δ_H 5.32), and between bisallylic proton H-11′ (δ_H 2.70) and olefinic protons H-10', H-12' (δ_H 5.32), and between H-3 (δ_H 4.55), and H-4 (δ_H 2.20), and between H-6 (δ_H 5.20),and H-7 (δ_H 2.18), respectively.

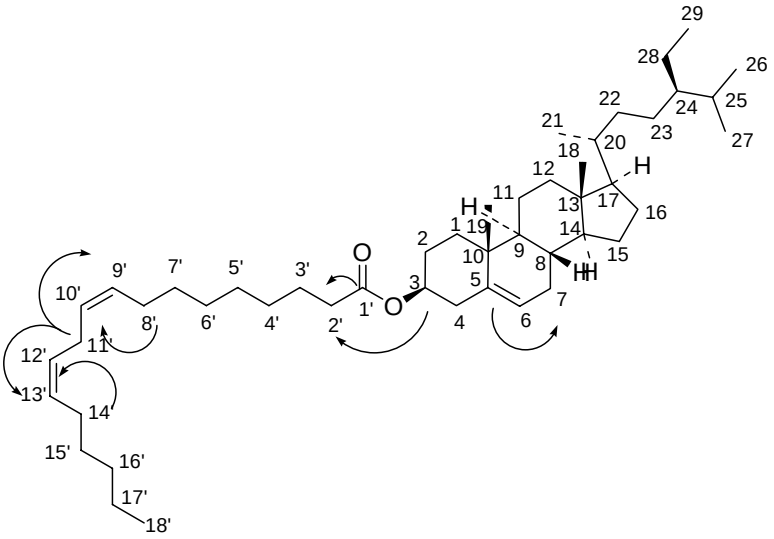

The HMBC spectrum (Fig 3.31) was clearly manifested the correlations between C-1′ (δ_C 173.6) and H-2′ (δ_H 2.20) between C-8′ (δ_C 27.1) and H-10′ (δ_H 5.32), between C-14′ (δ_C 27.2) and H-12′ (δ_H 5.26) between C-11′ (δ_C 25.6) and H-9′ (δ_H 5.32), H-13′ (δ_H 5.26) between C-3 (δ_C 70.2) and H-2′ (δ_H 2.21), C-5 (δ_C 140.0) and H-7 (δ_H 2.18), respectively.

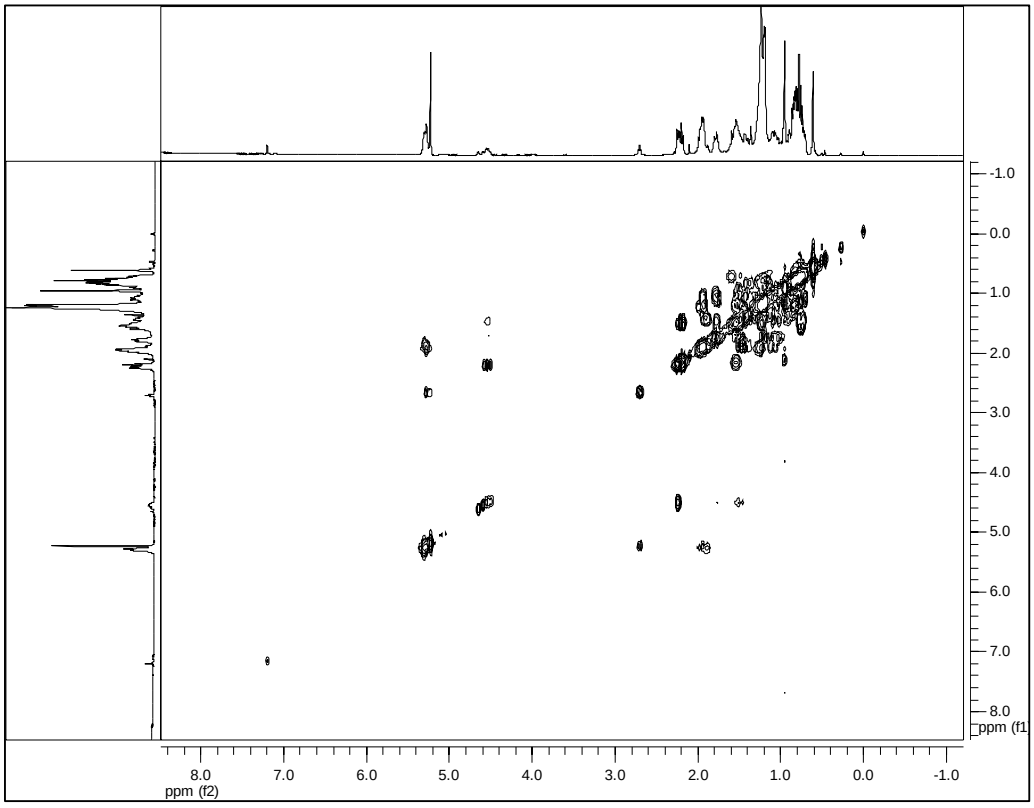

Figure 3.30 The COSY spectrum of compound **9**

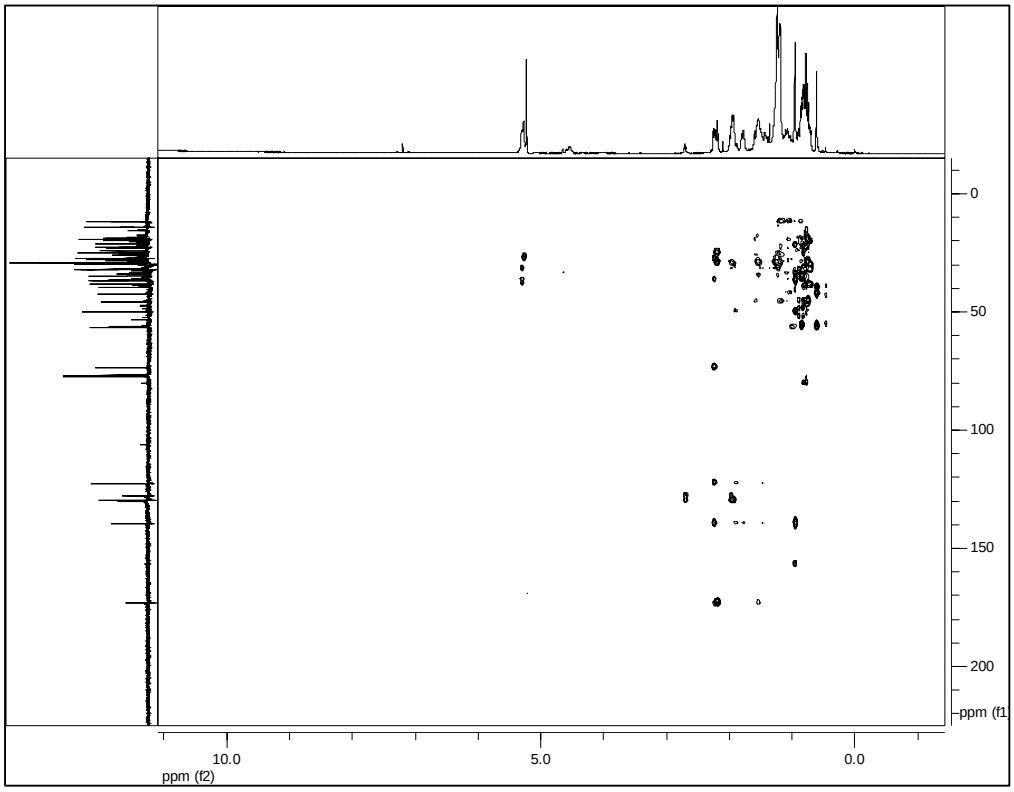

Figure 3.31 The HMBC spectrum of compound **9**

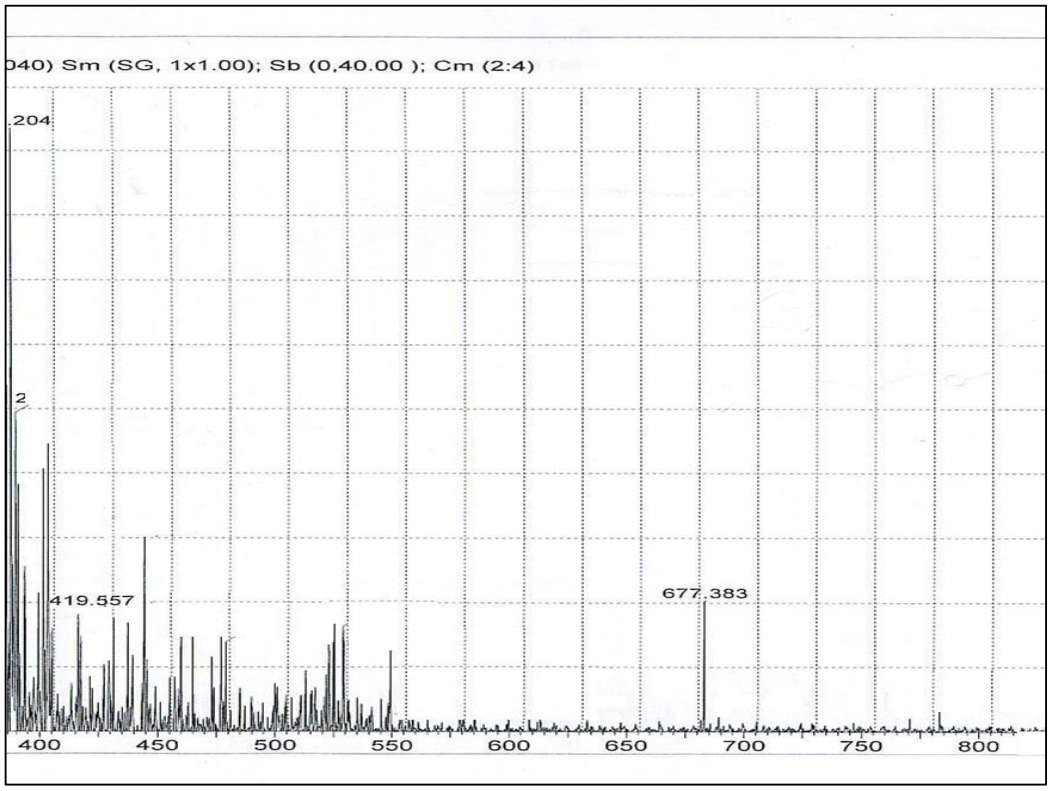

Figure 3.32 The mass spectrum of compound **9**

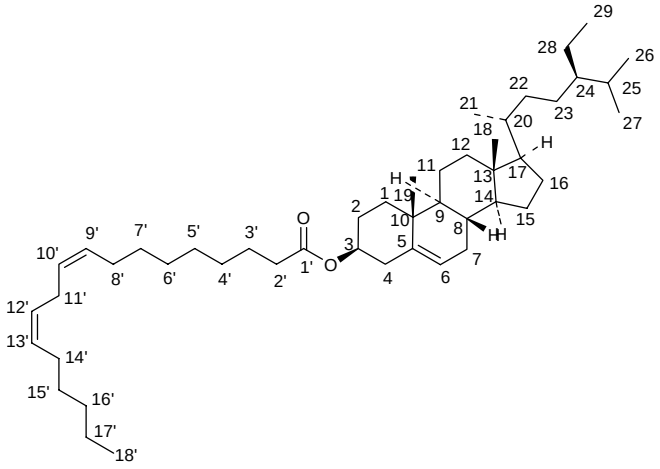

β-sitosteryl linoleate

To confirm the molecular weight of compound 9, this compound was further analyzed by ESI-MS-MS technique. The mass spectrum (Fig 3.32) provided a molecular ion $[M+1]^+$ peak at 677.

From the aforementioned data, this compound was truly identified as *β*-sitosteryl linoleate.

17.73 g of sub-fraction **Mor3** was re-separated by silica gel column eluting with 100%hexane-50%EtOAc/hexane as a solvent system. The further separation of sub-fraction **Mor3E (**20%EtOAc/hexane) yielded compound **10** (Table 3.21).

3.22.3 Structural elucidation of compound 10

Compound **10** was obtained as a pale yellow oil (890 mg, 1.89% w/w of Fraction VI) with R_f 0.59 (hexane/ether 6:1).

The ^{1}H-NMR spectrum ($CDCl_3$) (Fig 3.33) exhibited the chemical shift of olefinic proton and α-proton of a carbonyl group at δ_H 5.32 and 2.33, respectively. The signals at δ_H 2.04, 1.61 and 0.87 could be assigned for allylic, β- and methyl protons, respectively. The presence of the signals at δ_H 4.08, 5.20 and 4.12 were assigned to the protons at H-1′, H-2′ and H-3′ positions [31].

The ^{13}C-NMR spectrum (Fig 3.34) displayed three carbonyl signals for an ester group of C-1′ and C-1‴ at δ_C 174.3 and another signal at δ_C 173.4 of C-1″. The signals at δ_C 129.6 and 129.9 for six olefinic carbons were exhibited. Three carbons connected with oxygen atom were inferred from the observation of three carbon signals at δ_C 62.1 and 68.9. Forty-eight sp^3 carbons were in addition observed at δ_C 14.2-34.2. All spectroscopic data of this compound were compared with that of reported data. Therefore, this isolated compound was truly 1,2,3-triolein and its structure is shown below.

The tentative assignments of ^{1}H and ^{13}C-NMR chemical shifts of compound **10** are tabulated in Table 3.30.

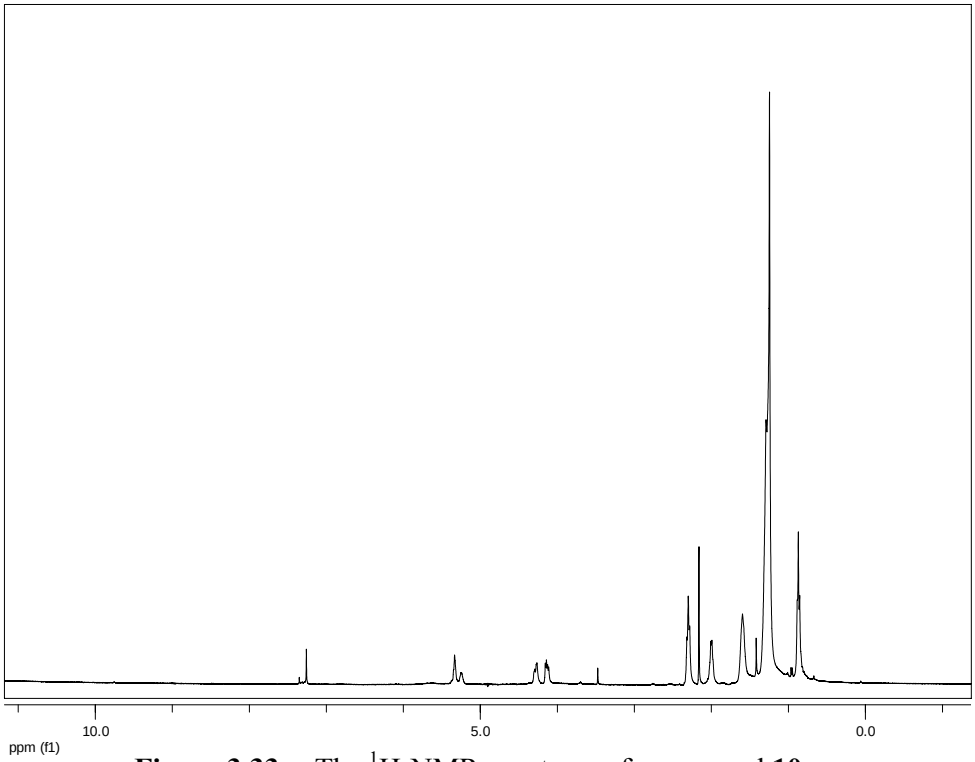

Figure 3.33 The ^{1}H-NMR spectrum of compound **10**

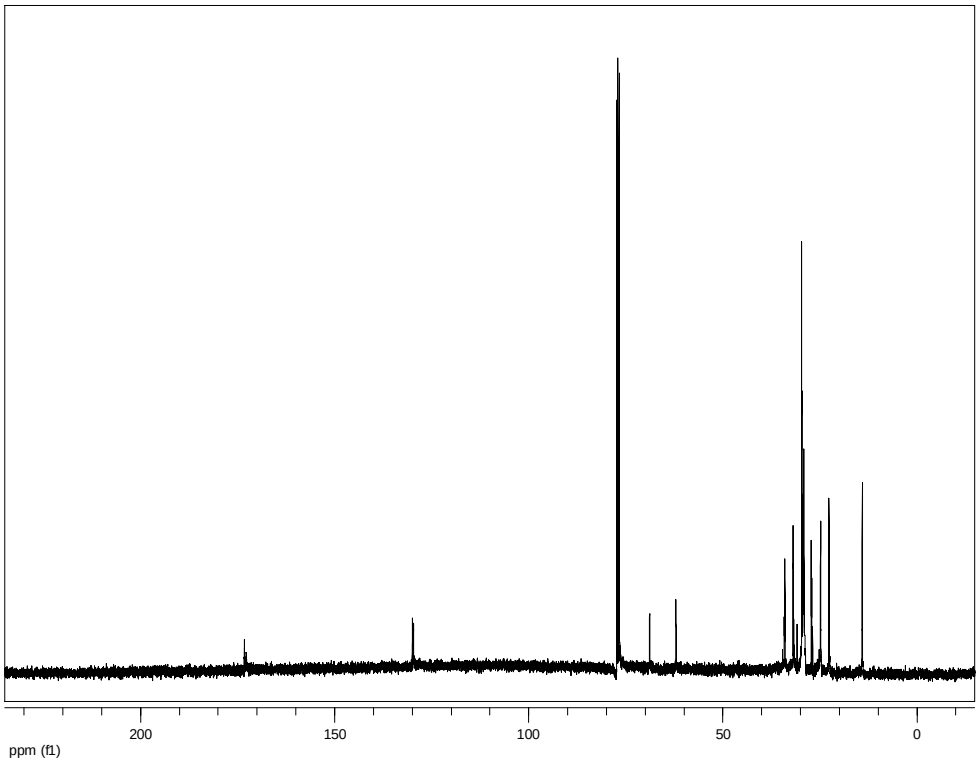

Figure 3.34 The ^{13}C-NMR spectrum of compound **10**

Table 3.30 The ^{1}H and ^{13}C chemical shift assignment of 1,2,3-triolein [31]

Position	Chemical shift(ppm)		Position	Chemical shift(ppm)		Position	Chemical shift(ppm)	
	^{1}H	^{13}C		^{1}H	^{13}C		^{1}H	^{13}C
1′	-	173.2	1″	-	173.1	1‴	-	173.2
2′	2.32	34.2	2″	2.32	34.1	2‴	2.32	34.2
3′	1.61	24.8	3″	1.61	24.8	3‴	1.61	24.8
4′	*	29.7	4″	*	29.7	4‴	*	29.7
5′	*	29.6	5″	*	29.5	5‴	*	29.6
6′	*	29.2	6″	*	29.2	6‴	*	29.2
7′	*	29.1	7″	*	29.1	7‴	*	29.1
8′	2.02	27.2	8″	2.02	27.2	8‴	2.02	27.2
9′	} 5.33	129.9	9″	} 5.33	129.9	9‴	} 5.33	129.9
10′		129.6	10″		129.6	10‴		129.6
11′	2.03	27.2	11″	2.03	27.2	11‴	2.03	27.2
12′	*	29.3	12″	*	29.9	12‴	*	29.3
13′	*	29.2	13″	*	29.2	13‴	*	29.2
14′	*	29.1	14″	*	29.8	14‴	*	29.1
15′	*	30.0	15″	*	28.2	15‴	*	30.0
16′	*	32.5	16″	*	30.0	16″	*	32.5
17′	*	23.1	17″	*	24.1	17″	*	23.1
18′	0.87	14.2	18″	0.87	14.2	18″	0.87	14.2
1	4.12	62.1						
2	5.20	68.9						
3	4.12	62.1						

Note : The methylene signals of 1,2,3-triolein * were resonated at 1.29 ppm

Table 3.31 The ^{1}H and ^{13}C chemical shift assignment of compound **10**

Position	Chemical shift (ppm)		Position	Chemical shift (ppm)		Position	Chemical shift (ppm)	
	^{1}H	^{13}C		^{1}H	^{13}C		^{1}H	^{13}C
1′	-	174.3	1″	-	173.1	1‴	-	174.3
2′	2.32	34.2	2″	2.32	34.1	2‴	2.32	34.2
3′	1.61	24.8	3″	1.61	24.5	3‴	1.61	24.8
4′	*	29.7	4″	*	29.7	4‴	*	29.7
5′	*	29.6	5″	*	29.6	5‴	*	29.6
6′	*	29.2	6″	*	29.2	6‴	*	29.2
7′	*	29.1	7″	*	29.1	7‴	*	29.1
8′	2.04	27.2	8″	2.04	27.1	8‴	2.04	27.2
9′	} 5.33	129.9	9″	} 5.33	129.9	9‴	} 5.33	129.9
10′		129.6	10″		129.6	10‴		129.6
11′	2.04	27.2	11″	2.04	27.2	11‴	2.04	27.2
12′	*	29.3	12″	*	29.6	12‴	*	29.3
13′	*	29.2	13″	*	29.2	13‴	*	29.2
14′	*	29.1	14″	*	29.3	14‴	*	29.1
15′	*	30.0	15″	*	28.2	15‴	*	30.0
16′	*	32.5	16″	*	30.0	16‴	*	32.5
17′	*	23.1	17″	*	24.1	17‴	*	23.1
18′	0.87	14.2	18″	0.87	14.2	18‴	0.87	14.2
1	4.08	62.1						
2	5.20	68.9						
3	4.12	62.1						

Note : The methylene signals of compound 10* were resonated at 1.29 ppm

Additionally, the structure of compound **10** was deduced from the analysis of COSY and HMBC spectra. The COSY spectrum of compound **10** (Fig 3.35) reasonably exposed the correlations between H-1 (δ_H 4.08) and H-2 (δ_H 5.20), between H-3 (δ_H 4.12) and H-2 (δ_H 5.20), between H-2′ (δ_H 2.32) and H-3′ (δ_H 1.61),

between allylic protons H-8′ (δ_H 2.02), H-11′ (δ_H 2.04) and olefinic proton H-9′ (δ_H 5.33), H-10′ (δ_H 5.33), respectively.

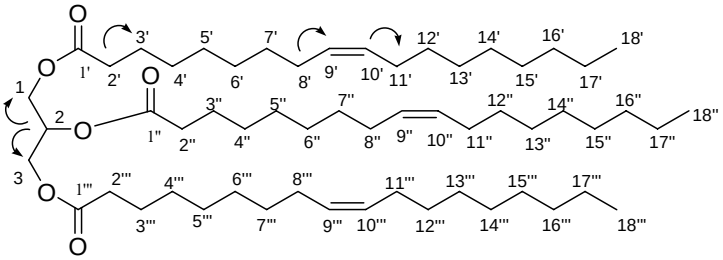

The HMBC spectrum (Fig 3.36) clearly manifested the correlations between C-1′ (δ_C 174.3) and H-2′ (δ_H 2.32), H-3′ (δ_H 1.61), H-1 (δ_H 4.08), between C-8′ (δ_C 27.2) and H-10′ (δ_H 5.33), between C-1 (δ_C 62.1) and H-2 (δ_H 5.20) between C-1′′′ (δ_C 174.3) and H-2′′′ (δ_H 2.32), H-3′′′ (δ_H 1.61), H-3 (δ_H 4.12), respectively.

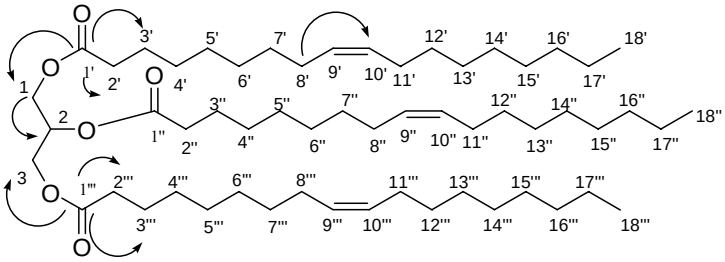

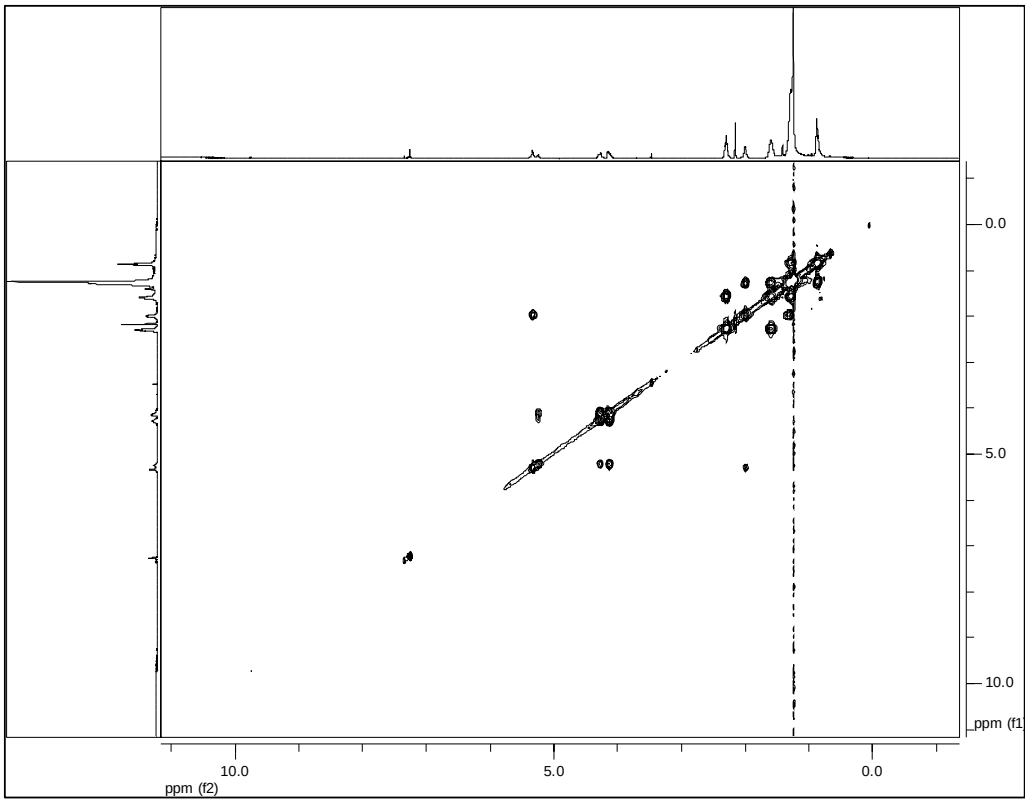

Figure 3.35 The COSY spectrum of compound **10**

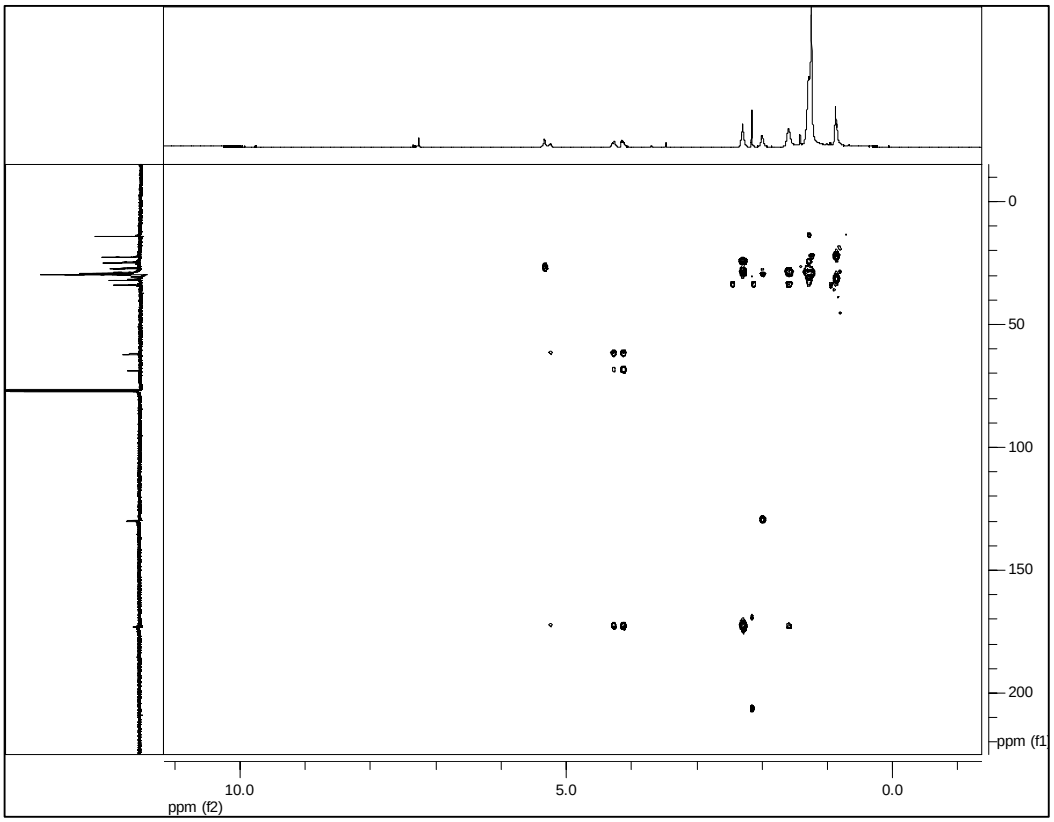

Figure 3.36 The HMBC spectrum of compound **10**

3.23 Separation of sub-fraction Mor4

3.45 g of sub-fraction **Mor4** was re-separated by silica gel column eluting with 100%hexane-80%EtOAc/hexane. The results of the separation are presented in Table 3.32.

Table 3.32 The separation of sub-fraction **Mor4**

Fraction	Solvent system	Remarks	Weight(g)
Mor4A	100%hexnae	Brownish solid	0.56
Mor4B	10%EtOAc/Hexane	Brownish solid + substance **11**	0.23
Mor4C	20%EtOAc/Hexane	Brownish solid + substance **12**	0.12
Mor4D	30-40%EtOAc/Hexane	Dark brown semisolid	1.22
Mor4E	50-80%EtOAc/Hexane	Dark brown semisolid	0.58

The separation of **Mor4B** yielded bright white plate, substance **11** (0.23 g, 0.51%w/w of Fraction VI). Its spectroscopic data was resemble to that of substance **1**, thus this substance was a long chain alcohol.

The separation of **Mor4C** gave white powder solid, substance **12** (0.12 g, 0.25%w/w of Fraction VI). According to the ^{1}H-NMR spectrum, it was close to that of substance **2,** thus this substance should be a long chain ketone.

Sub-fraction **Mor5** was a white solid, 1.23 g, 2.61% w/w of Fraction VI. According to the ^{1}H- and ^{13}C-NMR spectra and GC, this mixture was found to be the same as mixture **3**.

3.24 Separation of sub-fraction Mor6

Sub-fraction **Mor6** 2.56 g was obtained from the separation of Fraction VI eluting by 40-60% EtOAc/hexane. This fraction was further separated with silica gel column using a mixture of CH_2Cl_2 and hexane and the results are presented in Table 3.33.

Table 3.33 The results of the separation of sub-fraction **Mor6**

Fraction	Solvent system	Remarks	Weight(g)
Mor6A	25%CH_2Cl_2/hexane	Write soild + compound **11**	23 mg
Mor6B	25%CH_2Cl_2/hexane	Brownish solid	1.86
Mor6C	25%CH_2Cl_2/hexane	Brownish solid	1.15
Mor6D	25%CH_2Cl_2/hexane	Brownish solid	0.36

3.24.1 Structural elucidation of compound 11

Compound **11** as white oil (23 mg, 0.05%w/w of Fraction VI) R_f 0.48 (50% EtOAc/hexane), m.p. 127°C. This compound was soluble in $CHCl_3$, CH_2Cl_2 and EtOAc.

This compound was subjected to GC-MS. The GC-MS analysis revealed the retention time at 14.22 min (Figs 3.37-3.38). From the comparison of the mass spectrum with standard data, it was found that retention time showed the molecular ion peak, M^+, at *m/z* 121, corresponding to C_7H_7NO (Calcd. MW 121.05) and other important fragmentation peaks at *m/z* 105 and 77 (Fig 3.38).

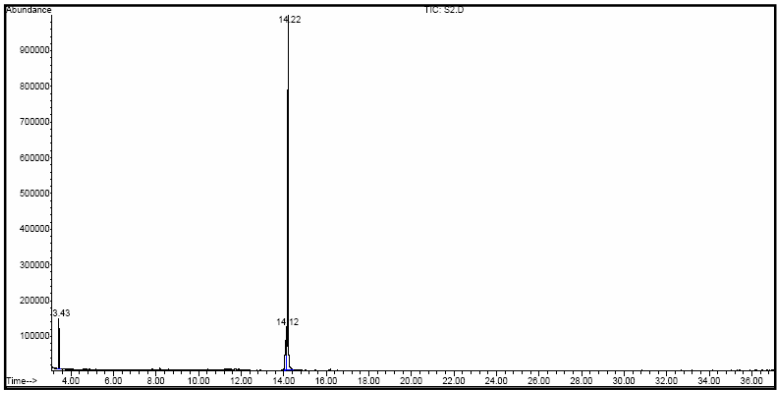

Figure 3.37 The GC chromatogram of compound **11**

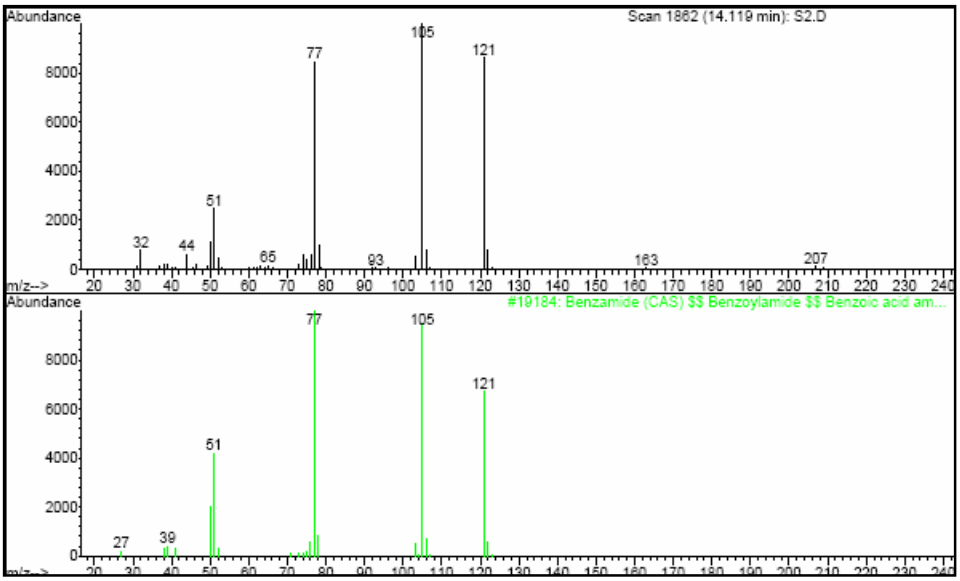

Figure 3.38 The mass spectrum of compound **11**

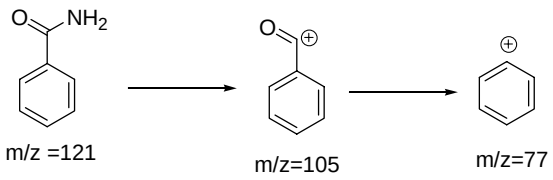

The IR spectrum of this mixture (Fig 3.39), exhibited the absorption peaks of amid in region of 3358 cm^{-1}, carbonyl group at 1648 cm^{-1}. Other signals were tentatively assigned in Table 3.34.

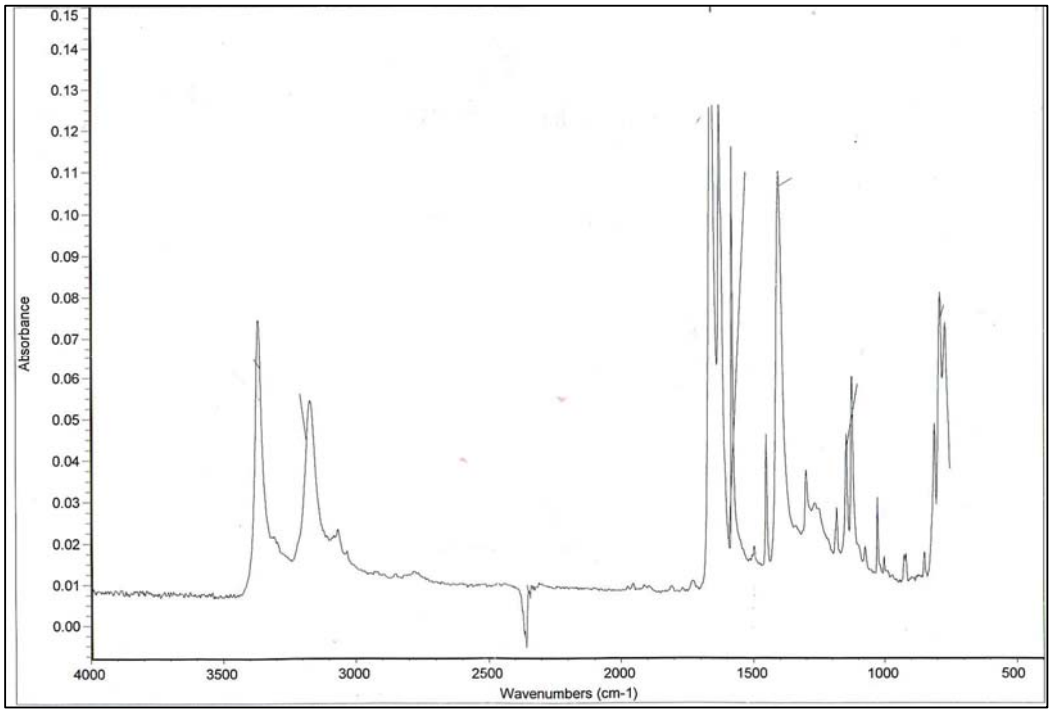

Figure 3.39 The IR absorption band assignments of compound **11**

Table 3.34 The IR absorption band assignment of compound **11**

Wavenumber (cm^{-1})	**Intensity**	**Tentation assignments**
3100-3300	Strong	N-H stretching vibration of amide
1648	Strong	C=O stretching vibration of carbonyl

The ^{1}H-NMR spectrum of compound **11** (Fig 3.40) exhibited the signals of the aromatic protons for H-1 at δ_H 7.53, for H-2 and H-6 at δ_H 7.41, for H-3 and H-5 at δ_H 7.82.

The ^{13}C-NMR spectrum ($CDCl_3$) of compound **11** (Fig 3.41) displayed the important carbon signals at δ_C 169.0 of carbonyl group. The carbon signals of C-3,5 at δ_C 127.0, C-2,6 at δ_C 128.0, C-1 at δ_C 131.0 and C-4 at δ_C 133.0 were also observed.

The tentative ^{1}H- and ^{13}C-NMR chemical shift assignments of compound **11** compared with that of reported benzamide are tabulated in Table 3.35.

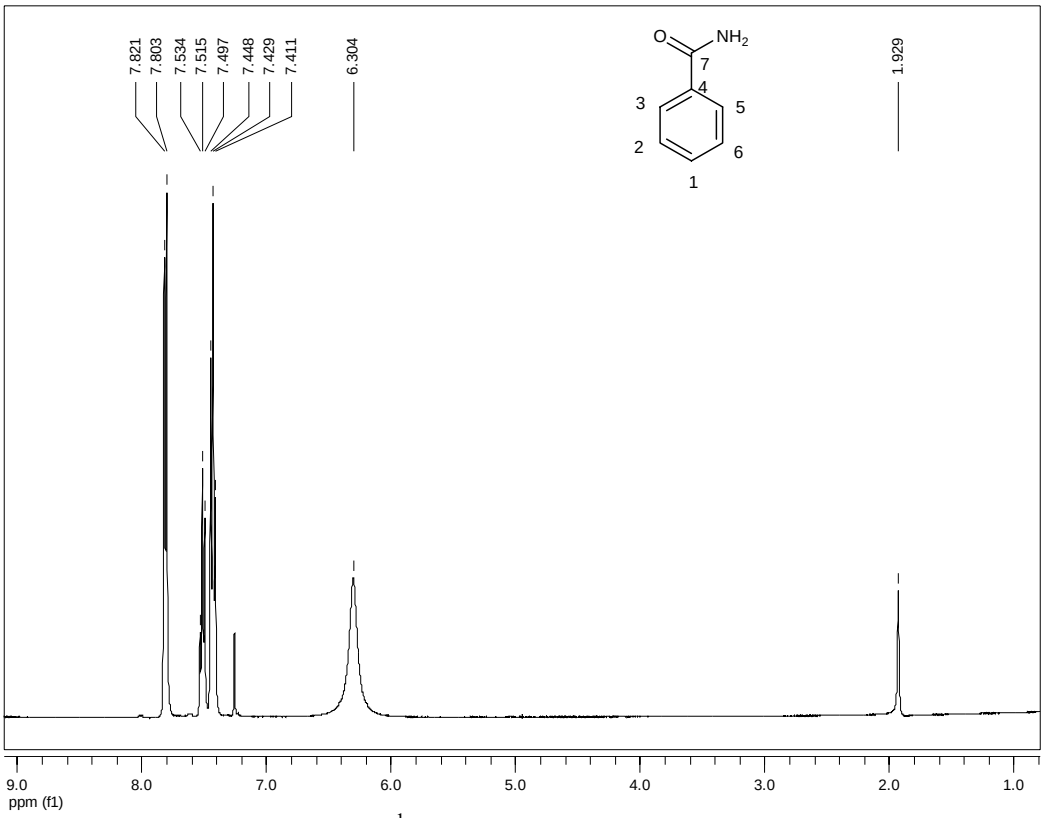

Figure 3.40 The ^{1}H-NMR spectrum of compound **11**

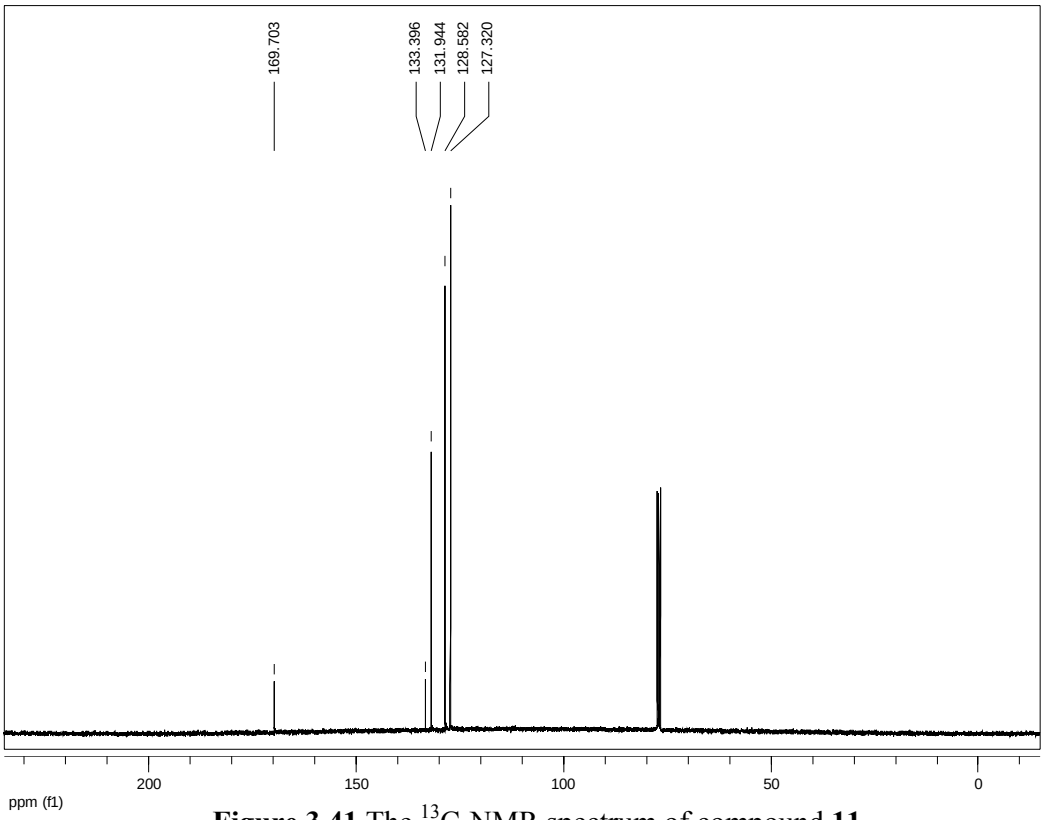

Figure 3.41 The ^{13}C-NMR spectrum of compound **11**

Table 3.35 The ^{1}H and ^{13}C-NMR chemical shift assignment of compound **11**

Position	Chemical shift (ppm) Compound **11**		Position	Chemical shift (ppm) **Benzamid [32]**	
	^{1}H	^{13}C		^{1}H	^{13}C
1	7.53 (t, 1H, *J* = 7.30 Hz)	131.0	1	7.53 (t, 1H, *J* = 7.33 Hz)	131.0
2	7.41 (t, 2H, *J* = 7.70 Hz)	128.0	2	7.43 (t, 2H, *J* = 7.75 Hz)	128.0
3	7.82 (d, 2H,*J* = 7.30 Hz)	127.0	3	7.80 (d, 2H, *J* = 7.33 Hz)	127.0
4	-	133.0	4	-	133.0
5	7.82 (d, 2H, *J* = 7.30 Hz)	127.0	5	7.82 (d, 2H,*J* = 7.32 Hz)	127.0
6	7.41 (t, 2H, *J* = 7.70 Hz)	128.0	6	7.41 (t, 2H, *J* = 7.70 Hz)	128.0
7	-	169.0	7	-	169.0

3.25 Separation of sub-fraction Mor7

4.23 g of sub-fraction **Mor7** in 60-70% EtOAc/hexane was further separated with silica gel column using a mixture of EtOAc and hexane. The results of the separation of this sub-fraction are presented in Table 3.36.

Table 3.36 The results of the separation of sub-fraction **Mor7**

Fraction	Solvent system	Remarks	Weight(g)
Mor7A	50-60% EtOAc/hexane	Write soil + compound **12**	4.23
Mor7B	60-70% EtOAc/hexane	Brownish solid	1.86

3.25.1 Structural elucidation of compound 12

Compound **12** (1.50 g, 3.19%w/w of CH_2Cl_2 crude extract) was obtained from sub-fraction compound **12** by eluting with 60-70%EtOAc/hexane. This compound had m.p. 203-206 $^{\circ}C$ and R_f 0.75 (80% MeOH/H_2O). Compound **12** gave a violet color to Liebermann-Burchard indicating the presence of triterpenoidal skeleton.

The ^{1}H-NMR spectrum (DMSO-d_6) of this compound (Fig 3.42) showed the signals in the range of δ_H 0.53-2.39, which were the signals of CH_3, CH_2 and CH groups of steroid. The multiplet signals at δ_H 2.85-3.15 were assigned to the protons of a sugar moiety. The proton on the carbon attached to a hydroxyl group appeared as the multiplet signal at δ_H 3.58 and the signal at δ_H 4.20 belonged to the anomeric proton. The multiple signal at δ_H 5.20 was the signal of trisubstituted vinyl proton (-CH=C-).

The ^{13}C-NMR spectrum (DMSO-d_6) of this compound (Fig 3.43) revealed a group of six carbon signals resonated at δ_C 106.0, 75.8, 77.4, 72.0, 76.6 which were assigned for C1′, C2′, C3′,C4′, C5′ and C6′ respectively. Table 3.37 summarizes the ^{13}C-NMR assignment of compound **12** compared with *β*-sitosterol-3-*O*-*β*-D-gluco-pyranoside.

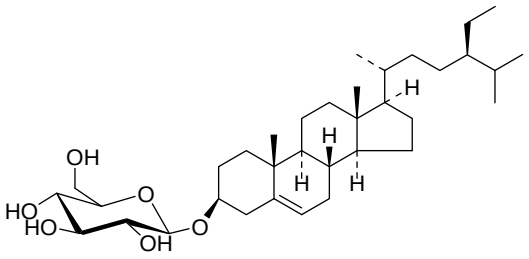

β-sitosterol-3-*O*-*β*-D-glucopyranoside

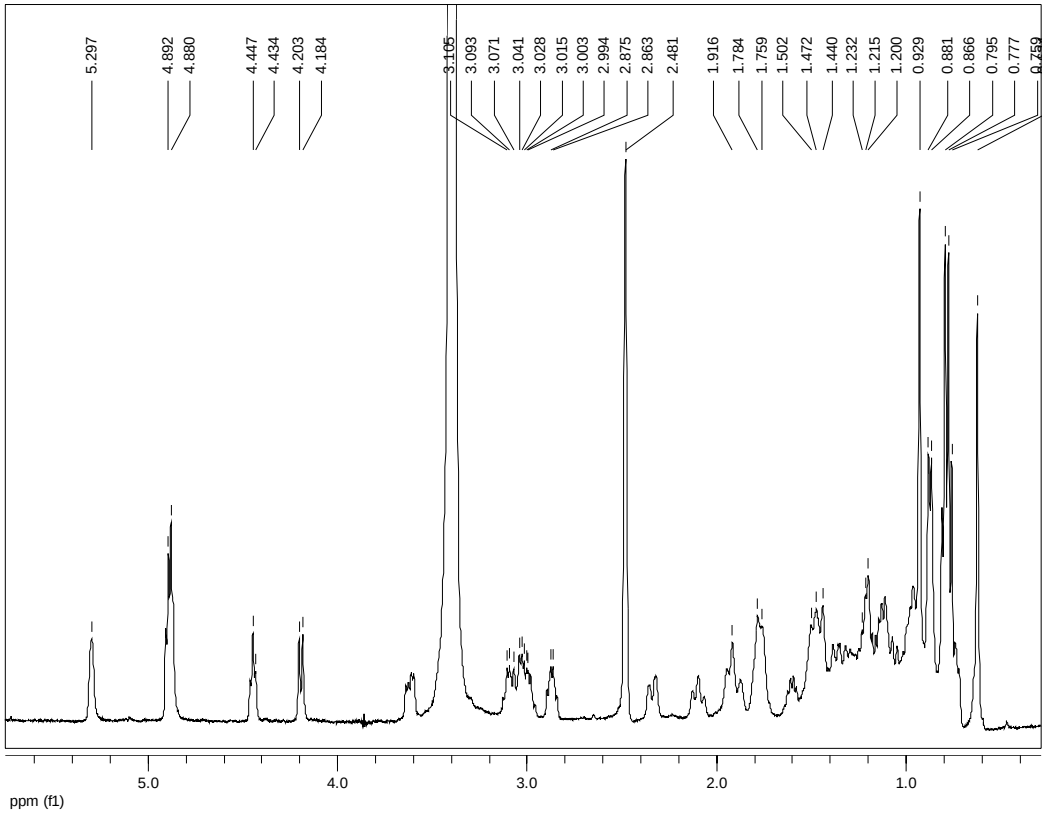

Figure 3.42 The ^{1}H-NMR spectrum of compound **12**

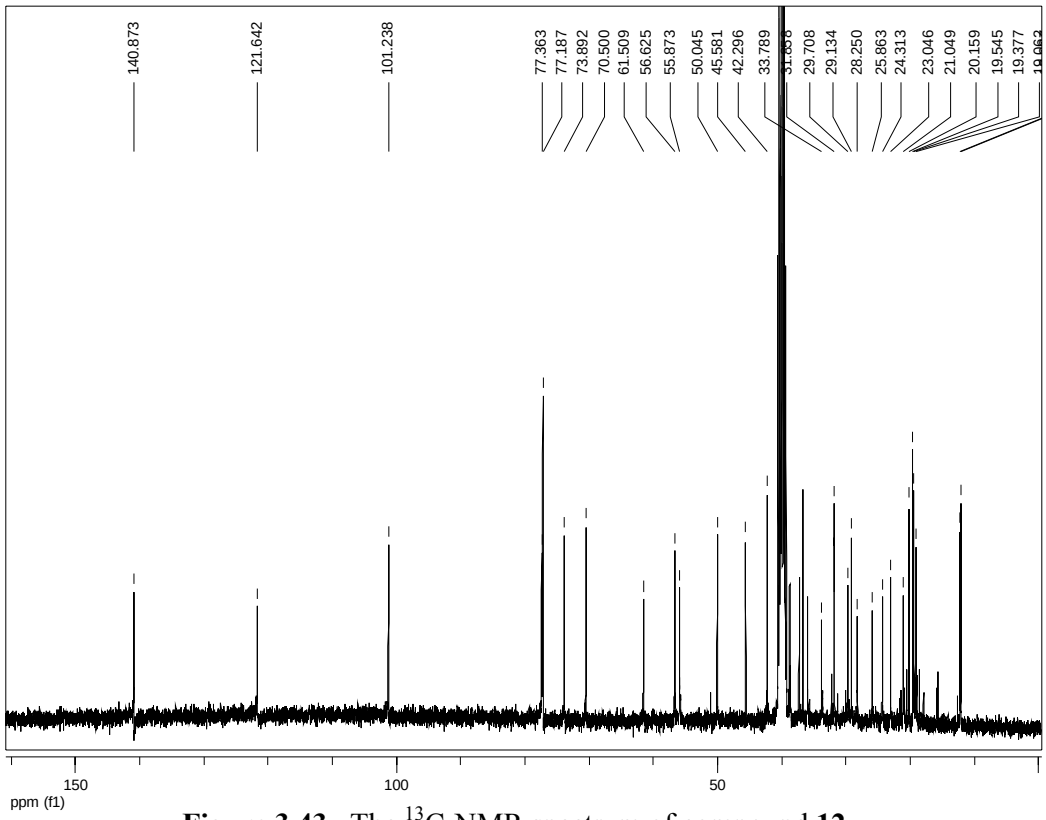

Figure 3.43 The ^{13}C-NMR spectrum of compound **12**

Table 3.37 The ^{13}C-NMR assignment of compound **12** and *β*-sitosterol-3-*O*- *β*-D-glucopyranoside

Carbon	**Chemical(ppm)**	
	Compound **12**	***β*-sitosterol -3-*O*- *β*-D-glucopyranoside [27]**
C1	36.7	37.5
C2	31.9	30.3
C3	77.4	78.2
C4	39.4	39.4
C5	140.9	140.9
C6	121.6	121.9
C7	31.8	32.2
C8	33.8	32.1
C9	50.0	50.4
C10	36.7	36.9
C11	21.0	21.3
C12	39.3	39.9
C13	42.3	42.5
C14	56.6	56.9
C15	24.3	24.6
C16	28.3	28.6
C17	56.6	56.3
C18	12.0	12.0
C19	19.3	19.3
C20	36.7	36.4
C21	19.0	19.1
C22	33.8	34.3
C23	25.9	26.4
C24	45.6	46.1
C25	29.7	29.5
C26	19.2	19.5
C27	20.5	20.0
C28	23.0	23.4
C29	12.6	12.2
C1′	101.2	102.6
C2′	77.2	75.4
C3′	77.4	78.7
C4′	70.5	71.8
C5′	77.4	78.5
C6′	61.5	62.9

3.26 Synthesis of benzamides and esters

Since benzamide, isolated from the CH_2Cl_2 crude extract from the roots exhibited promising antioxidant activity, benzamide derivatives was therefore prepared to search for new and potent antioxidants. Moreover, certain ester derivatives were synthesized to thoroughly analyze the structure-activity relationships of benzamide and ester derivatives.

3.26.1 Structural elucidation of compound A

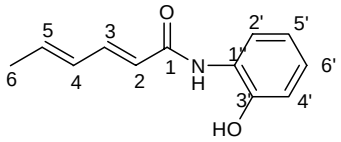

compound **A**

The structure of compound **A** was deduced from the analysis of COSY and HMBC. The COSY spectrum of compound **A** (Fig A-3) reasonably exposed correlations between H-6 (δ_H 1.80) and H-5 (δ_H 5.99), between H-4 (δ_H 6.15) and H-3 (δ_H 7.31), between H-2′ (δ_H 7.10) and H-5′ (δ_H 7.01), between H-5′ (δ_H 7.01) and H-6′ (δ_H 7.09), respectively.

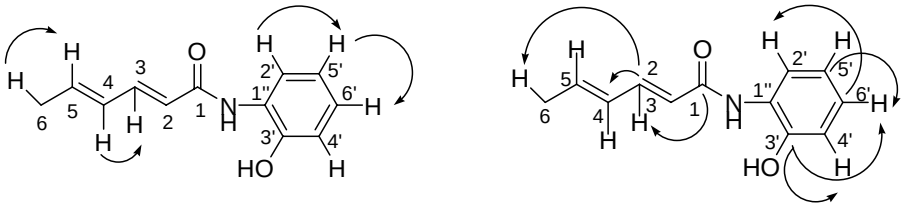

COSY **HMBC**

The HMBC spectrum of compound A (Fig A-4) reasonably exposed correlations between C-3 (δ_C 145.0) with H-6 (δ_H 1.80) and H-4 (δ_H 6.15), between C-3′ (δ_C 149.0) with H-4′ (δ_H 6.80) and H-6′ (δ_H 7.09) between C-6′ (δ_C 126.0) with H-2′ (δ_H 7.10), between C-5′ (δ_C 119.0), with H-6′ (δ_H 7.09) and between C-1 (δ_C 166.0), with H-3 (δ_H 7.31), respectively.

3.26.2 Structural elucidation of compound B

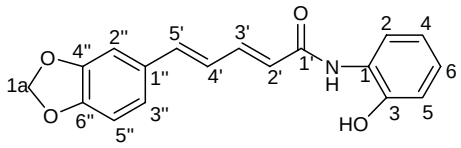

The structure of compound **B** was deduced from the analysis of COSY and HMBC. The COSY spectrum of compound **B** (Fig B-3) clearly exposed the correlations between H-5″ (δ_H 6.94) and H-3″ (δ_H 7.41) between H-5′ (δ_H 7.06) and H-4′ (δ_H 6.85) between H-4′ (δ_H 6.85) and H-3′ (δ_H 6.85) and between H-2 (δ_H 7.47) and H-4 (δ_H 6.91), respectively.

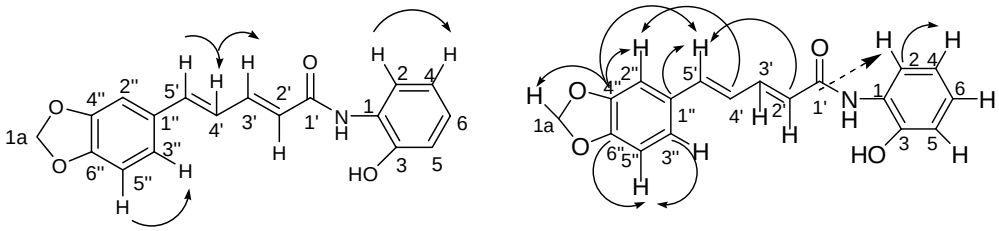

COSY **HMBC**

The HMBC spectrum of compound **B** (Fig B-4) manifestly revealed the correlations between C-4″ (δ_C 148.4) and H-2″ (δ_H 7.22) and H-5′ (δ_H 7.06) and H-1a, (δ_H 6.06) between C-6″ (δ_C 148.0) and H-5″ (δ_H 6.94) between C-3″ (δ_C 119.7) and H-5″ (δ_H 6.94), between C-1″ (δ_C 128.0) and H-5′ (δ_H 7.06), between C-4′ (δ_C 122.2) and H-2″ (δ_H 7.22) between C-2′ (δ_C 121.7) and H-5′ (δ_H 7.06) between C-1′ (δ_C 166.0) and H-2 (δ_H 7.47) and C-2 (δ_C 123.0) and H-4 (δ_H 6.91), respectively.

3.26.3 Structural elucidation of compound C

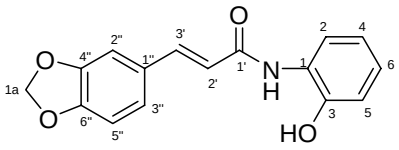

The structure of compound **C** was deduced from the analysis of COSY and HMBC**.** The COSY spectrum of compound **C** (Fig C-3) clearly indicated the correlations between H-5″ (δ_H 6.94) and H-3″ (δ_H 6.88) between H-3′ (δ_H 7.46) and H-2′ (δ_H 2.80) between H-2 (δ_H 7.72) and H-4 (δ_H 7.00) between H-4 (δ_H 7.00) and H-6 (δ_H 6.94) and between H-6 (δ_H 6.94) and H-5 (δ_H 6.88), respectively.

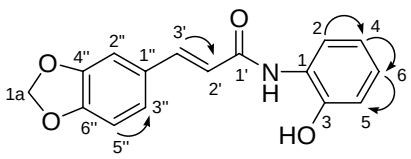

COSY

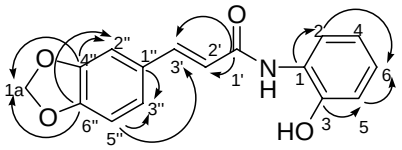

HMBC

The HMBC spectrum of compound **C** (Fig C-4) undoubtedly exposed the correlations between C-4″ (δ_C 148.7) and H-1a (δ_H 6.06) and H-2″ (δ_H 7.20) between C-6″ (δ_C 148.0) and H-1a (δ_H 6.06), H-2″ (δ_H 7.20) between C-5″ (δ_C 109.0) and H-3″ (δ_H 6.88), H-3′ (δ_H 7.46) between C-1′ (δ_H 165.0) and H-2′ (δ_H 6.80), H-3′ (δ_H 7.46) between C-1 (δ_C 125.0) and H-2 (δ_H 7.72) between C-2 (δ_C 122.0) and H-6 (δ_H 6.94) between C-3 (δ_C 148.0) and H-5 (δ_H 6.88) between C-5 (δ_C 116.1) and H-6 (δ_H 6.94), respectively.

3.26.4 Structural elucidation of compound I

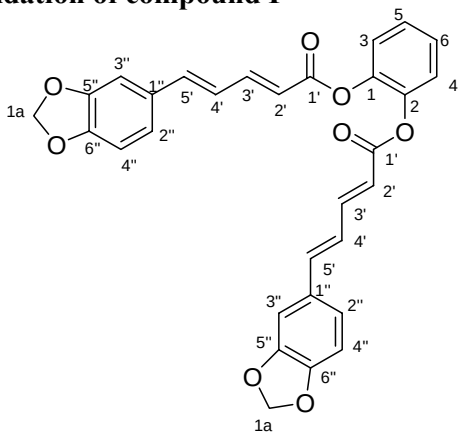

The structure of compound **I** was deduced from the analysis of COSY and HMBC. The COSY spectrum of compound **C** (Fig I-3) reasonably exposed the correlations between H-4″ (δ_H 7.06) and H-2″ (δ_H 6.83) between H-5′ (δ_H 7.76) and H-4′ (δ_H 6.83) between H-3′ (δ_H 6.85) and H-2′ (δ_H 6.74) between H-3 (δ_H 7.04) and H-5 (δ_H 7.05) between H-4 (δ_H 7.38) and H-6 (δ_H 7.38), respectively.

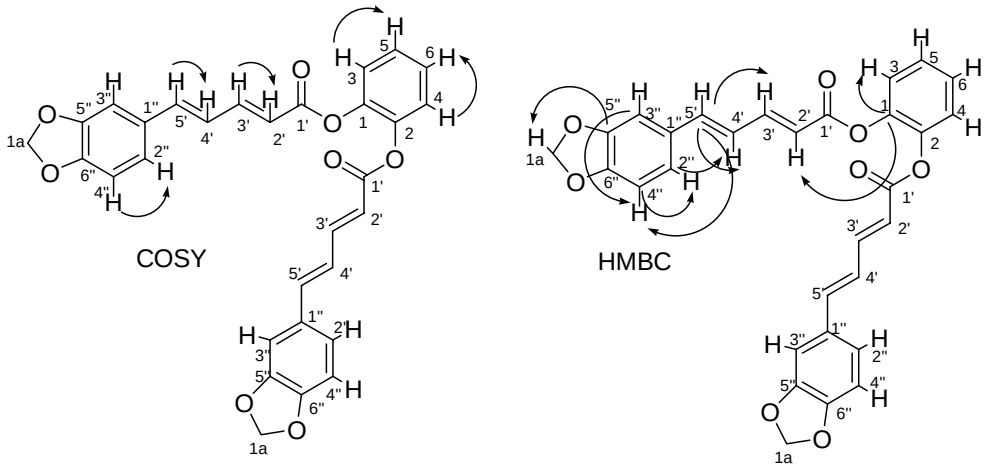

The HMBC spectrum of compound **I** (Fig I-4) clearly indicated the correlations between C-5″ (δ_C 148.7) and H-1a (δ_H 6.06) between C-2″ (δ_C 108.0) and H-4′ (δ_H 7.06) between C-4″ (δ_C 115.2) and H-2″ (δ_H 6.65) between C-3″ (δ_C 119.4) and H-4″ (δ_H 6.83) between C-5′ (δ_C 132.7) and H-3′ (δ_H 6.85), H-4″ (δ_H 7.06), H-4′ (δ_H 6.83) between C-1 (δ_C 146.1)and H-2′ (δ_H 6.74), H-3 (δ_H 6.74), respectively.

3.26.5 Structural elucidation of compound J

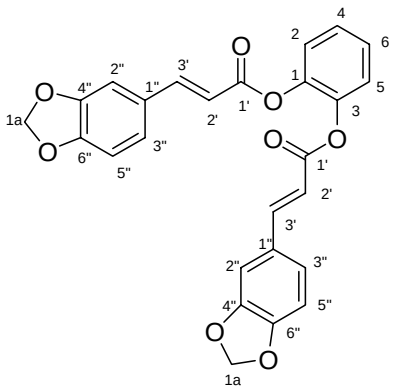

The structure of compound **J** was deduced from the analysis of COSY and HMBC. The COSY spectrum of compound **J** (Fig J-3) manifestly displayed the correlations between H-2′ (δ_H 6.40) and H-3′ (δ_H 7.70) between H-3″ (δ_H 7.00) and H-5″ (δ_H 6.80) between H-2 (δ_H 7.30) and H-4 (δ_H 7.29), respectively.

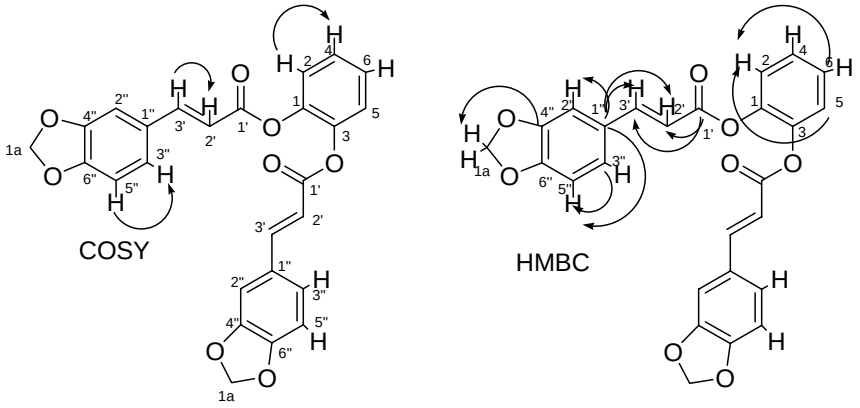

The HMBC spectrum of compound **J** (Fig J-4) reasonably exposed the correlations between C-4″ (δ_C 148.0) and H-1a (δ_H 6.06), between C-1″ (δ_C 128.0) and H-2″ (δ_H 6.41), H-3′ (δ_H 7.70), H-2′ (δ_H 6.40) between C-1′ (δ_C 164.0) and H-2′ (δ_H 6.40), H-3′ (δ_H 7.70), between C-3″ (δ_C 106.0) and H-5″ (δ_H 6.80) between C-1″ (δ_C 128.0) and H-5″ (δ_H 6.80) between C-5 (δ_C 122.0) and H-2 (δ_H 7.30) and between C-6 (δ_C 126.0) and H-2 (δ_H 7.30), respectively.

3.27 Biological activities of isolated substances from the CH_2Cl_2 extract of *M. oleifera*

3.27.1 Antioxidant

The radical scavenger effect on DPPH radical of benzamide and benzylisothiocyanate, isolated from a natural source, and their synthetic derivatives including *N*-phenyl-benzamide, *N,N*-diethyl-benzamide and benzonitrile were subjected for radical scavenging effect on DPPH radical by TLC autographic assay. The results are demonstrated in Table 3.38.

Table 3.38 Antioxidant of isolated compounds from a natural source and their synthetic compounds

Substance	Structure	Radical scavenging effect on DPPH
Benzylisothiocyanate	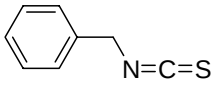	-
benzamide	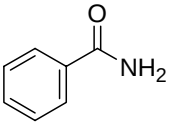	++
N-phenyl-benzamide	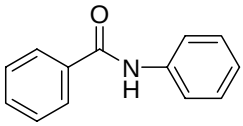	-
N,N-diethyl-benzamide	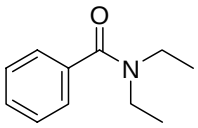	-
Benzonitrile	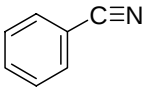	-

Note : + positive results observed within 10 min
++ positive results observed within 5 min
+++ positive immediately

As the result above, benzamide showed significant activity against DPPH radical, whereas benzylisothiocyanate and benzonitrile did not show antioxidant activity. This observation prompted to prepare the benzamide analogues with the expectation to gain more potent compounds that possessed antioxidant activity. Benzamides derivatives were synthesized according to the reported protocols [23] and subjected to radical scavenging test on DPPH radical by TLC autographic assay. Unfortunately, both *N*-phenyl-benzamide and *N,N*-diethyl-benzamide could disappear the pleasant antioxidant activity. These results indicated that the substituents, aliphatic and aromatic moieties, on nitrogen atom did not affect to increase of radical scavenging effect on DPPH radical. To try to search for potent antioxidant activity, other amide derivatives were additionally prepared from various structural amines and carboxylic acids and the results are demonstrated in Table 3.39. From the literature reviews, phenolic compounds were found as a good antioxidant agent, suggesting that

the compound contained phenolic group may be caused a higher antioxidant activity of prepared amides.

Table 3.39 Antioxidant activity of synthesized benzamides and ester derivatives

Substance	Structure	Radical scavenging effect on DPPH
A	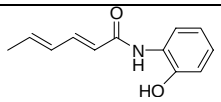	+++
B	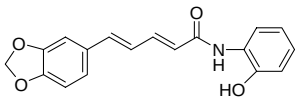	+++
C	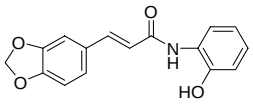	+++
D	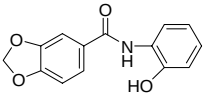	+++
F	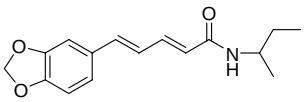	-
G	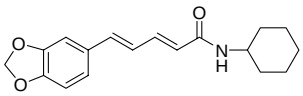	-
H	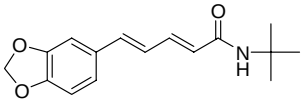	-
I	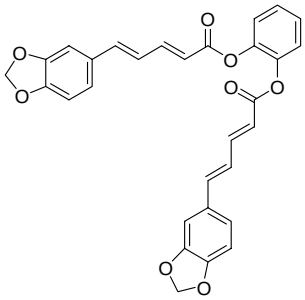	-

Table 3.39 (cont)

Substance	Structure	Radical scavenging effect DPPH
J	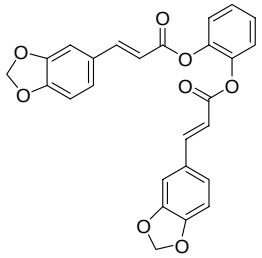	-
L	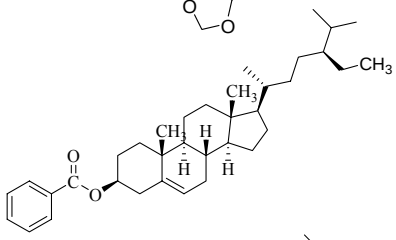	-
K	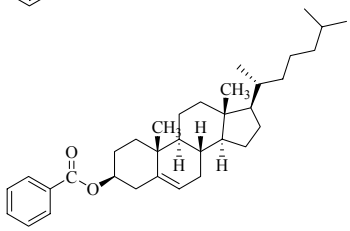	-
Benzamide	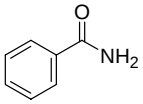	++

The synthesized compounds **A-D** and benzamide exhibited the best activity against DPPH radical. All compounds were then investigated for the IC_{50} value. The quantitative analysis for determination IC_{50} value of those substances was performed using spectrophotometric method and the results are presented in Table M-1. The curve was plotted between the percentage of radical scavenging and the concentration of each sample. Ascorbic was used as a standard compound. The IC_{50} value of each substance was calculated from the logarithmic equation of its curves and are tabulated in Table 3.40.

Table 3.40 IC_{50} values of synthesized compounds for radical scavenging on DPPH radical

Compound	Structure	IC_{50} (mM)
A	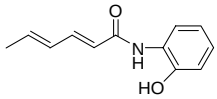	0.518
B	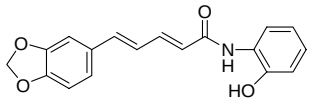	0.470
C	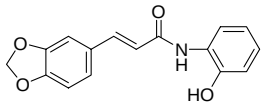	0.494
D	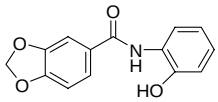	0.836
Benzamide	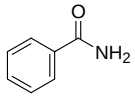	>1
Ascorbic acid	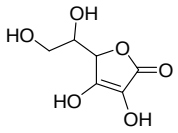	0.12

Compounds **A**, **B** and **C** revealed high antioxidant activity in scavenging of DPPH radical with IC_{50} of 0.470-0.518, while benzamide showed low antioxidant activity. The structure and activity relationships of all compounds were then analyzed. The presence of hydroxyl group at *ortho*- position of aromatic ring connecting to nitrogen atom enhanced the antioxidant activity. In the case of amide and ester functional groups, the antioxidant activity of compounds containing an amide group was better than that of ester group.

3.27.2 Inhibition of cholinesterase activity

The inhibition of cholinesterase activity of the isolated compounds of *M. oleifera* and synthetic benzamide derivatives was investigated by the assay described Ellman. All compounds including *β*-Sitosterol-3-O-*β*-D-glucopyranoside **(12)**, isothiocyanatomethylbenzene **(7)** a mixture of steroids **(3)**, linoleic acid **(6)**, *β*-sitosteryl linoleate **(9)**, 1,2,3-triolein **(10)**, a mixture of 1,3-dilinoleoyl-2-olein, 3-

dioleoyl-2-linolein, 12,3-trilinolein **(8)**, benzamide **(11)**, compounds **A**, **B**, **D**, **F**, **G** and **H** were tested.

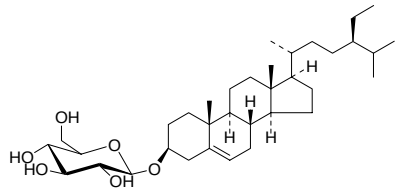

β-Sitosterol-3-O- *β*-D-glucopyranoside **(12)**

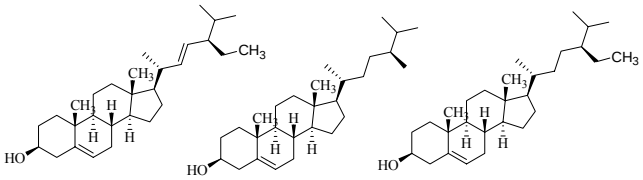

Mixture steroids **(3)**

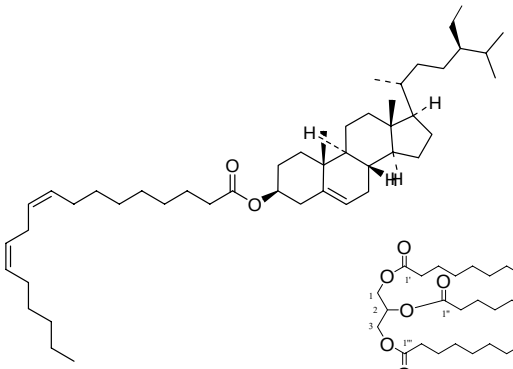

B-sitosteryl linoleate **(9)**

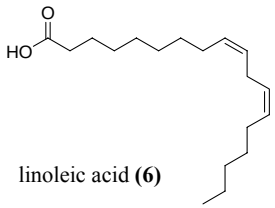

linoleic acid **(6)**

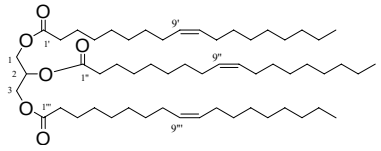

1,2,3-triolein **(10)**

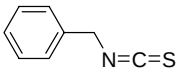

Isothiocyanatomethyl benzene **(7)**

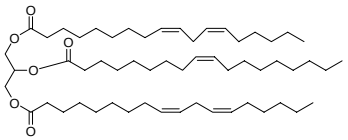

1,3-dilinoleoyl-2-olein

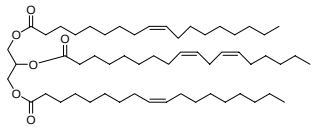

1,3-dioleoyl-2-linolein

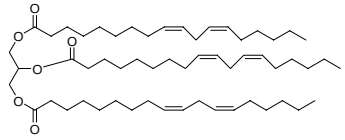

1,2,3-trilinolein **(8)**

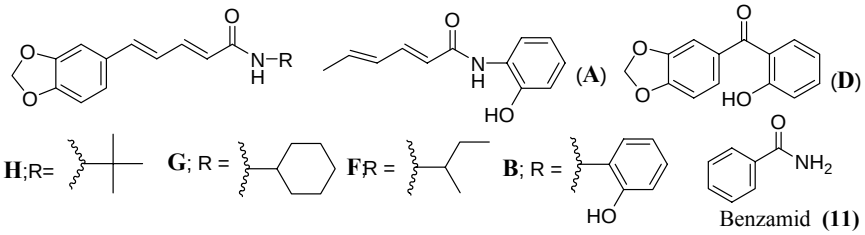

H;R= **G**; R = **F**; R = **B**; R = Benzamid **(11)**

From the inhibition of cholinesterase activity results, all compounds did not display the inhibition of cholinesterase activity.

3.27.3 α-Amylase inhibitor

α-Amylase inhibition was assayed according to the method of Kanda pancreatic porcine α-amylase [22]. *β*-Sitosterol-3-*O*-*β*-D-glucopyranoside (compound **12**) and *β*-sitosteryl linoleate (compound **9**) were tested for α-amylase inhibition. The results are accumulated in Table 3.41.

Table 3.41 The percentage of α-amylase inhibition *β*-sitosterol-3-*O*-*β*-D-glucopyranoside and *β*-sitosteryl linoleate

Substance	Concentration (mg/mL)	% inhibition			
		1	2	3	Average
β-sitosterol-3-*O*-*β*-D-glucopyranoside	1.000	63.47	64.04	63.14	63.55
	0.500	58.17	58.12	58.58	58.29
	0.250	49.04	47.45	48.45	48.31
	0.125	28.68	28.83	27.09	28.20
	0.000	0.000	0.000	0.000	0.000
β-sitosteryl linoleate	1.000	29.83	29.52	29.30	29.55

Only *β*-sitosterol-3-*O*-*β*-D-glucopyranoside showed α-amylase inhibition with the IC_{50} of 0.326 mM. *β*-Sitosterol-3-*O*-*β*-D-glucopyranoside (compound **12**) which contained a hydroxyl group of glucose revealed 63.55% inhibition more than *β*-sitosteryl linoleate (compound **9**) which have no hydroxyl group (29.55%). This was in line with previous study [28] that a hydroxyl group formed a hydrogen bonding with enzyme affected not be possible for forming of enzyme-substrate complex.

3.27.4 Trolox equivalent antioxidant capacity (TEAC) assay

The ABTS radical cation scavenging activity of *N*-(2-hydroxylphenyl)-5-(3,4-methylenedioxyphenyl)-*2E,4E*-pentadieneyl amide was tested comparing with trolox at 1 mM. All tests are carried out in triplicate and average values are calculated in Table 3.42.

Table 3.42 Antioxidant activities of compound **B** towards the ABTS radical

Compound	Antioxidant activity(equivalent to trolox) ABTS
Trolox	1
B	0.9948 ± 0.0090

As the result above, ABTS value of compound **B** was similar to that of trolox. Therefore, compound **B** was a good candidate revealing antioxidant activity.

CHAPTER IV

CONCLUSION

4.1 Bioactive constituents from the roots of *G. inodorum*

Three known substances: long chain saturated alcohol, long chain saturated ketone and a mixture of steroids were isolated from the CH_2Cl_2 extract of the whole plant of *G. inodorum.* In addition, two known compounds (**4** and **5**) were isolated from *n*-BuOH crude extract. All isolated substances were elucidated their structures by means of physical properties and spectroscopic evidences, and explored biological activity including scavenging effect on DPPH radical, α-amylase inhibitor and cholinesterase inhibitory activity. The structures of isolated substances are depicted as shown in Fig 4.1. The results of their biological activity are summarized as presented in Table 4.1.

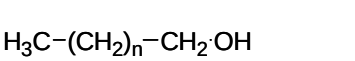

Substance **1**

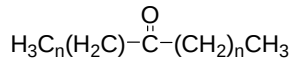

Substance **2**

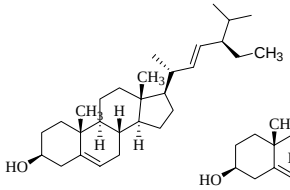

Stigmasterol

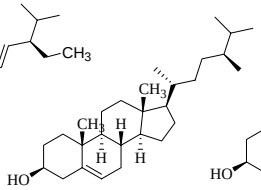

Campesterol

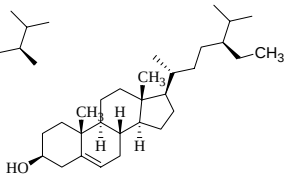

β-sitosterol

Mixture **3**

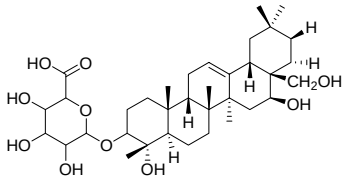

Compound **4**

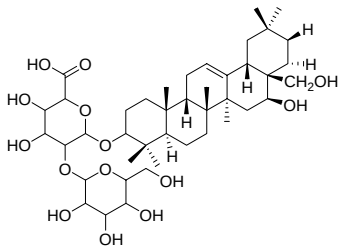

Compound **5**

Table 4.1 The results of biological activity of isolated substances from the CH_2Cl_2 and *n*-BuOH crude extracts of *G. inodorum*

Substance	Antioxidant TLC assay	% α-amylase inhibition	Inhibition of cholinesterase activity	
			(AChE)	(BuChE)
Substance **1**	-	Not tested	-	-
Substance **2**	-	Not tested	-	-
Mixture **3**	-	Not tested	-	-
Compound **4**	Not tested	9.80	-	-
Compound **5**	++	38.59	-	-

Note antioxidant : + positive results observed within 10 min
++ positive results observed within 5 min
+++ positive immediately

Only compound **5** was active for radical scavenging effect on DPPH radical. In addition, all compounds did not present the inhibition of cholinesterase activity at all. The α-amylase inhibition of compound **5** (38.59 %) was better than that of compound **4** (9.80 %) approximately four folds.

4.2 Bioactive constituents from the roots of *M.oleifera*

Four known components: a long chain alcohol, a long chain ketone, a mixture of *β*-sitosterol, campesterol and stigmasterol, and a mixture of triglycerides as 1,3-dilinoleoyl-2-olein, 1,3-dioleoyl-2-linolein and 1,2,3-trilinolein were isolated from the CH_2Cl_2 crude extract of the roots of *M. oleifera*. In addition, five known compounds were isolated from this crude extract and could be identified as: linoleic acid, isothiocyanatomethylbenzene, 1,2,3-triolein, benzamide, *β*-sitosterol-3-O-*β*-D-gluco-pyranoside and *β*-sitosteryl linoleate. Certain benzamide and ester derivatives were manipulated to explore structure-activity relationship as depicted in Fig 4.2. The results of their biological activity are summarized as presented in Table 4.2.

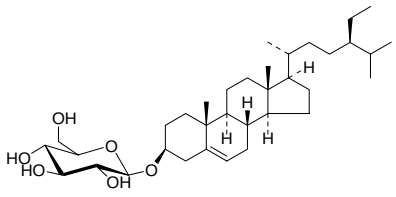

β-Sitosterol-3-O- *β*-D-glucopyranoside **(12)**

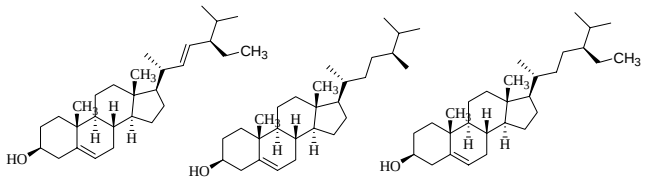

Mixture steroids **(3)**

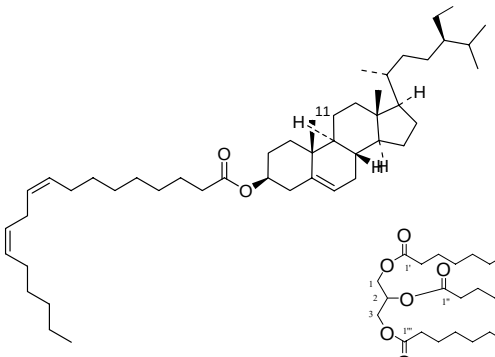

β-Sitosteryl linoleate **(9)**

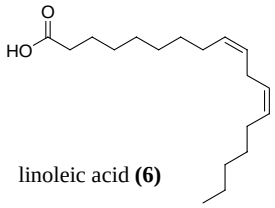

linoleic acid **(6)**

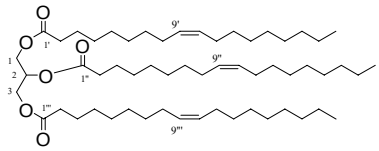

1,2,3-triolein **(10)**

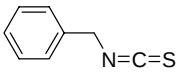

Isothiocyanatomethyl benzene **(7)**

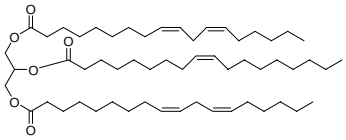

1,3-dilinoleoyl-2-olein

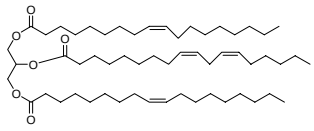

1,3-dioleoyl-2-linolein

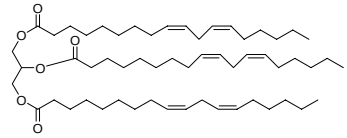

1,2,3-trilinolein **(8)**

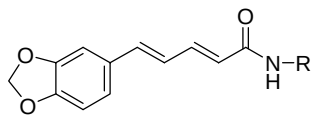

D

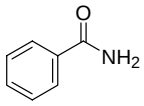

Benzamide **(11)**

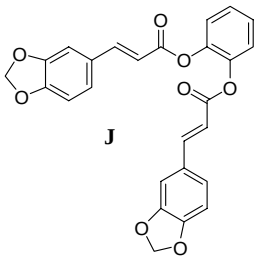

J

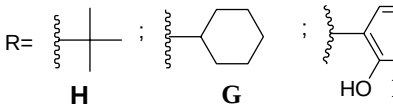

H **G** **B** **F**

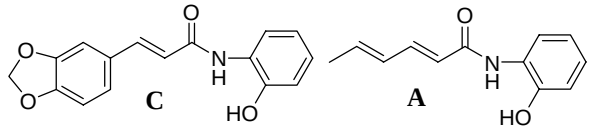

C **A**

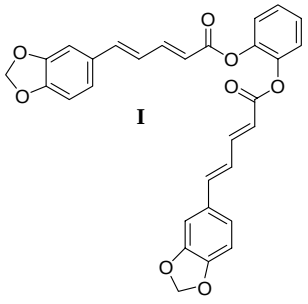

I

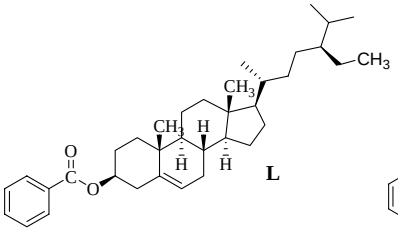

L

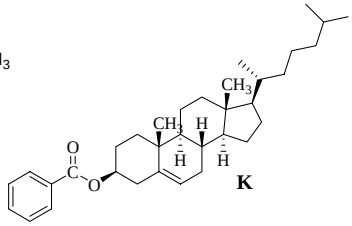

K

Table 4.2 Biological activity of isolated substances from the CH_2Cl_2 crude extract of the roots of *M. oleifera*, certain benzamide and ester derivatives

Substance	Antioxidant		Inhibition of cholinesterase activity		α-Amylase inhibition	
	TLC	IC_{50}	(AChE)	(BuChE)	% α-amylase inhibition	IC_{50}
1	-	a	-	-	a	a
2	-	a	-	-	a	a
3	-	a	-	-	a	a
4	-	a	-	-	a	a
5	-	a	-	-	a	a
6	-	a	-	-	a	a
7	-	a	-	-	a	a
8	-	a	-	-	a	a
9	-	a	-	-	29.55	a
10	-	a	-	-	a	a
11	++	>1	-	-	a	a
12	-	a	-	-	63.55	0.326
A	+++	0.518	-	-	a	a
B	+++	0.470	-	-	a	a
C	+++	0.494	-	-	a	a
D	+++	0.836	-	-	a	a
F	-	a	-	-	a	a
G	-	a	-	-	a	a
H	-	a	-	-	a	a
I	-	a	-	-	a	a
J	-	a	-	-	a	a
K	-	a	-	-	a	a
L	-	a	-	-	a	a

Note : a : No test, - : not active

(Antioxidant) Note : + positive results observed within 10 min

++ positive results observed within 5 min

+++ positive immediately

Benzamide, isolated from the CH_2Cl_2 crude extract of the roots of *M. oleifera* showed the highest scavenging activity on DPPH. While *β*-sitosterol-3-O-*β*-D-glucopyranoside was found as a good inhibitor for α-amylase inhibition with IC_{50} of 0.326 mM

The synthetic derivatives of benzamide and ester were prepared to evaluate for scavenging effects on DPPH radical. Compound **B** showed highly active toward radical scavenging effect on DPPH radical with IC_{50} of 0.470 mM.

The β-sitosterol-3-O-β-D-gluco-pyranoside was further examined for α-amylase inhibitory activities by evaluating their IC_{50} values. The IC_{50} value is the half maximal inhibitory concentration, representing the concentration of an inhibitor that is required for 50% inhibition of its targeted enzyme and it is commonly used as a measure of inhibitor effectiveness. Table 4.2 shows the IC_{50} value of β-sitosterol-3-O-β-D-glucopyranoside . Although the inhibitory potency was still lower than that of the therapeutic durg, acarbose, observed data clearly indicated the potential of this β-sitosterol-3-O-β-D-gluco-pyranoside as inhibitor for α-amylase.

Proposal for the future work

As the results showed the CH_2Cl_2 crude extract of *M. oleifera* leaves disclosed abundant biological activities: antioxidant and α-amylase inhibitor. Therefore, the study on the exploration of other pharmaceutical activities such as antimicrobial, anticancer and anti-inflammatory can be future investigated. This finding is particular interesting in the future design and preparation of novel medicine.

REFERENCES

[1]. Tiew, P., Ioset, J. R., Kokpol, U., Chavasiri, W., and Hostettmann, K. **2003.** Antifungal, antioxidant, and larvicidal activities of compounds isolated from the heartwoods of *Mansonia gagei*. *Phytother. Res*. 17: 190-193.

[2]. Couladis, M., Baziou, P., Verykokidou, E., and Loukis, A. **2002.** Antioxidant activity of polyphenols from *Hypericum triquetrifolium* Turra. *Phytother. Res.* 16: 769-770.

[3]. Conforti, F., Statti, G. A., Tundis, R., Menichini, F., and Houghton, P. **2002.** Antioxidant activity of methanolic extract of *Hypericum triquetrifolium* Turra aerial part. *Fitoterapia* 73: 479-483.

[4]. วุฒิ วุฒิธรรมเวช. **2540**. สารานุกรมสมุนไพร รวมหลักเภสัชกรรมไทย. พิมพ์ครั้งที่ 1. กรุงเทพมหานคร: สำนักพิมพ์โอเดียนสโตร์.

[5].Morton, J. F. **1962.** Ornamental plants with toxic and or irritant properties II. *Proc. Fla. State Hort. Soc*. 75: 484.

[6]. Mokkhasmit, M., Swasdimongkol, K., and Satrawaha, P. **1971**. Study on toxicity of Thai medicinal plants. *Bull Dept. Med. Sci*. 12(2/4): 36-65.

[7]. Mokkhasmit, M., Swasdimongkol, K., Ngarmwathana, W., and Permphiphat, U. **1971**. Study on toxicity of Thai medicinal plants (continue). *J. Med. Assoc. Thai* 54(7): 490-504.

[8]. Bhawasar, G. C., Guru, L. V., and Chadda, A. K. **1965**. Antibacterial activity of some indigenous medicinal plants. *Med. Surg*. 5: 11-14.

[9]. Dhawan, B. N., Dubey, M. P., Mehrotra, B. N., Rastogi, R. P., and Tandon, J. S. **1980.** Screening of Indian plants for biological activity Part IX. *Indian J. Experimental Biol*. 18: 594-7.

[10]. Ghasi, S., Nwobodo, E., and Ofili, J. O. **2000.** Hypocholesterolemic effects of crude extract of leaf of *Moringa oleifera* Lam in high-fat fed Wistar rats. *J. Ethnopharm*. 69: 5-21.

[11]. Tahiliani, P., and Kar, A. **2000.** Role of *Moringa oleifera* leaf extract in the regulation of thyroid hormone status in adult male and female rats. *Pharmacol. Res*. 41: 319-23.

[12]. Makonnen, E., Hunde, A., Damecha, G. **1977.** Hypoglycaemic effect of *Moringa stenopetala* aqueous extracts in rabbits. *Phytother. Res*. 11: 147-8.

[13]. Pal, S. K., Mukherjee, P. K., and Saha, B. P. **1995**. Studies on the antiulcer activity of *Moringa oleifera* leaf extract on gastric ulcer models in rats. *Phytother Res*. 9: 463-5.

[14]. Guevara, A. P., Vagas, C., Sakurai, H., Fujiwara, Y., Hashimoto, K., Maoka, T., Kozuka, M., Ito, Y., Tokuda, H., and Nishino, H. **1999.** An antitumor promoter from *Moringa oleifera* Lam. *Mutat. Resgen. Toxan. 440*: 181-188.

[15]. Faizi, S., Siddiqui, S. B., Saleem, R., Siddiqui, S., and Aftab, K. **1994**. Isolation and structure elucidation of new nitrile and mustard oil glycosides from *Moringa oleifera* and their effect on blood pressure. *J. Nat. Prod*. 57: 1256-1261.

[16]. Ye, W., Liu, X., Zhang, Q., Che, C. T., and Zhao, S. **2001.** Antisweet saponins from *Gymnema sylvestre*. *J. Nat. Prod*. 64: 232-235.

[17]. Shimizu, K., Ozeki, M., Iino, A., Nakajyo, S., Urakawa, N., and Atsuchi, M. **2001.** Structure-activity relationships of triterpenoid derivatives extracted from *Gymnema inodorum* leaves on glucose absorption. *J. Pharmacol*. *86*: 223-229.

[18]. Hosttettmann, K., Terreaux, C., Marston, A., and Potterat, O. **1997**. The role of planar chromatography in the rapid screening and isolation of bioactive compound from medicinal plants. *J. Pla. Chro*. 10: 251-257.

[19]. Pongtip, S., Roongtawan, S., and Wandee, G. **2005.** Antioxidant activity of Siamese neem tree (VP 1209). *J. Ethnopharm*. 99: 109-112..

[20]. Halid, A., Kamran, M. A., Parveen S., Rahman, A., and Choudhary, M. I. **2005.** Structural basis of acetylcholinesterase inhibition by triterpenoidal alkaloids. *Biochem. Bioph. Res. Co*. 331: 1528-1532.

[21]. Viegas, C. Jr., Bolzani, V. S., Pimentel, L. S. B., Castro, N. G., Cabral, R. F., Costa, R. S., Floyd, C., Rocha, M. S., Young, M. C. M., Barreiro, E. J., and Fraga, C. A. M. **2005.** New selective acetylcholinesterase inhibitors designed from natural piperidine alkaloids. *Bioorgan. Med. Chemistry* 13: 4184-4190.

[22]. Kandra, L., Zajacz, A,, Remenyik, J., Gyemant, G. **2005.** Kinetic investigation of a new inhibitor for human salivary alpha-amylase. *Biochem. Biophy. Res*. Co. 334: 824-8.

[23]. Chayaripongkal, S. **2003.** Reagent development for the preparation of acid chloride for synthesis of bioactive compounds, Master's thesis, Department of Chemistry, Chulalongkorn University.

[24]. Albert, M., and Karsten, K. **1972.** Synthesis of narciprimin and related compound. *Chemische. Berichte*.105(11): 3726-47.

[25]. Hauser, C. R., and Walker, H. G. Jr. **1969.** Condensation of certain esters by means of diethylaminomagnesium bromide. *J. Am. Chem. Soc.* 69: 295-297.

[26]. Hans, J. J., Driver, R. W., and Burke, S. D. **1999**. One-pot synthesis of amides and esters from 2,2,2-trihaloethyl esters using phosphorus(III) Reagents. *J. Org. Chem*. 64: 1430-1431.

[27]. Mizushina, Y., Nakanishi, R., Kuriyama, I., Kamiya, K., Satake, T., Shimazaki, N., Koiwai, O., Uchiyama, Y., Yonezawa, Y., Takemura, M., Sakaguchi, K., and Yoshida, H. **2006.** β-sitosterol-3-O-β-D-glucopyranoside: A eukaryotic DNA polymerase λ inhibitor. *J. Steroid Biochem. & Molec. Biol.* 99: 100-107.

[28]. Heidari, R., Zareae, S., and Heidarizadeh, M. **2005**. Extraction, purification, and inhibitory effect on α-amylase inhibitor from wheat (*Triticum aestivum* Var. *zarrin*). *J. Nutr.* 4(2): 101-105.

[29]. Ramsewak, S. R., Nair, G. M., Murugesan, S., Mattson, J. W., Zasada, J. **2001**. Insecticidal fatty acids and triglycerides from *Dirca palustris*. *J. Agri. Food Chem*. 49: 5852-5856.

[30]. Hanley, A. B., Heaney, R. K., Lewis, J., Sones, K., Spinks, E. A., Wilkinson, A. P., and Fenwiok, G. R. **1988.** Benzyl isothiocyanate in onion (*Allium cepa* L.) and mushroom(*Agaricus bisporus*)-A re-examination. *Food Chem*. 30: 157-162.

[31]. Pan, X., and Hussain, M. M. **2007**. Diurnal regulation of microsomal triglyceride transfer protein and plasma lipid levels. *J. Biochem.* 282(34): 24707-24719.

[32]. Collin, S., Tayar, N., Waterbeemd, H., Moureau, F., and Daniel, P. **1989.** QSAR of nortropane-substituted benzamides: use of lipophilic(RP-HPLC) and electronic (^{1}H NMR) parameters. *J. Med. Chem*. 24: 163-169.

APPENDIX

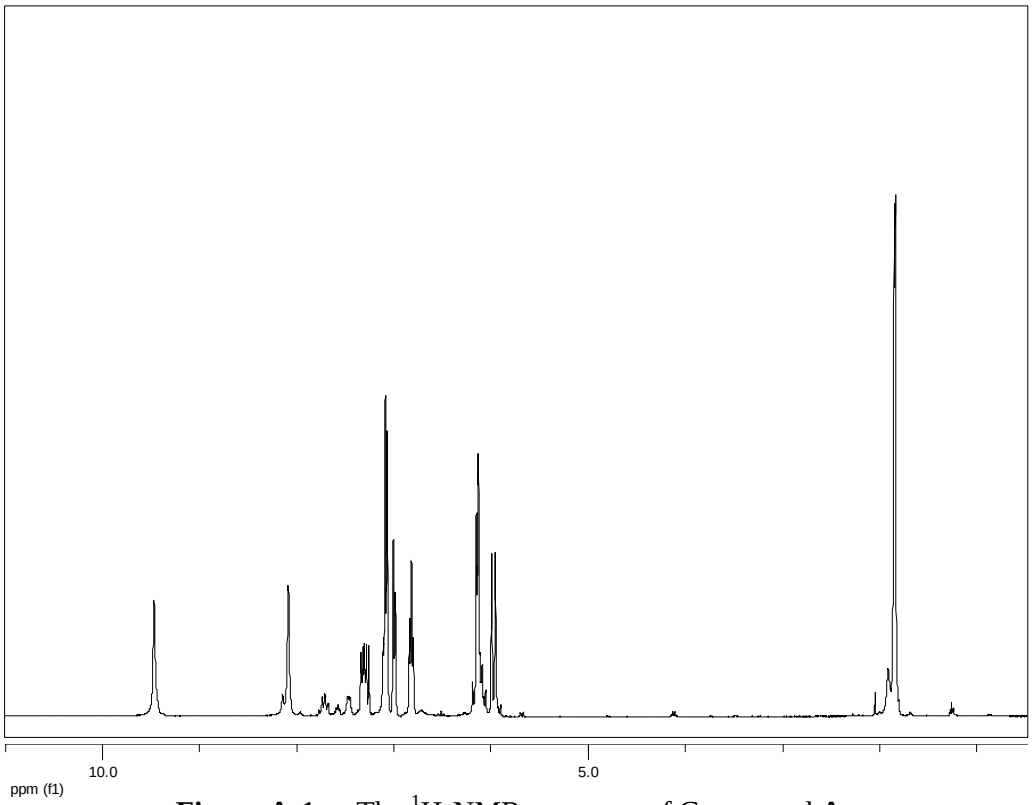

Figure A-1 The ^{1}H-NMR spectrum of Compound **A**

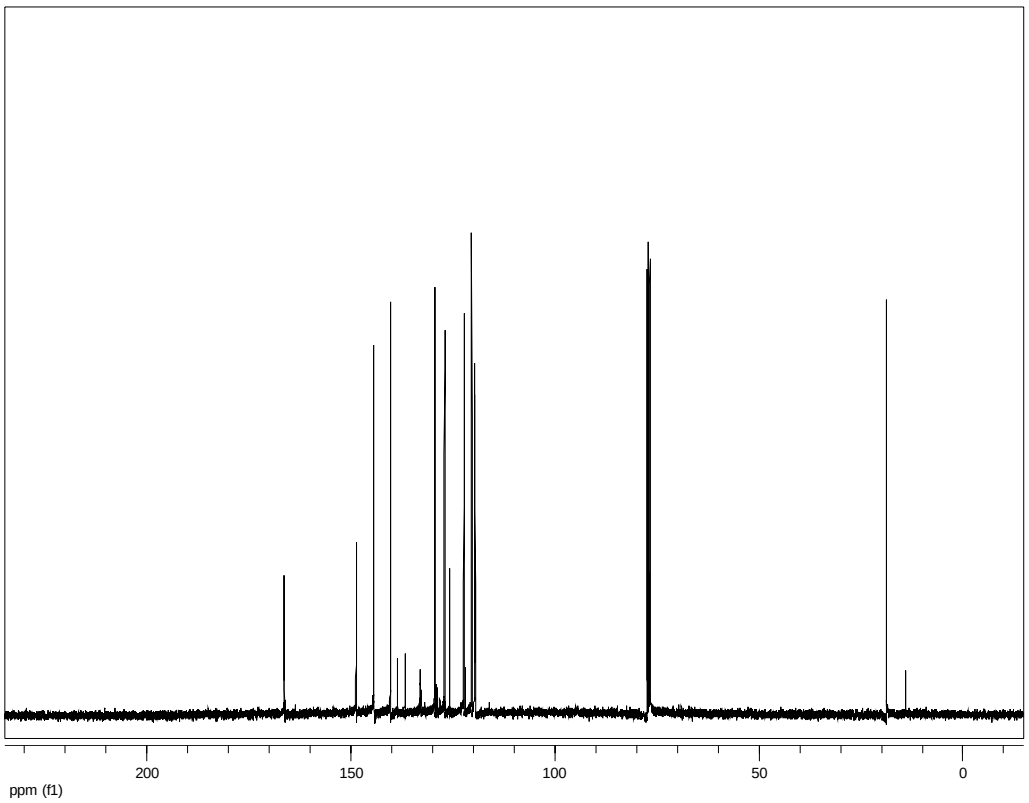

Figure A-2 The ^{13}C-NMR spectrum of Compound **A**

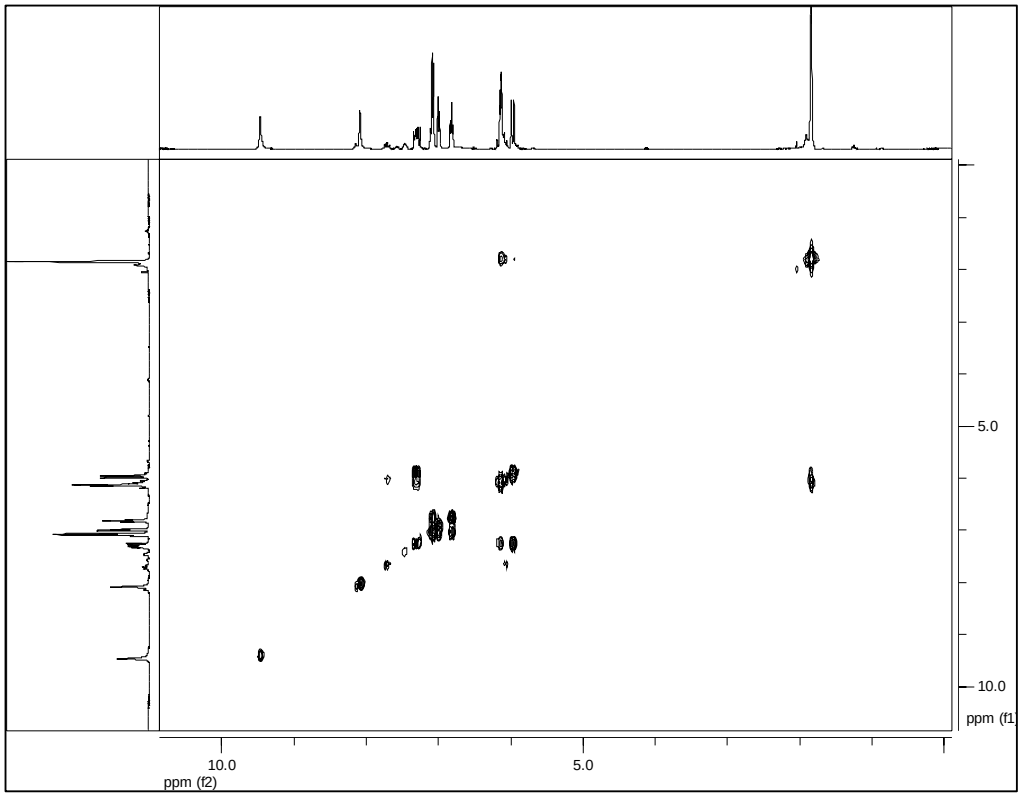

Figure A-3 The COSY spectrum of Compound **A**

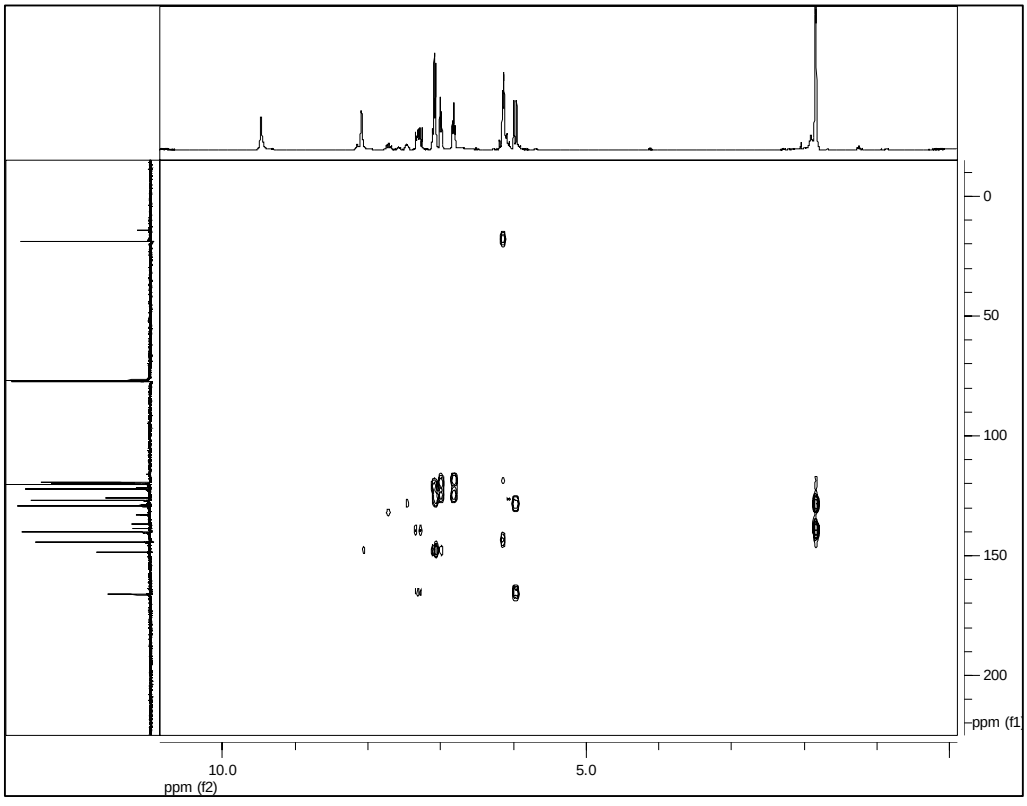

Figure A-4 The HMBC spectrum of Compound **A**

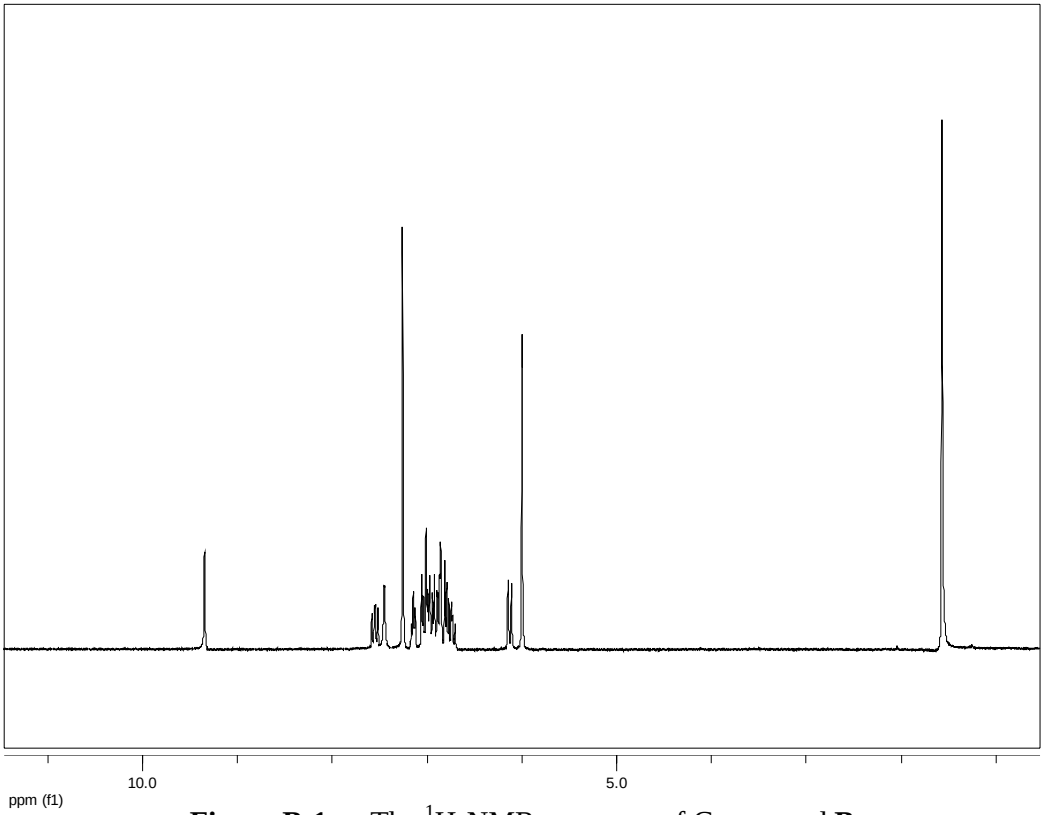

Figure B-1 The ^{1}H-NMR spectrum of Compound **B**

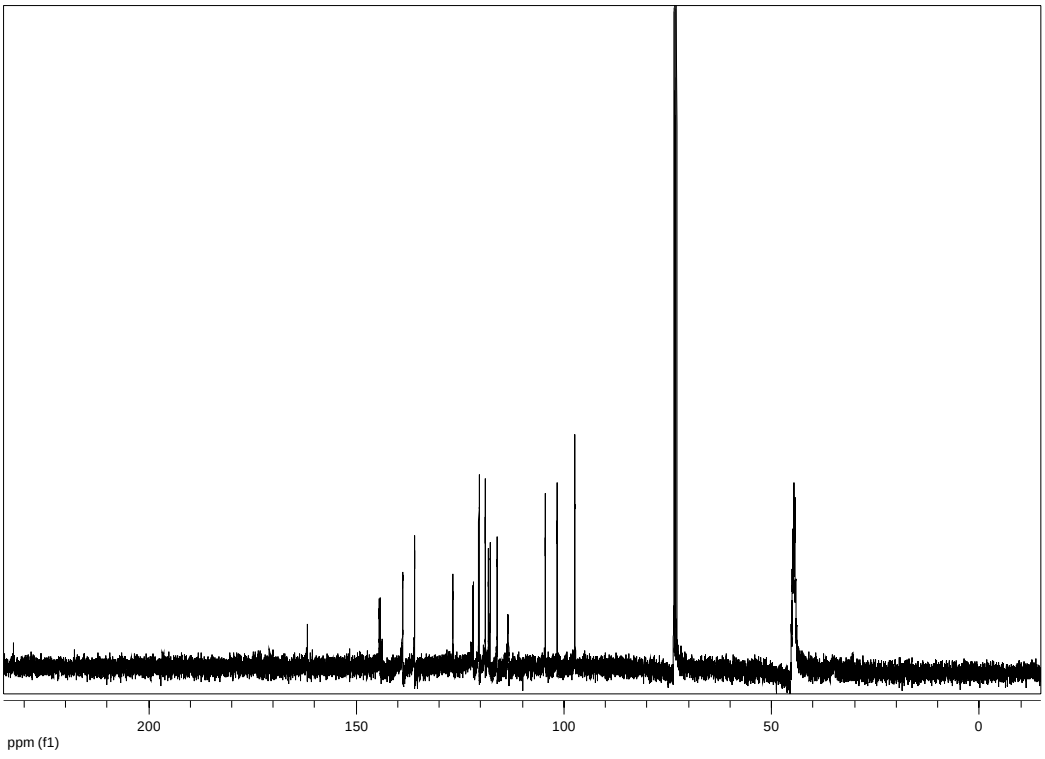

Figure B-2 The ^{13}C-NMR spectrum of Compound **B**

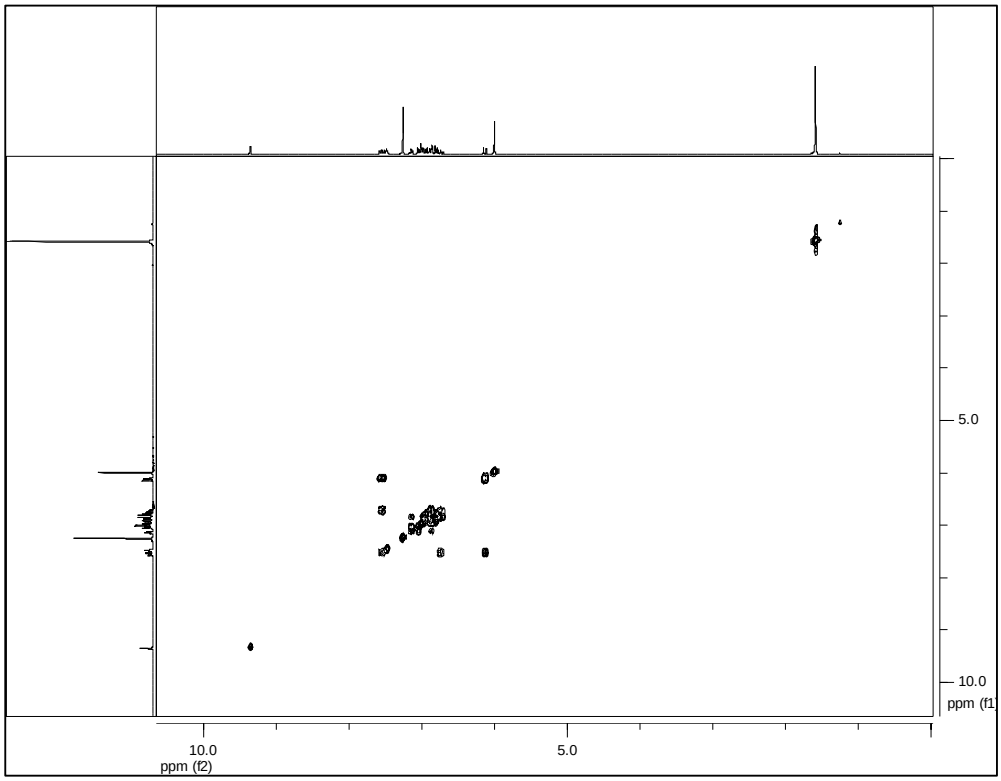

Figure B-3 The COSY spectrum of Compound **B**

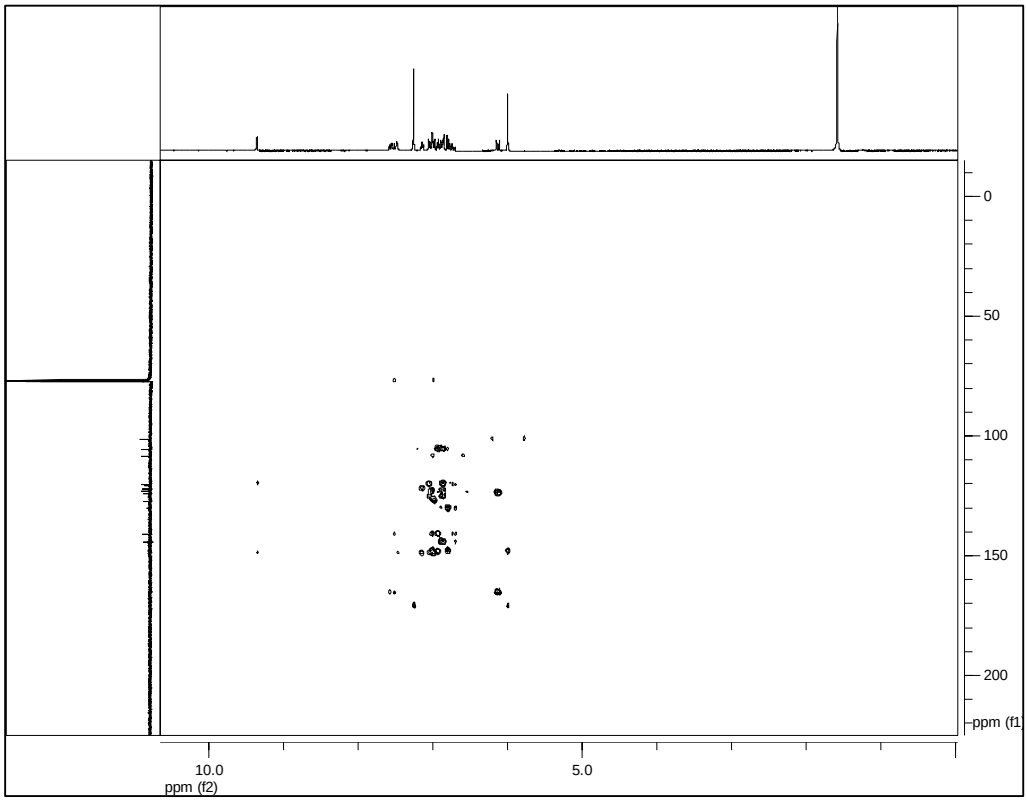

Figure B-4 The HMBC spectrum of Compound **B**

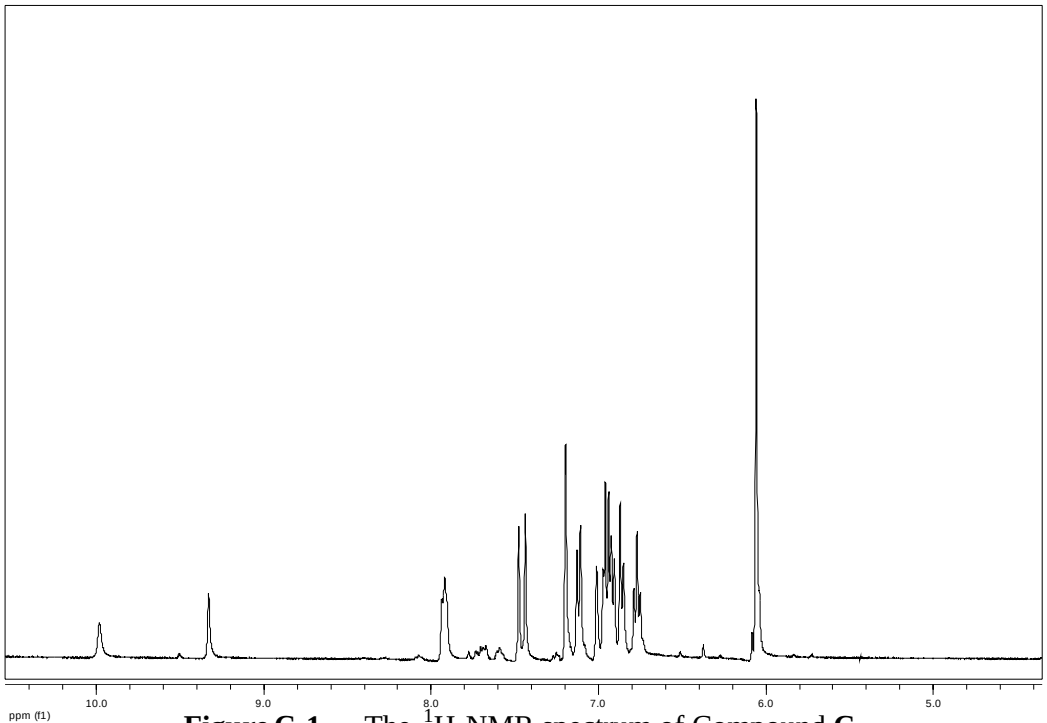

Figure C-1 The ^{1}H-NMR spectrum of Compound **C**

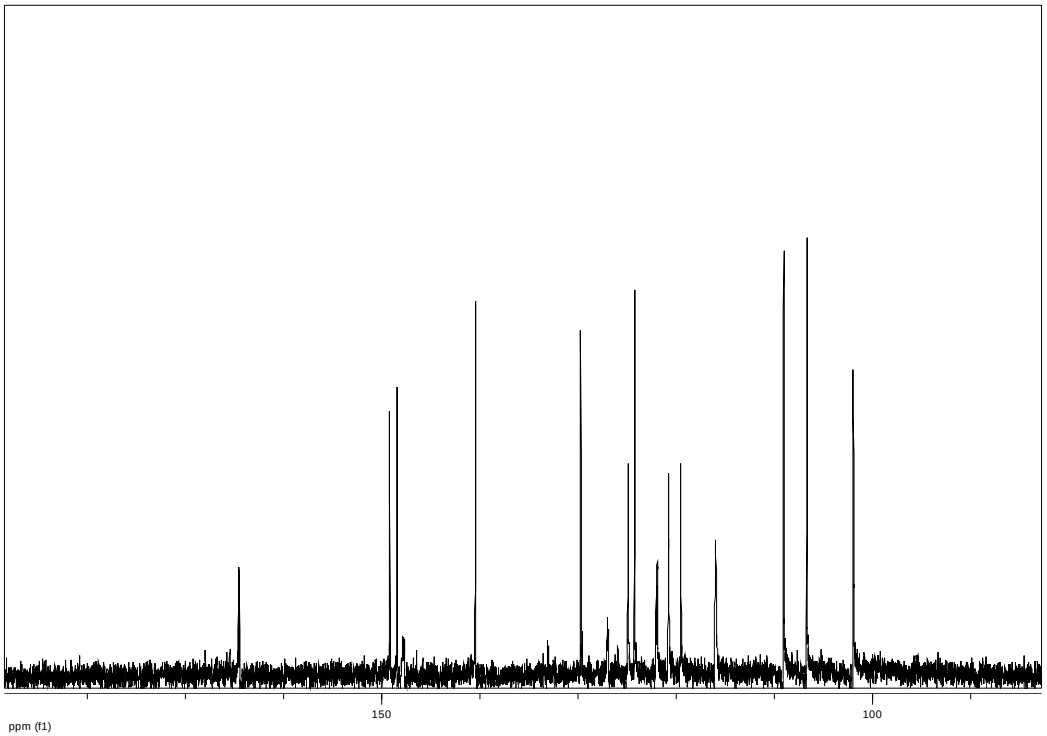

Figure C-2 The ^{13}C-NMR Carbon spectrum of Compound **C**

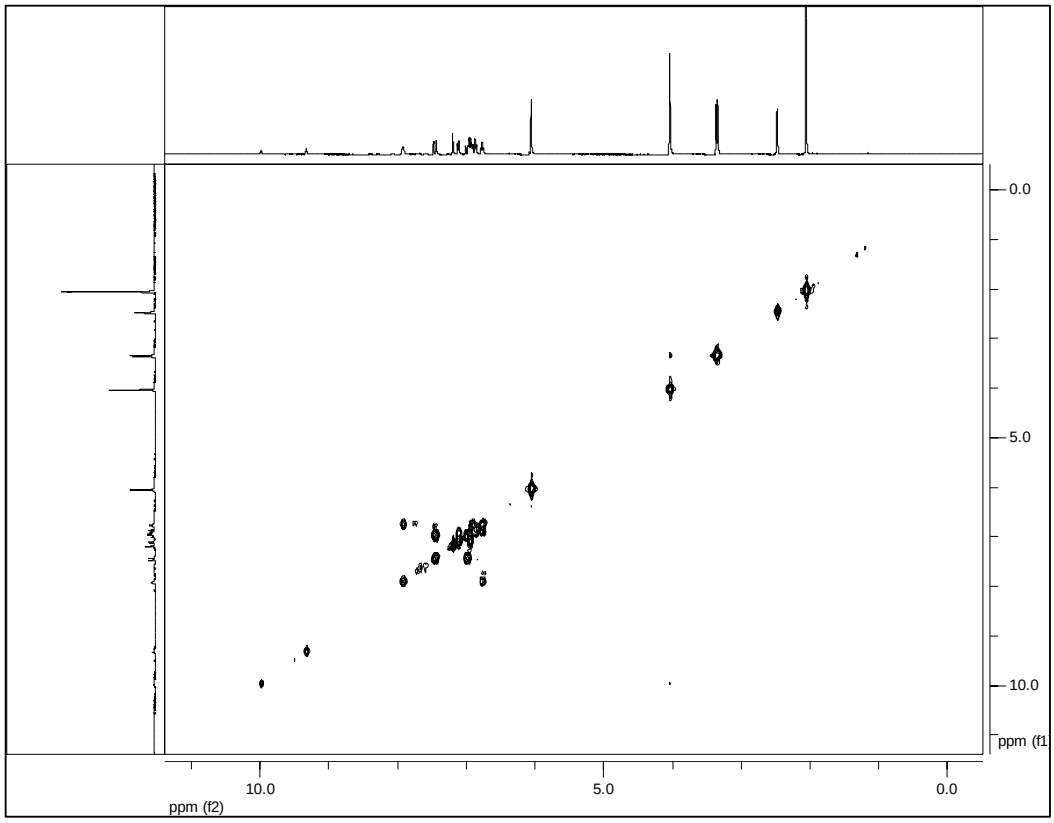

Figure C-3 The COSY spectrum of Compound **C**

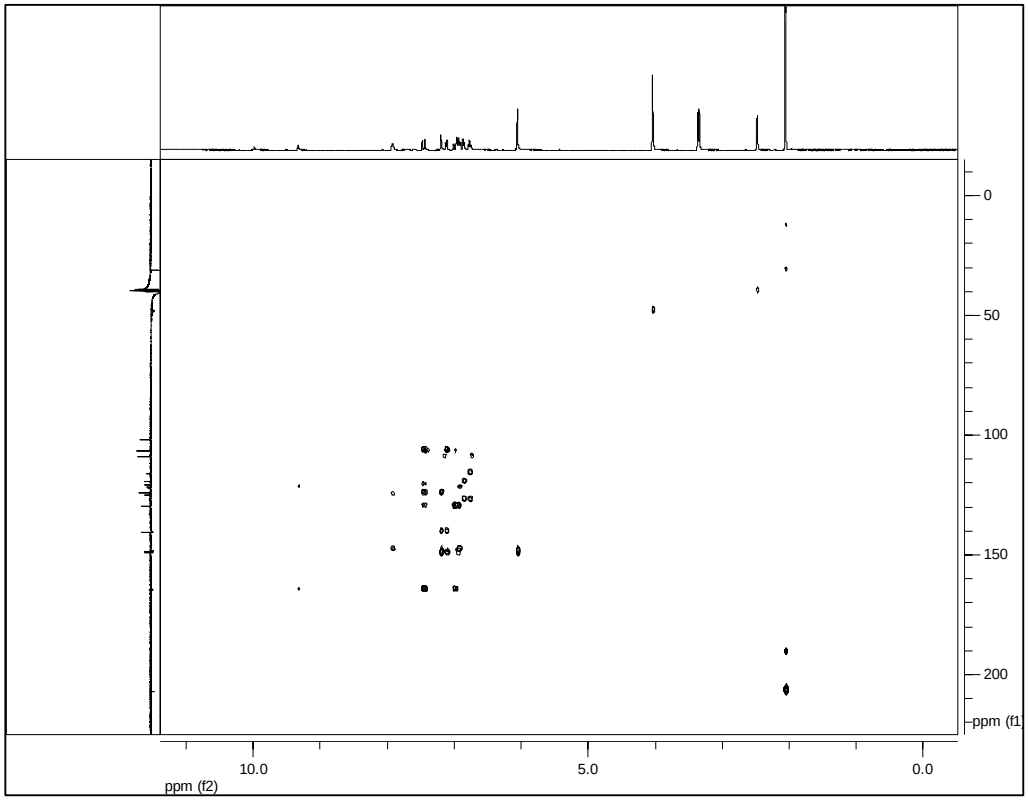

Figure C-4 The HMBC spectrum of Compound **C**

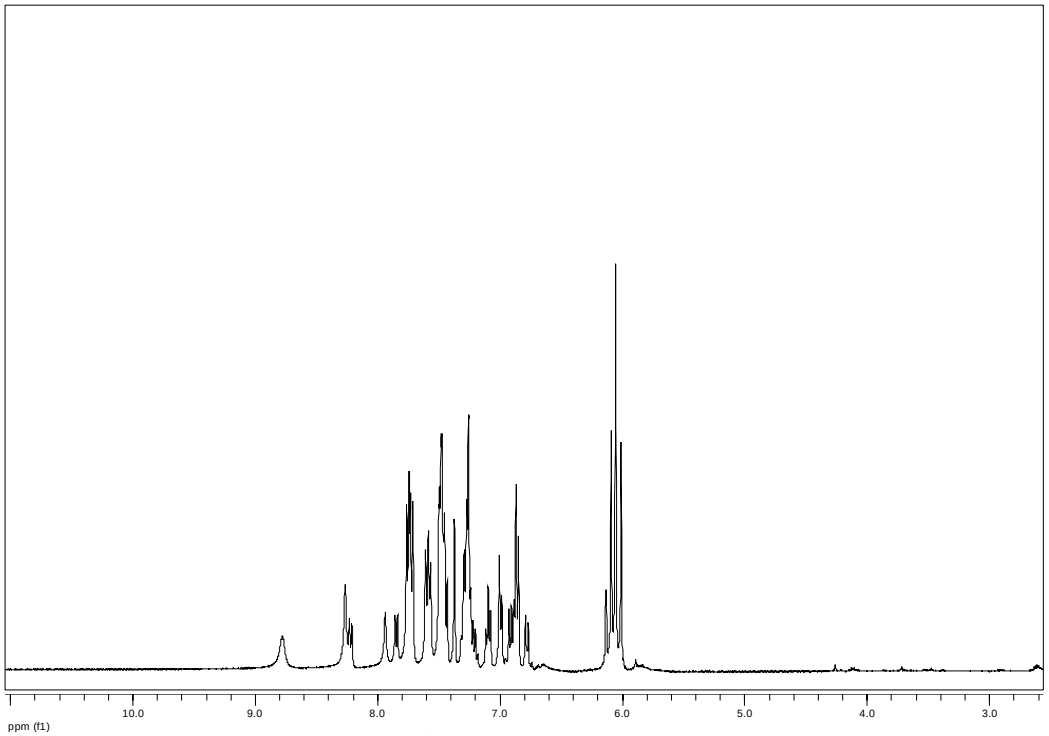

Figure D-1 The ^{1}H-NMR spectrum of Compound **D**

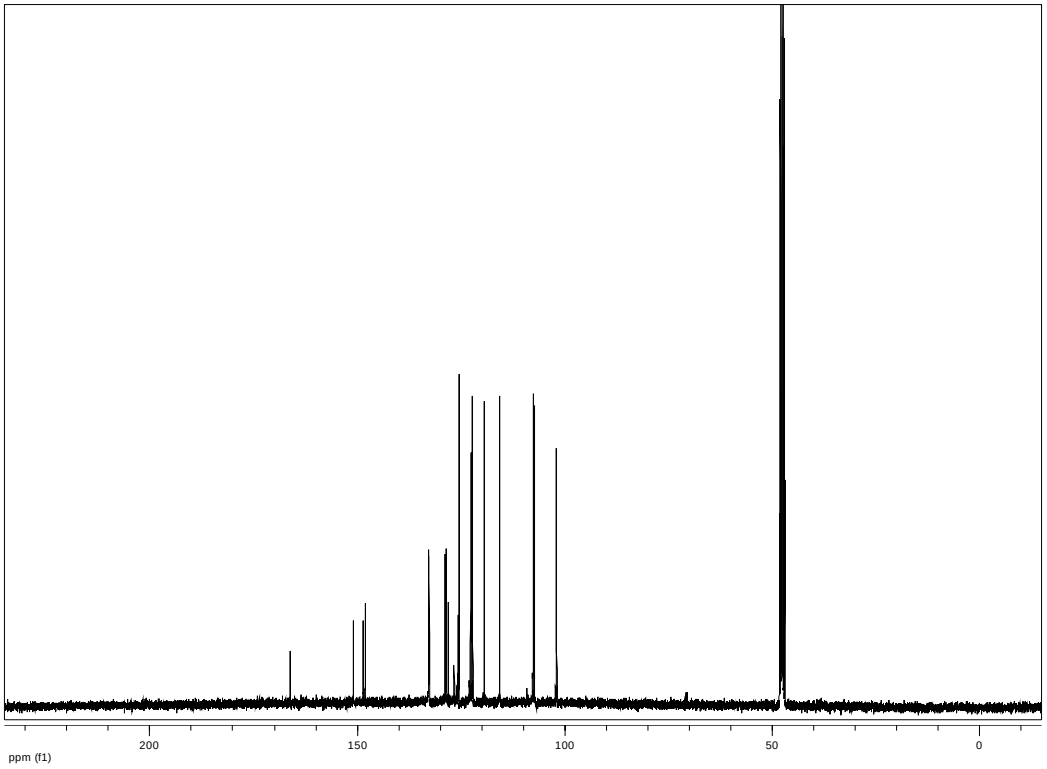

Figure D-2 The ^{13}C-NMR spectrum of Compound **D**

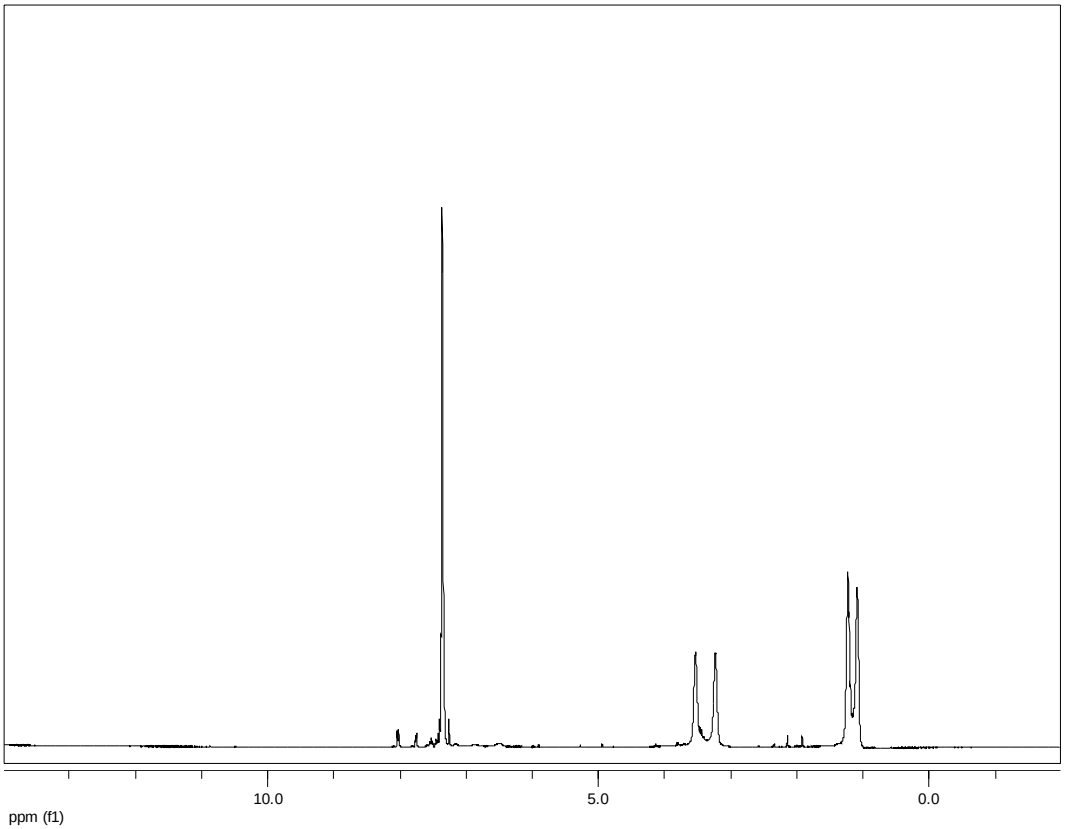

Figure E-1 The ^{1}H-NMR spectrum of Compound **E**

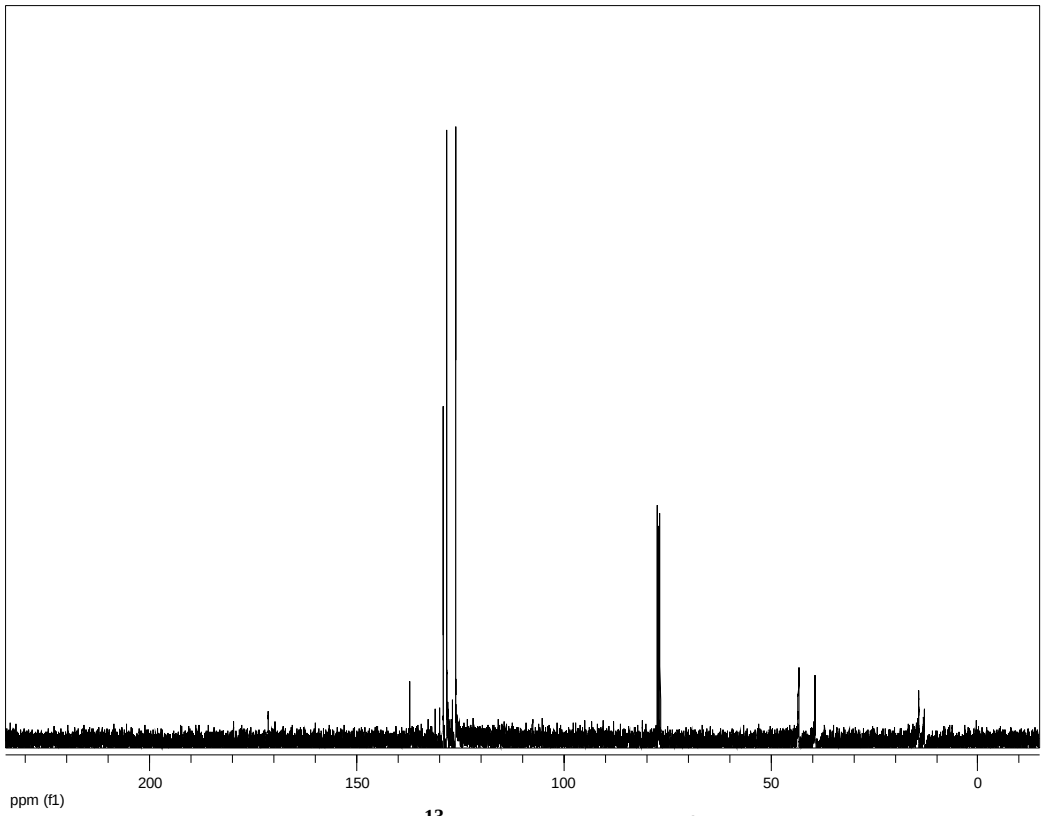

Figure E-2 The ^{13}**C**-NMR spectrum of Compound **E**

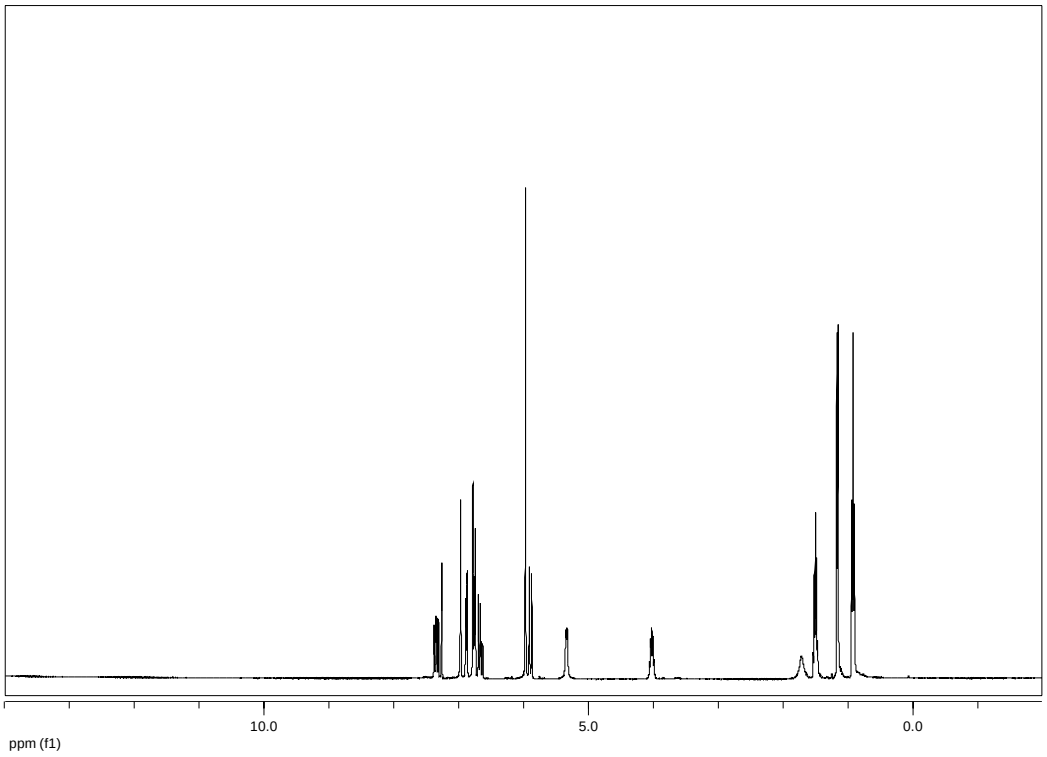

Figure F-1 The ^{1}H-NMR spectrum of Compound **F**

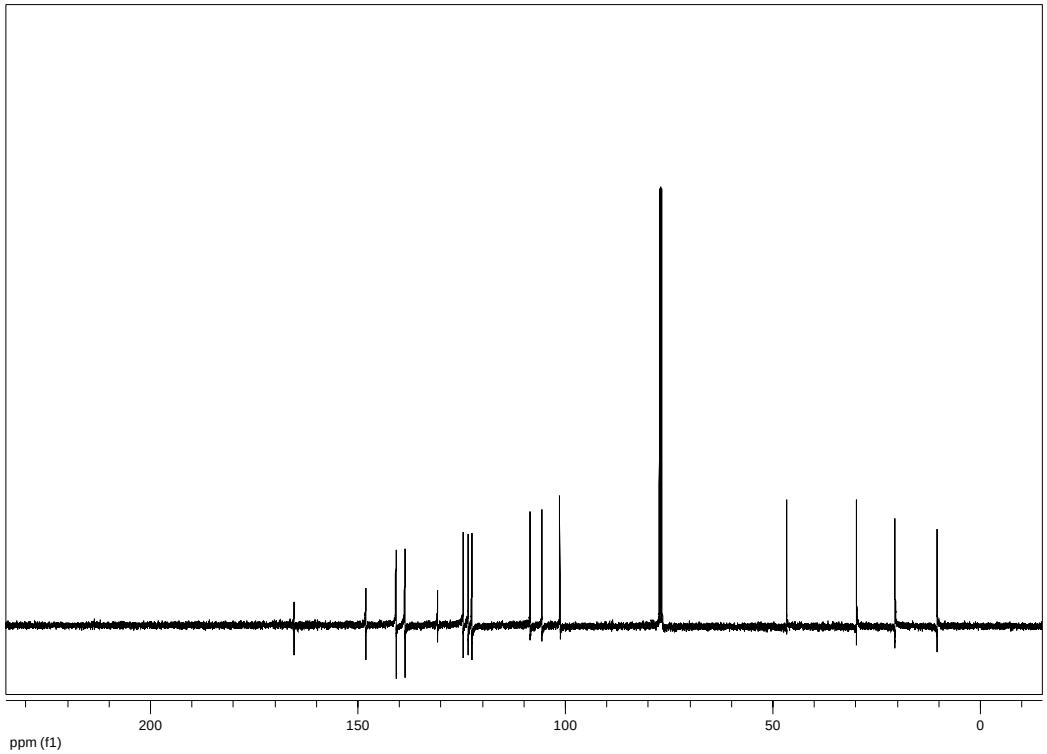

Figure F-2 The ^{13}C-NMR spectrum of Compound **F**

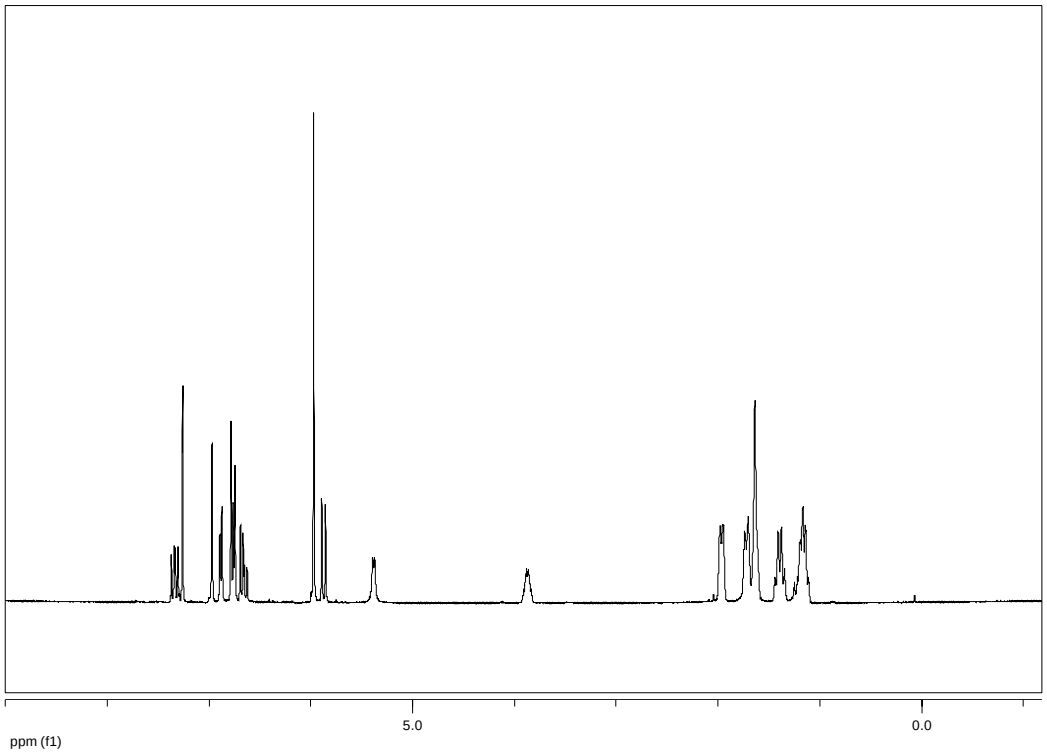

Figure G-1 The ^{1}H-NMR spectrum of Compound **G**

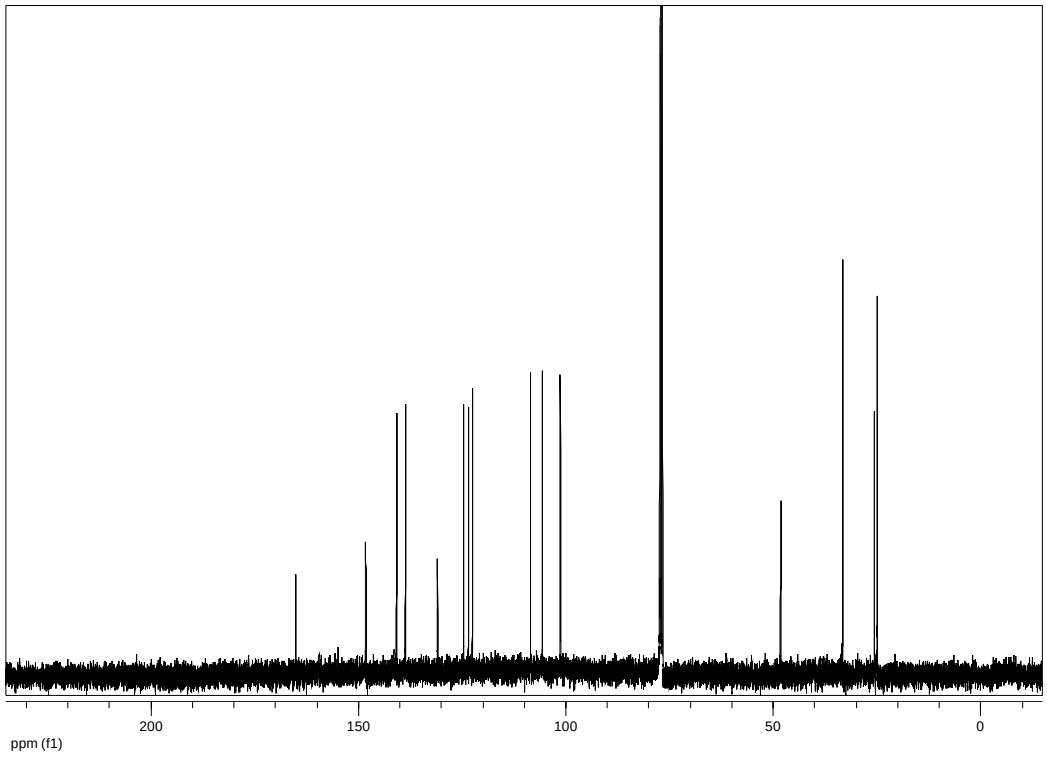

Figure G-2 The ^{13}C-NMR spectrum of Compound **G**

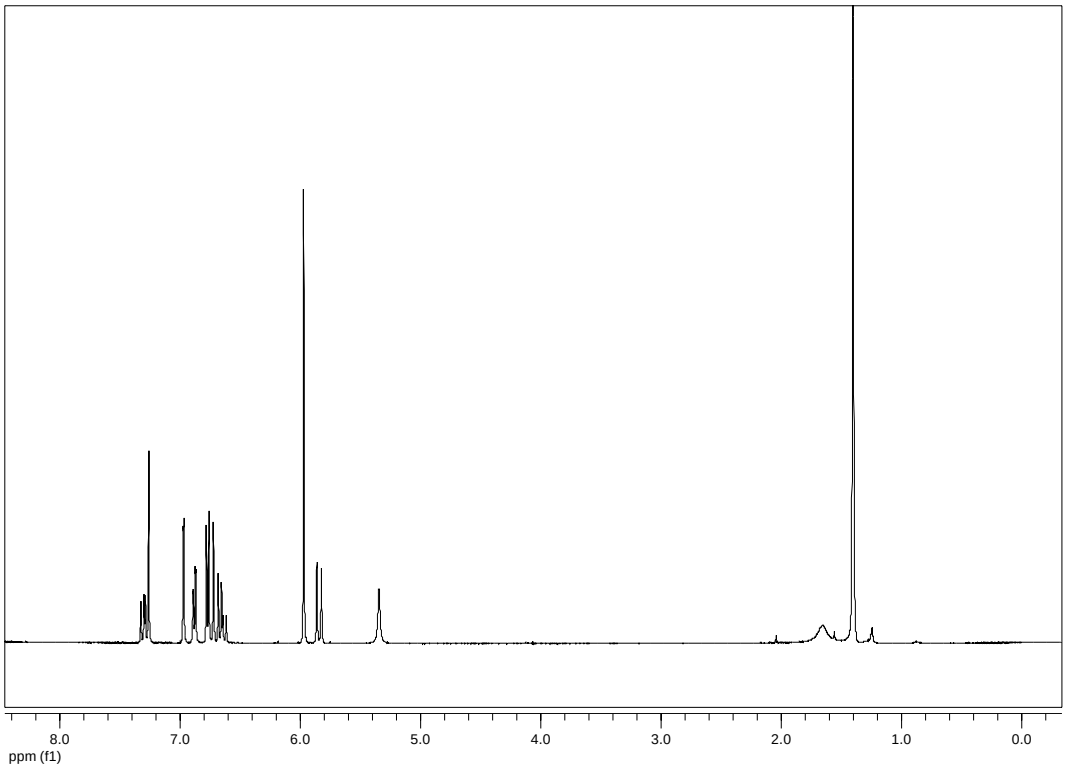

Figure H-1 The ^{1}H-NMR spectrum of Compound **H**

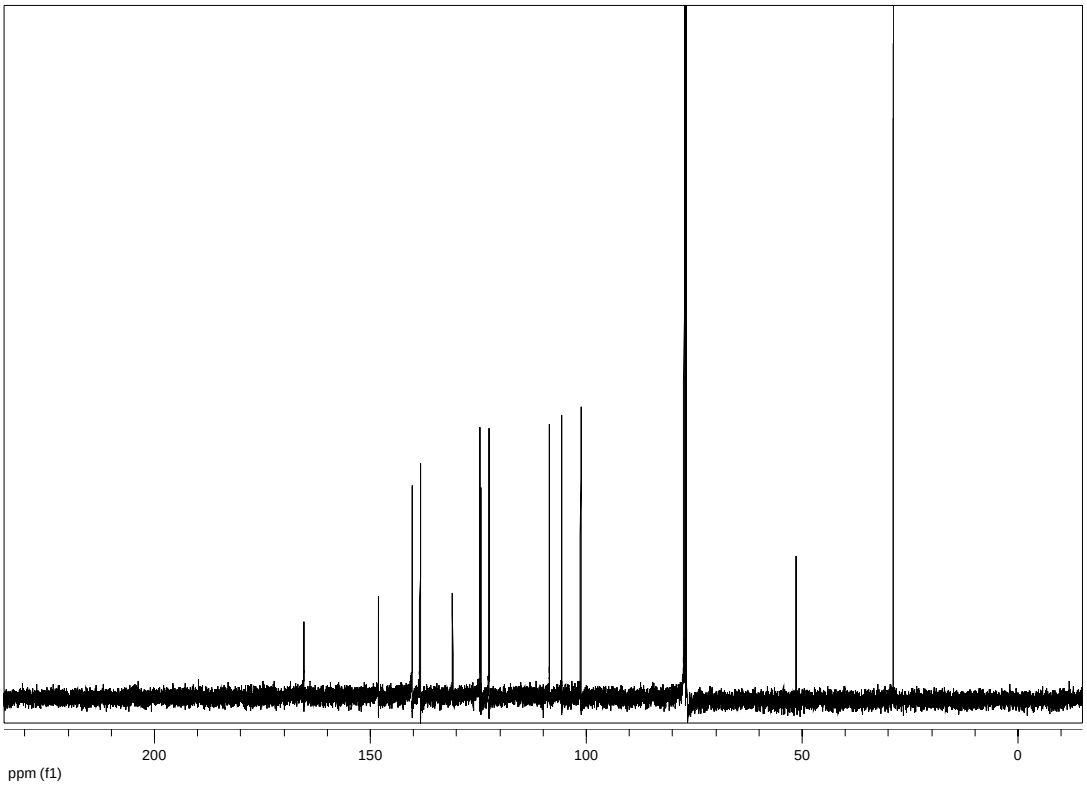

Figure H-2 The ^{13}C-NMR spectrum of Compound **H**

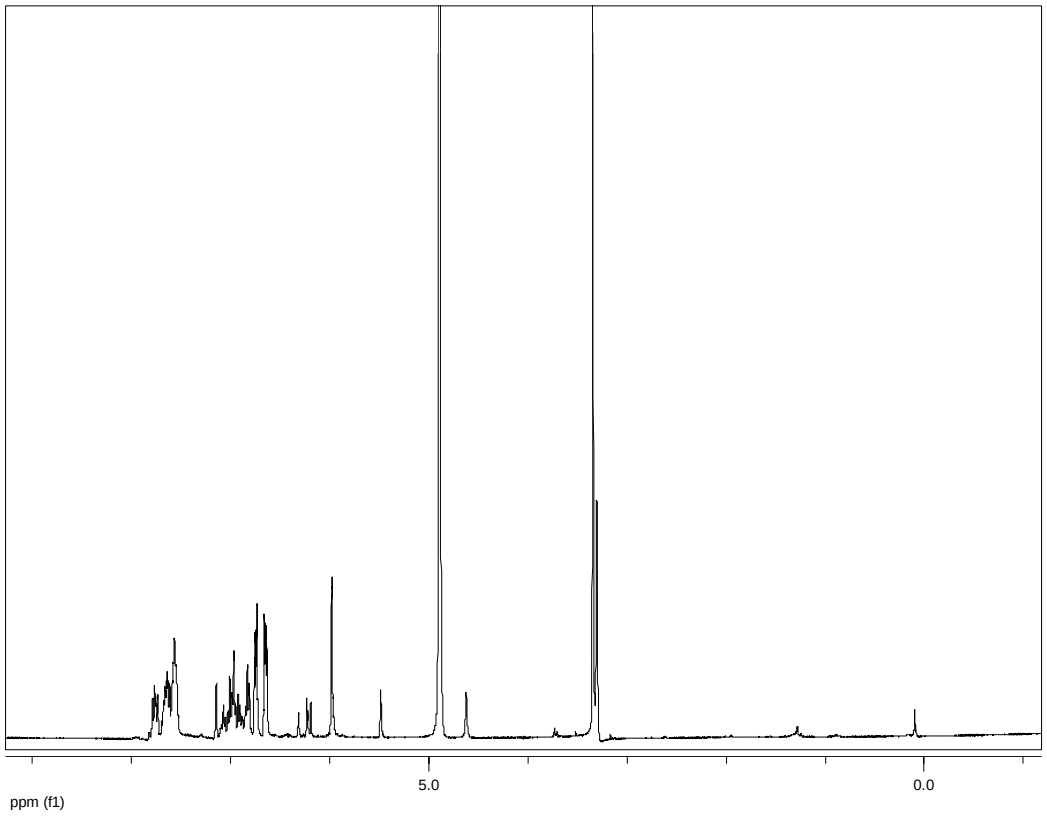

Figure I-1 The ^{1}H-NMR spectrum of Compound **I**

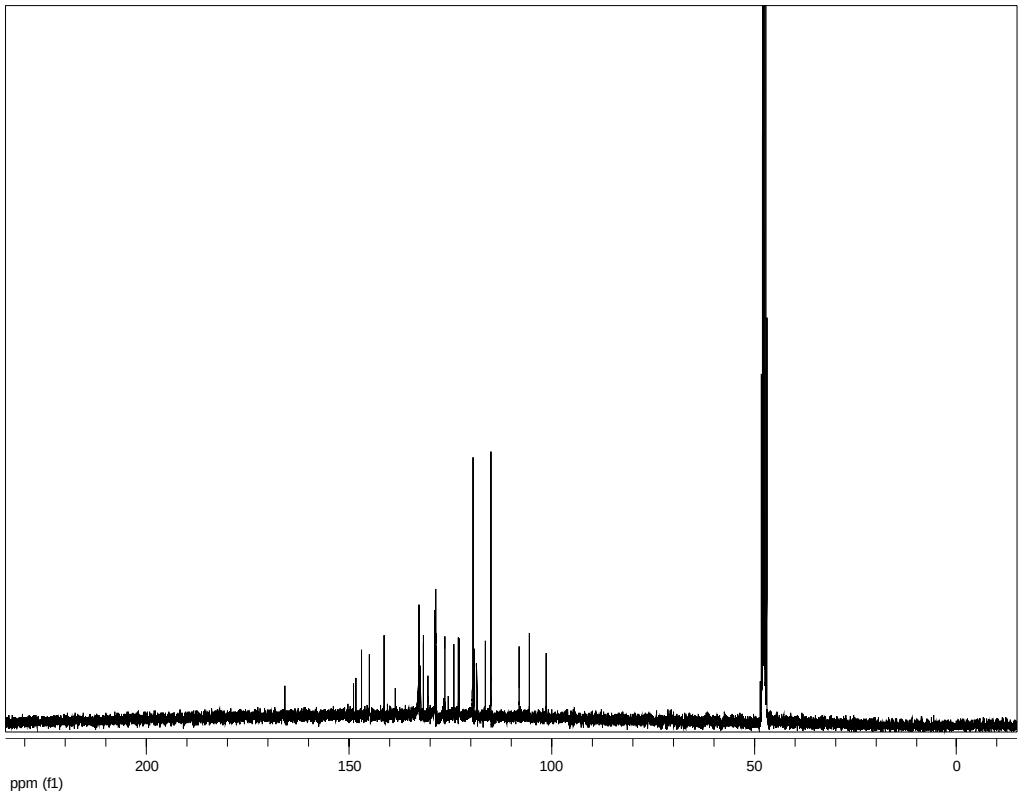

Figure I-2 The^{13}C-NMR spectrum of Compound **I**

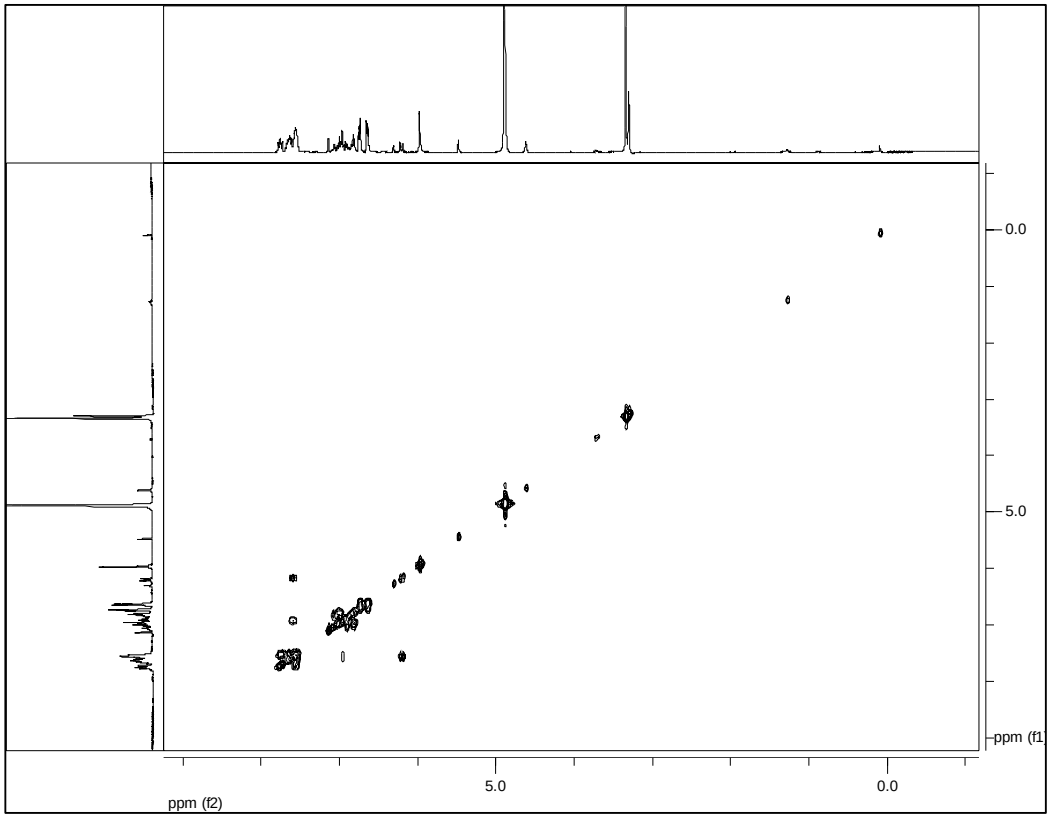

Figure I-3 The COSY spectrum of Compound **I**

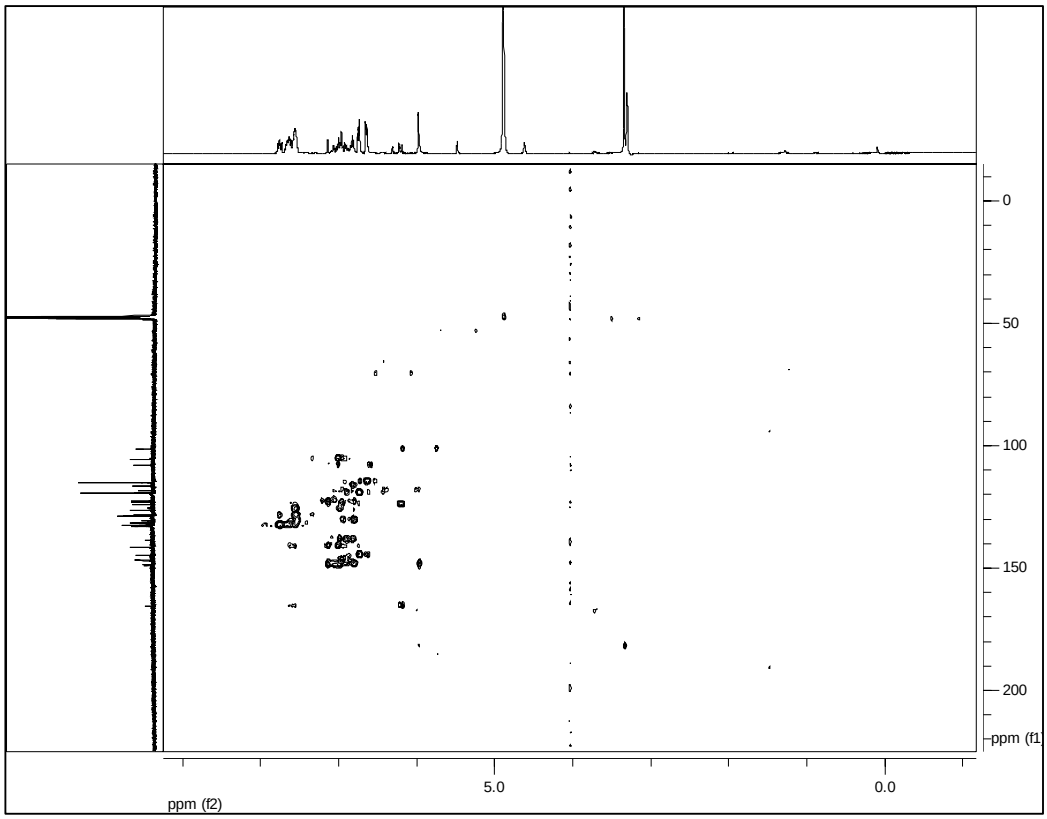

Figure I-4 The HMBC spectrum of Compound **I**

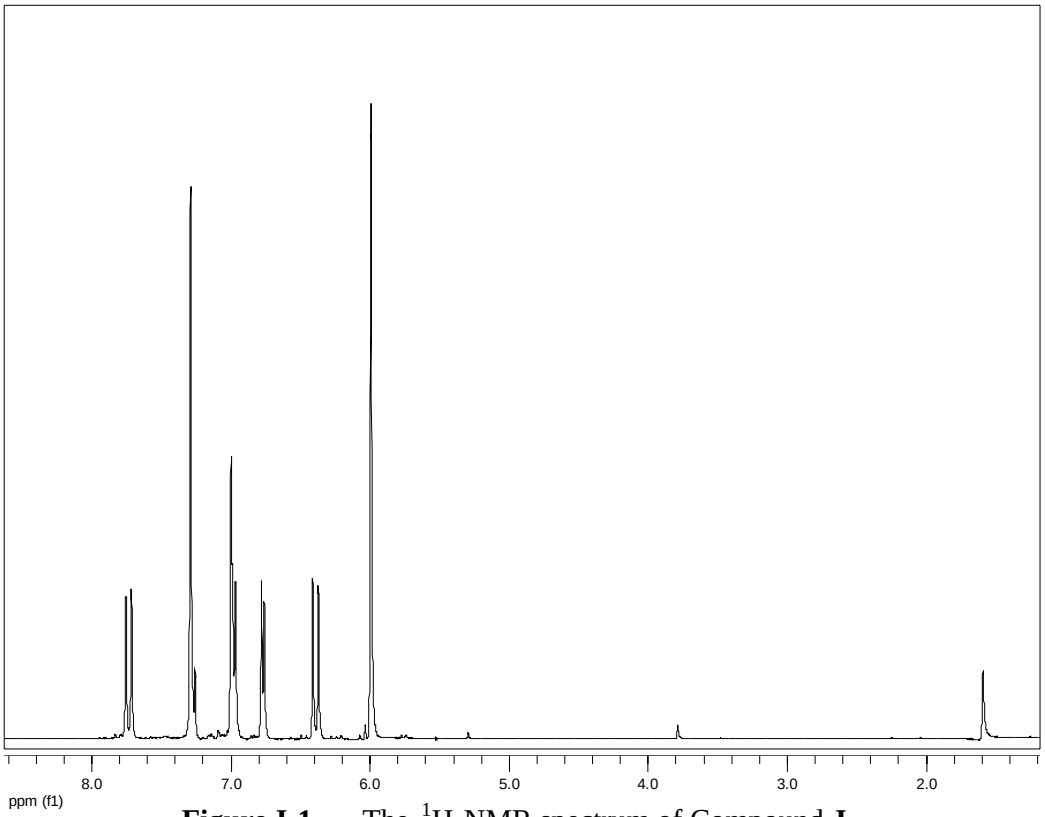

Figure J-1 The ^{1}H-NMR spectrum of Compound **J**

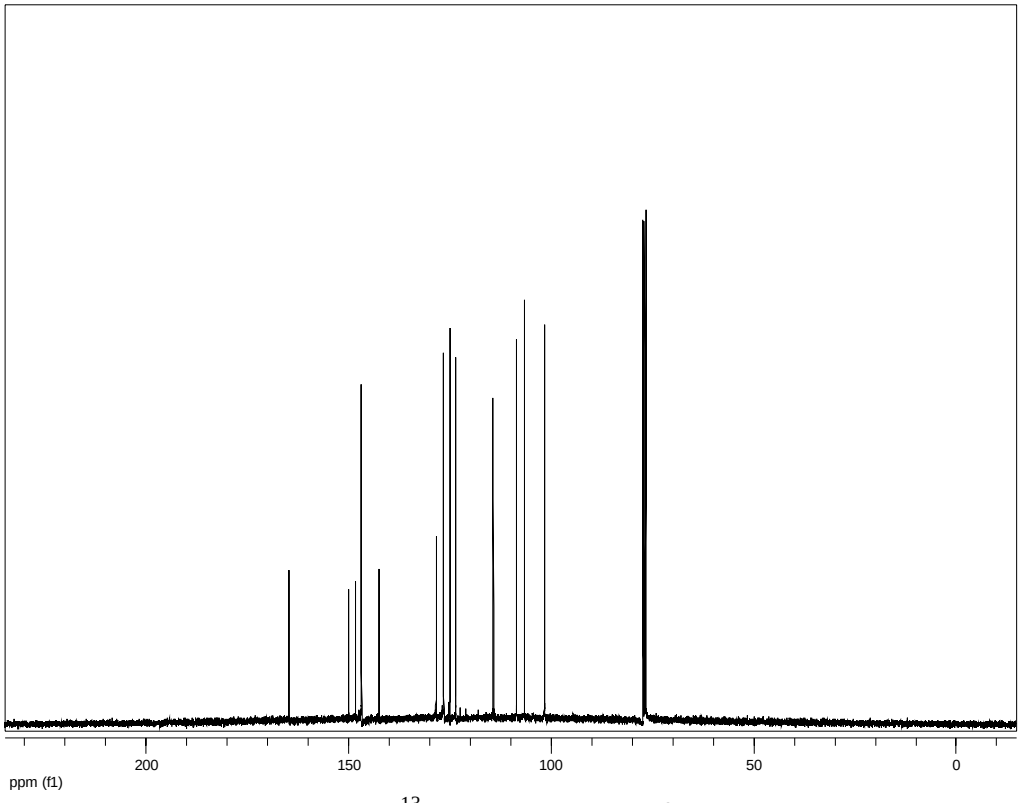

Figure J-2 The ^{13}C-NMR spectrum of Compound **J**

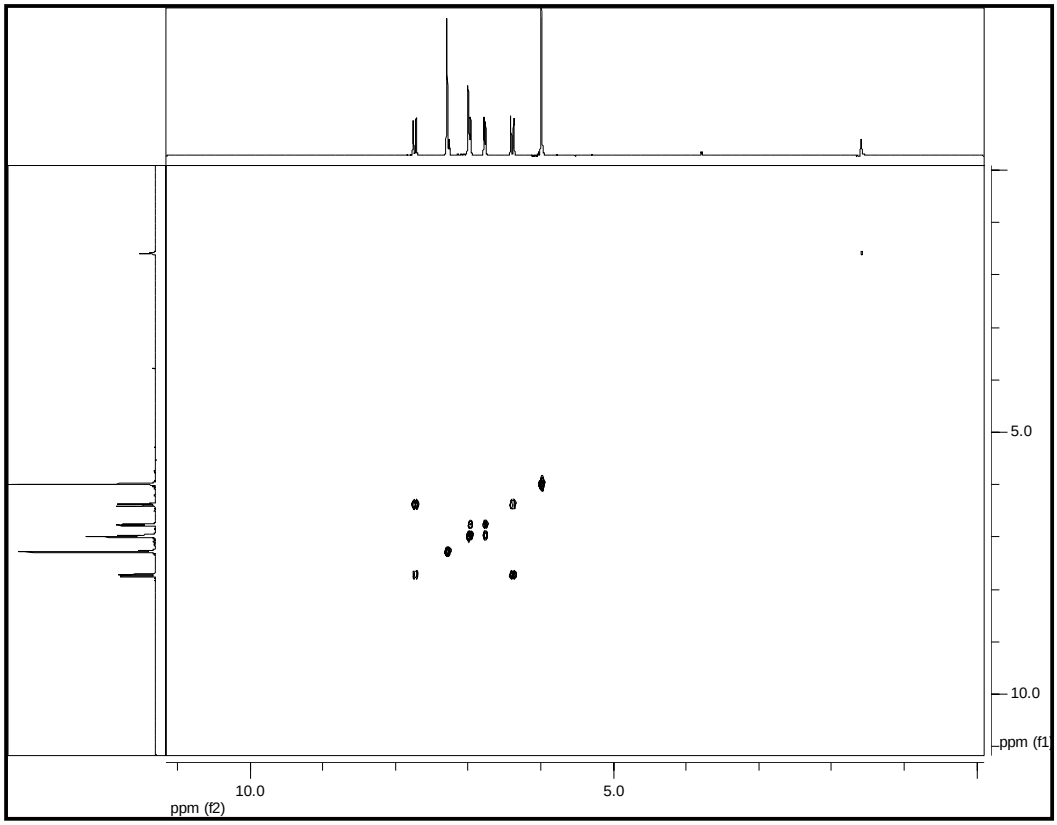

Figure J-3 The COSY spectrum of Compound **J**

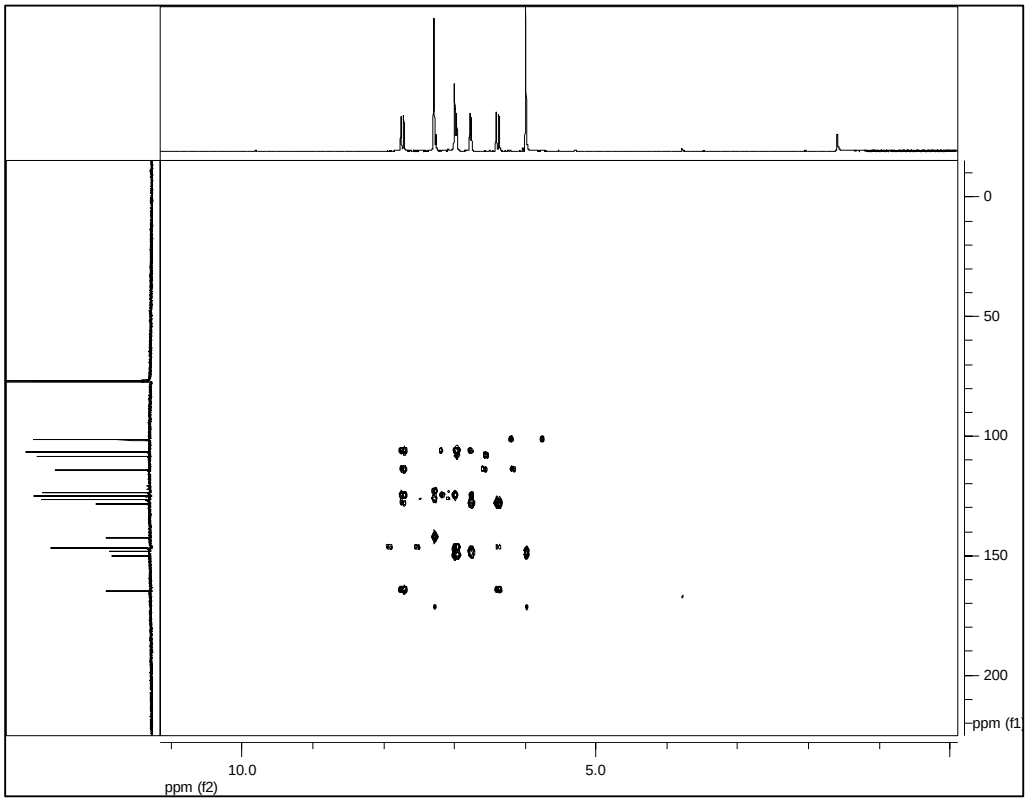

Figure J-4 The HMBC spectrum of Compound **J**

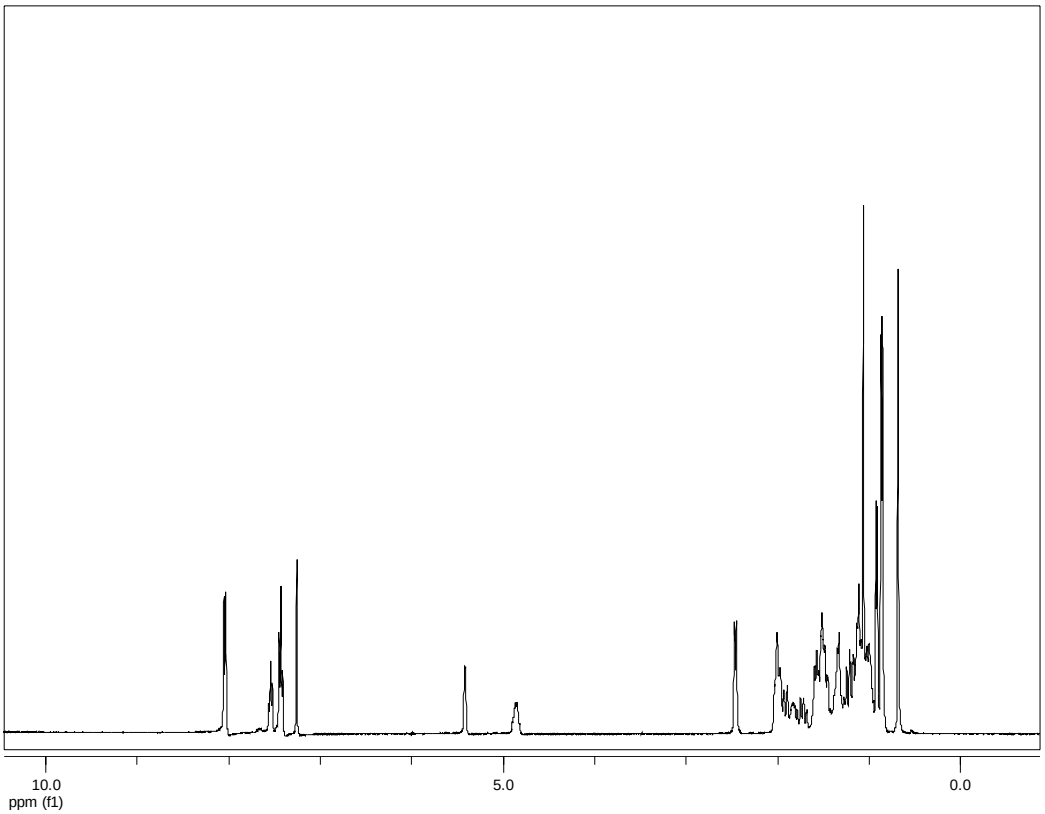

Figure K-1 The ^{1}H-NMR spectrum of Compound **K**

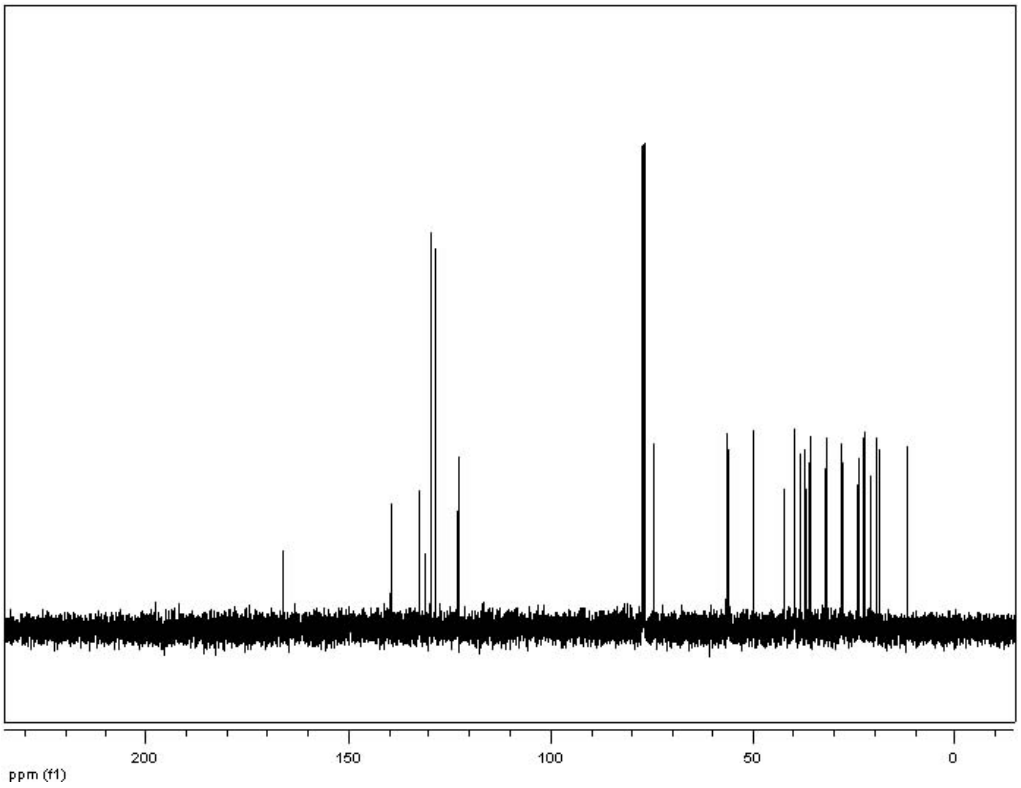

Figure K-2 The ^{13}C-NMRCarbom spectrum of Compound **K**

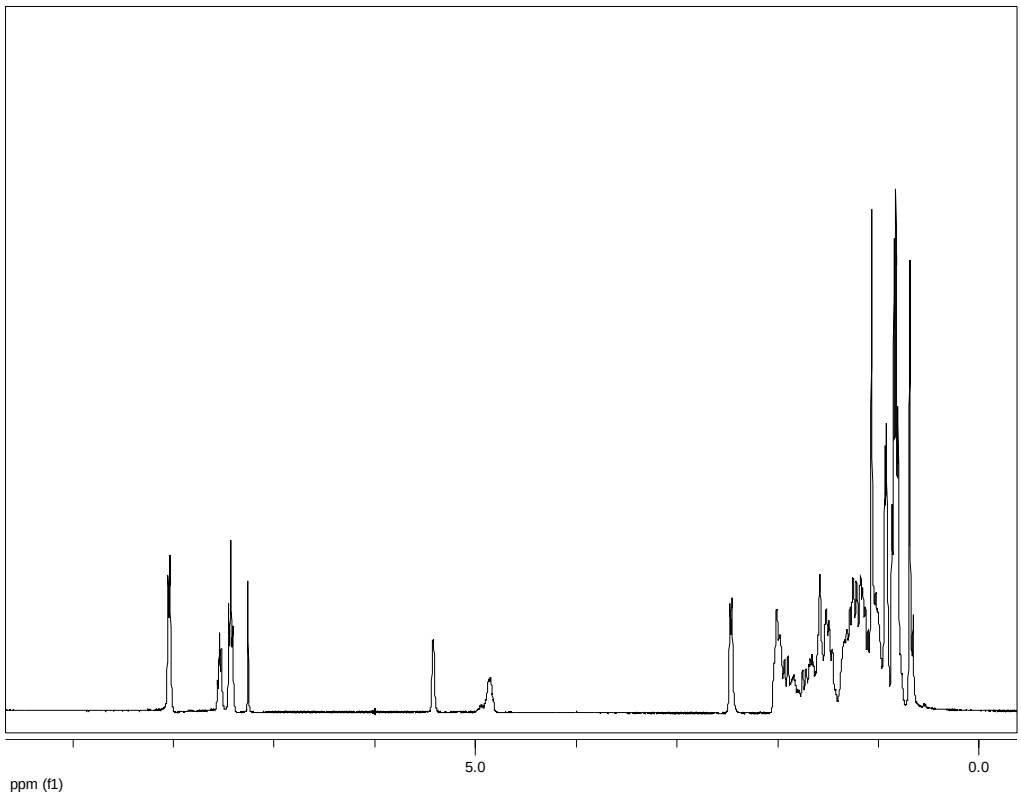

Figure L-1 The ^{1}H-NMR spectrum of Compound **L**

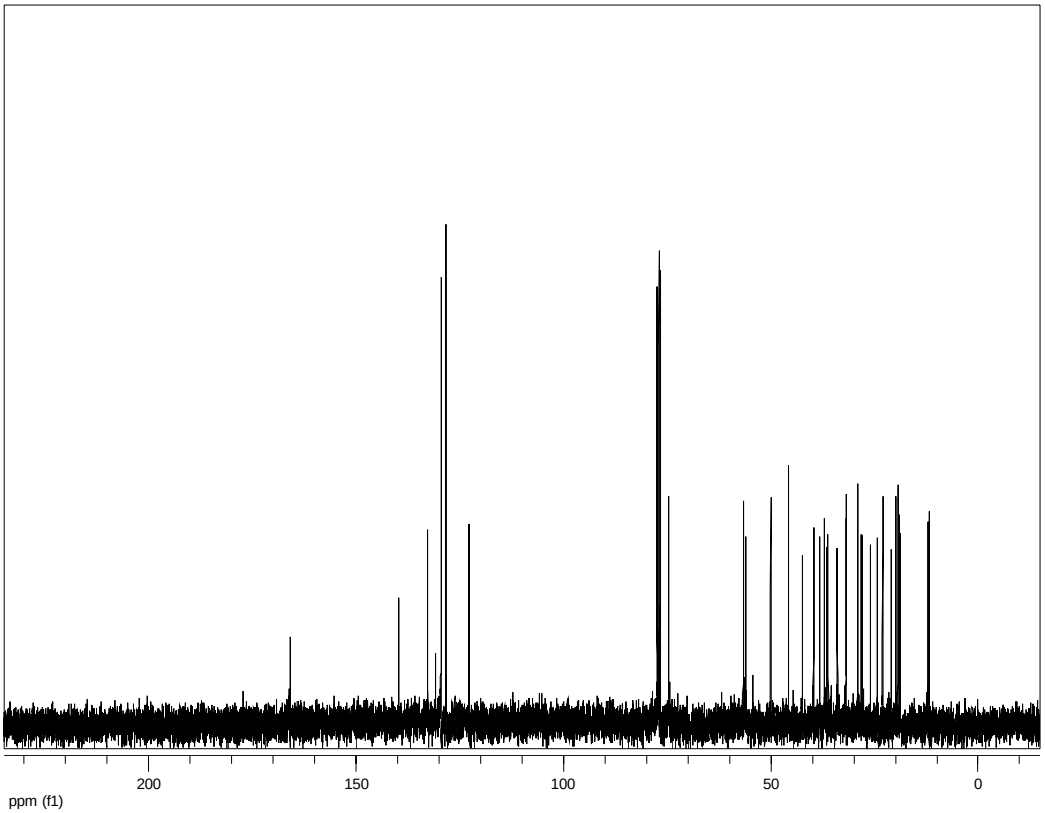

Figure L-2 The ^{13}C-NMR Carbon spectrum of Compound **L**

Table M-1 Radical scavenging effect on DPPH radical

Substance	**Concentration (mg/mL)**	**% radical scavenging**
Ascorbic acid	$1.25x10^{-2}$	93.98
	$6.25x10^{-3}$	80.00
	$3.125x10^{-3}$	60.00
	$1.5625x10^{-3}$	40.00
	$7.813x10^{-4}$	20.00
A	2.00000	62.02
	1.00000	46.78
	0.50000	32.25
	0.25000	15.61
	0.12500	7.47
B	0.50000	62.02
	0.25000	46.78
	0.12500	32.25
	0.06250	15.61
	0.03125	7.47
C	1.00000	75.13
	0.50000	62.64
	0.25000	48.94
	0.12500	31.67
	0.06250	20.20
D	2.00000	80.80
	1.00000	71.66
	0.50000	62.46
	0.25000	54.27
	0.12500	41.13

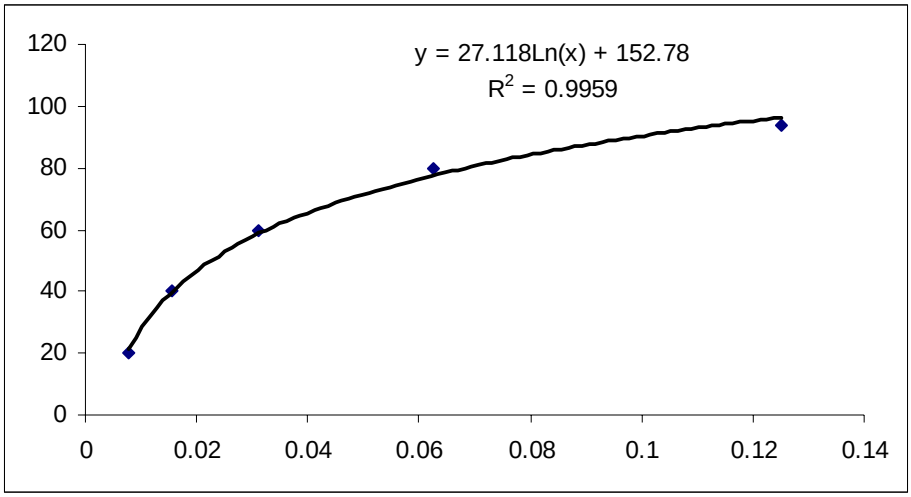

Figure M-1 DPPH radical scavenging effect of Ascorbic acid

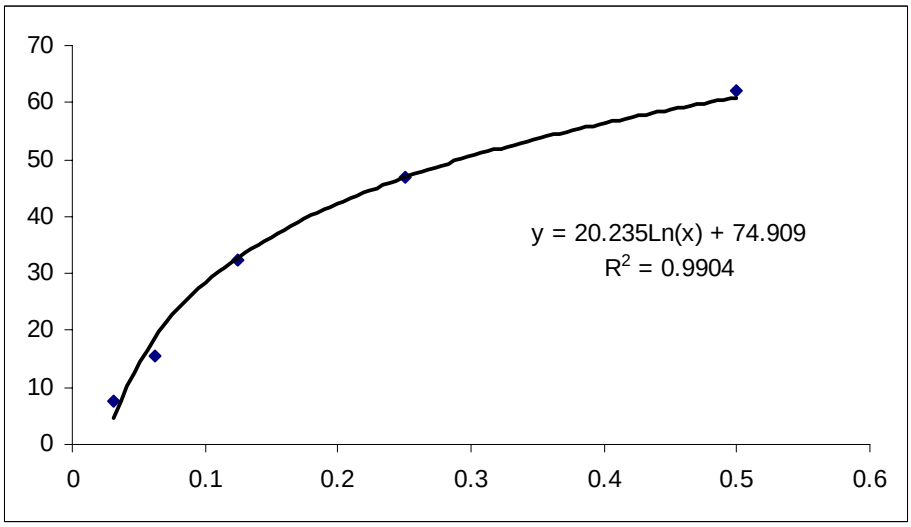

Figure M-2 DPPH radical scavenging effect of Compound **A**

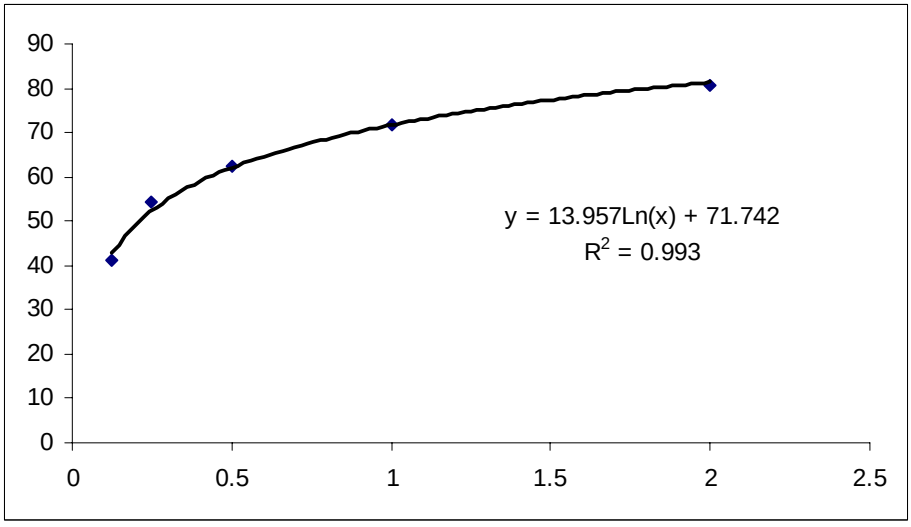

Figure M-3 DPPH radical scavenging effect of Compound **B**

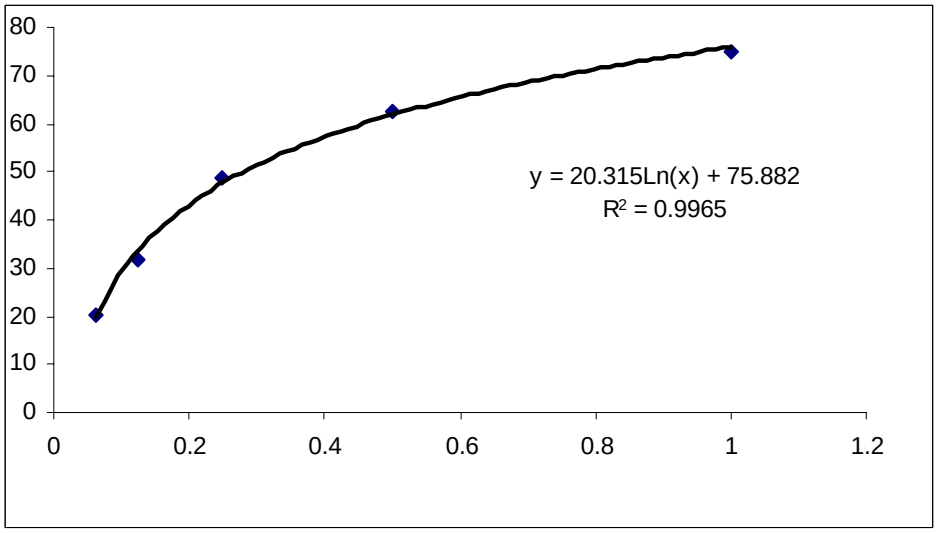

Figure M-4 DPPH radical scavenging effect of Compound **C**

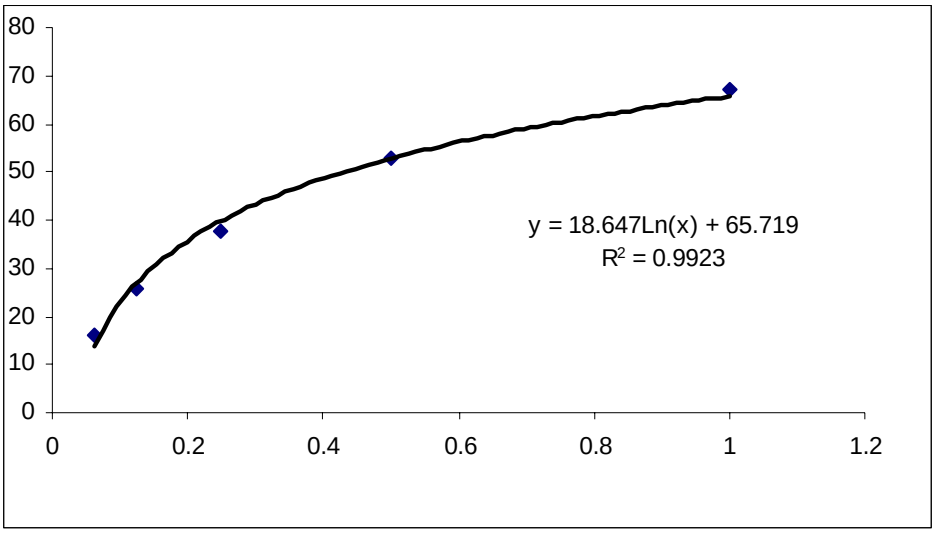

Figure M-5 DPPH radical scavenging effect of Compound **D**

VITA

Miss Dararat Yammuenart was born on June 17, 1978 in Tak Province, Thailand. She received a Bachelor Degree of Science in Chemistry from Rajabhat Insitute Kamphaengphet University in 1997. Since 2005, she has been a graduate student studying Organic Chemistry at Department of Chemistry, Faculty of Science, Chulalongkorn University, Bangkok, Thailand. She was supported by research grant for this Master Degree's thesis from the Graduate School, Chulalomgkorn University. During she was studying in master degree program, she was awarded a teaching assistant schola. Her present address is 78 Moo 9 Tombon Bantak Tak province Thailand.